# BIODEGRADATION OF DIPHENYLAMINE AND *CIS*-DICHLOROETHENE

A Dissertation
Presented to
The Academic Faculty

By

Kwanghee Shin

In Partial Fulfillment
Of the Requirements for the Degree
Doctor of Philosophy in Environmental Engineering in the
School of Civil and Environmental Engineering

Georgia Institute of Technology
May 2010

# BIODEGRADATION OF DIPHENYLAMINE AND *CIS*-DICHLOROETHENE

Approved by:

Dr. Jim C. Spain, Advisor
School of Civil and Environmental Engineering
*Georgia Institute of Technology*

Dr. Joseph B. Hughes
School of Civil and Environmental Engineering
*Georgia Institute of Technology*

Dr. Kostas. T. Konstantinidis
School of Civil and Environmental Engineering
*Georgia Institute of Technology*

Dr. Thomas DiChristina
School of Biology
*Georgia Institute of Technology*

Dr. E. Erin Mack
DuPont Corporate Remediation Group

Date Approved: March 16, 2010

**To my wife, son, and family**

## ACKNOWLEDGEMENTS

I would like to thank my advisor Jim Spain for his support and great guidance towards increasing my insight on science. His clear and thoughtful advisement has been an invaluable resource for my research endeavors. I thank my committee members: Joseph Hughes, Kostas Konstantinidis, Thomas DiChristina, and Erin Mack for their advisement and guidance. I acknowledge support for this work from DuPont Corporate Remediation Group and Strategic Environmental Research and Development Program (SERDP).

There are many graduate students, postdocs, and staff that provided me valuable comments and supported me with their friendship. I would like to thank Shirley Nishino for all of her help throughout my time at Georgia Tech. I appreciate Graham Pumphrey, Samantha Parks, Sarah Craven, Yi Qu, Zuzi Kurt, Anthony Ranchou-Peyruse, Balakrishna Pai, Ray Payne, and Sarah Schroeder for help in and around the lab. I thank all my friends at Georgia Tech who supported me with their friendship.

Finally, I would like to thank my father and mother for being supportive, my son for bringing happiness to my family, and my wife for always being with me.

## TABLE OF CONTENTS

## LIST OF TABLES

## LIST OF FIGURES

## SUMMARY

Past operational practices at chemical manufacturing facilities and widespread use of synthetic chemicals in agriculture, industry, and military operations have introduced many anthropogenic compounds to the biosphere. Some of them are readily biodegradable as a likely consequence of bacterial evolution of efficient degradation pathways, whereas others are partially degraded or persistent in the environment. Insight about biodegradation mechanisms and distribution of bacteria responsible provide the basis to predict the fate of synthetic chemicals in the environment and to enable bioremediation.

The main focus of the research described here encompasses basic science to discover pathways and evolutionary implications of aerobic biodegradation of two specific synthetic chemicals, *cis*-dichloroethene (*c*DCE) and diphenylamine (DPA). *c*DCE is a suspected carcinogen that frequently accumulates due to transformation of perchloroethene and trichloroethene at many contaminated sites. *Polaromonas* sp. strain JS666 is the only isolate able to use *c*DCE as the growth substrate, but the degradation mechanism was unknown. In this study, the degradation pathway of *c*DCE by strain JS666 and the genes involved were determined by using heterologous gene expression, inhibition studies, enzyme assays, and analysis of intermediates. The requirement of oxygen for *c*DCE degradation and inhibition of *c*DCE degradation by cytochrome P450 specific inhibitors suggested that cytochrome P450 monooxygenase catalyzes the initial steps of *c*DCE degradation. The finding was supported by the observation that an *E. coli* recombinant expressing cytochrome P450 monooxygenase catalyzes the transformation of *c*DCE to dichloroacetaldehyde and small amounts of the epoxide. Both the transient accumulation of dichloroacetaldehyde in cDCE degrading

cultures and dichloroacetaldehyde dehydrogenase activities in cell extracts of JS666 further support a pathway involving the degradation of *c*DCE through dichloroacetaldehyde. Molecular phylogeny of the cytochrome P450 gene and organization of neighboring genes suggest that the *c*DCE degradation pathway evolved in a progenitor capable of degrading dichloroacetaldehyde by the recruitment of the cytochrome P450 monooxygenase gene from alkane assimilating bacteria. The discovery provides insight about the evolution of the aerobic *c*DCE biodegradation pathway and sets the stage for field applications.

DPA has been widely used as a precursor of dyes, pesticides, pharmaceuticals, and photographic chemicals and as a stabilizer for explosives, but little was known about the biodegradation of the compound. Therefore, bacteria able to use DPA as the growth substrate were isolated by selective enrichment from DPA-contaminated sediment and the degradation pathway and the genes that encode the enzymes were elucidated. Transposon mutagenesis, the sequence similarity of putative open reading frames to those of well characterized dioxygenases, and $^{18}O_2$ experiments support the conclusion that the initial reaction in DPA degradation is catalyzed by a multi-component ring-hydroxylating dioxygenase. Aniline and catechol produced from the initial reaction of DPA degradation are then completely degraded via the common aniline degradation pathway. Molecular phylogeny and organization of the genes involved were investigated to provide insight about the evolution of DPA biodegradation.

The fate and transport of toxic chemicals are of a great concern at several historically contaminated sites where anoxic contaminant plumes emerge into water bodies. The release

of toxic chemicals to overlying water poses a potential source of environmental exposure. Bench scale studies were conducted to evaluate the impact of biodegradation on the transport of toxic chemicals across the sediment/water interface. These studies demonstrated that substantial populations of bacteria associated with organic detritus at the interface rapidly biodegrade toxic chemicals as they migrate from contaminated sediment to overlying water, suggesting that the natural attenuation processes serve as a remedial strategy for contaminated sediments and protect the overlying water.

# CHAPTER 1

# Introduction

## 1.1 DISSERTATION RESEARCH OVERVIEW

Past operational practices at chemical manufacturing facilities and widespread use of synthetic chemicals in agriculture, industry, and military operations have introduced many anthropogenic compounds to the biosphere. The release of synthetic chemicals to the biosphere provides microbial populations with selective pressure to evolve new catabolic pathways which enable some of them to exploit synthetic chemicals for their growth. New biodegradation pathways for synthetic chemicals can evolve through mutations that alter the substrate specificities of the existing enzymes and/or recruitment of genes that channel degradation intermediates to central metabolism (35, 36, 55). Thus existing microbial metabolic diversity provides the source for evolution of catabolic pathways for synthetic chemicals (78, 79). Some of the synthetic chemicals are, however, partially degraded or persistent in the environment, which can cause toxicity to humans and wildlife. Therefore, insight about biodegradation mechanisms and distribution of bacteria responsible must be determined to predict the fate of synthetic chemicals in the environment and to enable bioremediation at contaminated sites.

The main focus of the research encompasses basic science to discover pathways and evolutionary implications of aerobic biodegradation of two specific toxic chemicals, *cis*-dichloroethene (*c*DCE) and diphenylamine (DPA). More applied studies are included to

evaluate the impact of biodegradation on the fate and transport of contaminants at contaminated sites. This introduction demonstrates what is known and what remains to be discovered regarding biodegradation of *c*DCE and DPA. Chapter 1 ends with a review of systematic approaches to evaluate monitored natural attenuation of the synthetic chemicals at contaminated sites.

*c*DCE is a suspected carcinogen that frequently accumulates during biotransformation of perchloroethene and trichloroethene at many contaminated sites. *Polaromonas* sp. strain JS666 is the only isolate able to grow on *cis*-dichloroethene as the sole source of carbon and energy under aerobic conditions, but it remained to be discovered how it degraded *cis*-dichloroethene and how it evolved the capability to grow on the compound. The biodegradation pathway of *cis*-dichloroethene by *Polaromonas* sp. JS666 and the genes involved are described in Chapter 2. The discovery of the degradation pathway and the genes involved provides insight about the evolution of aerobic *cis*-dichloroethene biodegradation and sets the stage for field applications.

DPA has been widely used as a precursor of dyes, pesticides, pharmaceuticals, and photographic chemicals and as a stabilizer for explosives, but little is known about the biodegradation of the compound. Research described in Chapter 3 led to the discovery of aerobic bacteria able to use DPA as the growth substrate and then the elucidation of the degradation pathway and the genes that encode the enzymes involved. Molecular phylogeny and organization of the genes involved were investigated to provide insight about the evolution of DPA biodegradation.

At many of the aniline and diphenylamine manufacturing sites the soil and groundwater are extensively contaminated with not only aniline and diphenylamine, but

also nitrobenzene- a precursor of aniline. The fate and transport of the three chemicals are of a great concern at several historically contaminated sites where an anoxic contaminant plume emerges into a water body. The release of the toxic chemicals to overlying water poses a potential source of environmental exposure. Chapter 4 describes the impact of biodegradation on the transport of the three chemicals across the sediment/water interface at contaminated sites. These studies demonstrated that substantial populations of bacteria associated with organic detritus at the interface rapidly biodegrade toxic chemicals as they migrate from contaminated sediment to overlying water, suggesting that the natural attenuation processes serve as a remedial strategy for contaminated sediments and protect the overlying water.

## 1.2 *CIS*-DICHLOROETHENE (*c*DCE) BIODEGRADATION

### 1.2.1 Environmental relevance of *c*DCE

Chlorinated ethenes such as perchloroethene and trichloroethene have been widely used as de-greasing agents and solvents, resulting in soil and groundwater contamination throughout the world (76). Reductive dechlorination by anaerobic bacteria is a major route to detoxify the polychlorinated solvents by converting them to ethene (28, 29, 50) (Fig. 1.1). Incomplete reduction, however, frequently increases the risk by accumulating the toxic intermediates, *cis*-dichloroethene (*c*DCE) and vinyl chloride (VC) in the field (19, 54). *c*DCE degradation is a rate limiting step in natural attenuation processes for the chlorinated ethenes at many contaminated sites. The problem can be exacerbated by insufficient electron donors or by the absence of *Dehalococcoides* sp. able to dechlorinate

*c*DCE and VC (28). Migration of the toxic intermediates into an aerobic zone with groundwater flow increases the risk at the contaminated sites.

### 1.2.2 Aerobic biodegradation of *c*DCE and VC

*c*DCE and VC are biodegradable under aerobic conditions (9, 11) (Fig. 1.1). Several bacteria able to grow on VC have been isolated and they are widespread (10, 49). The initial step of VC degradation is a monooxygenase-mediated epoxidation that produces a chlorinated epoxyethane (chlorooxirane). Epoxyalkane coenzyme M transferase catalyzes conversion of the chlorooxirane to 2-chloro-2-hydroxyethyl-CoM which spontaneously

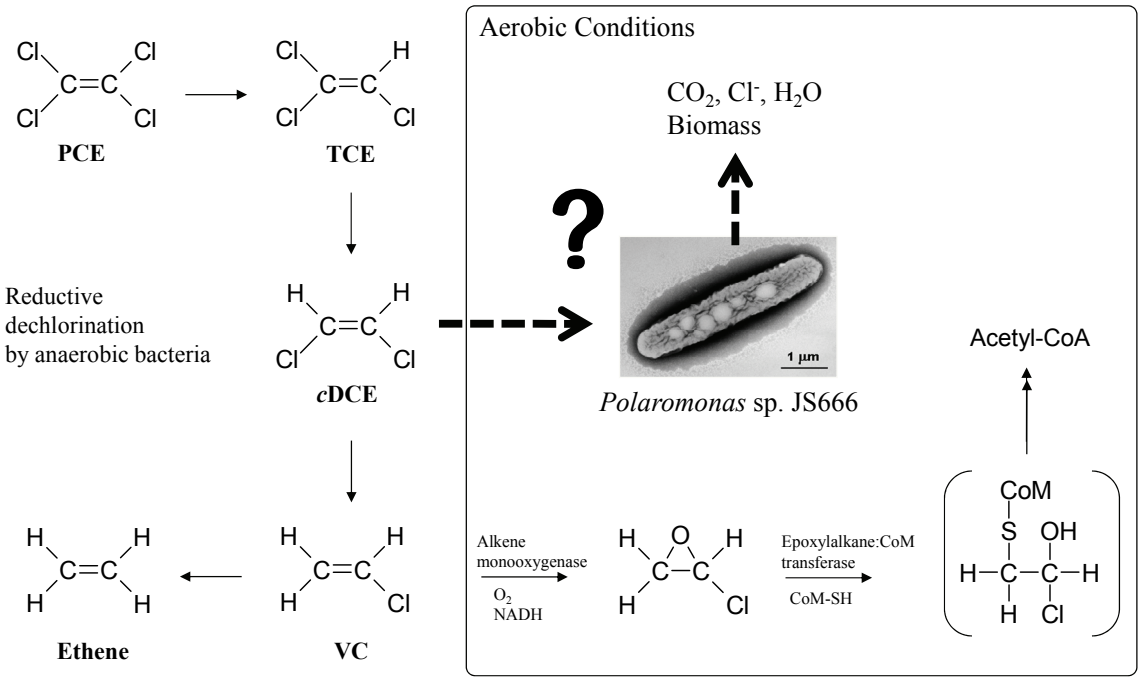


**Figure 1.1** Biodegradation of chlorinated ethenes.

releases chloride to form 2-hydroxyethyl-CoM, an intermediate in the ethene assimilation pathway (1, 11). The two enzymatic steps of the VC degradation pathway are analogous to those of aerobic ethene biodegradation (41, 42). The VC-assimilating bacteria are able to grow on ethene by the expression of the enzymes involved in VC degradation (49), which suggests that widespread ethene assimilating bacteria can readily adapt to use VC as their growth substrates (48, 49).

In contrast to the wide distribution of VC degrading bacteria, *Polaromonas* sp. strain JS666 is the only isolate able to grow on *c*DCE as the sole carbon and energy source under aerobic condition (9) despite many attempts to isolate *c*DCE degraders from several contaminated sites. Bioaugmentation with strain JS666 is therefore a promising strategy to clean up *c*DCE contaminated sites, but uncertainty about the degradation pathway and intermediates is a deterrent to the use of the strategy in practical application.

### 1.2.3 Cometabolic oxidation of cDCE

Cometabolism of chlorinated ethenes by oxygenases is a widespread mechanism in bacteria that leads to the formation of a toxic and highly reactive epoxide intermediates (18, 20, 40, 80). The epoxide intermediates can damage cellular constituents and eventually lead to cell death. The epoxidation of chlorinated ethenes is therefore an undesirable reaction unless the epoxide can be further metabolized. Vinyl chloride-degrading bacteria have evolved a strategy to metabolize vinyl chloride epoxide in a reaction catalyzed by coenzyme M transferase (11).

Rui et al (67, 68) exploited the epoxide formation as the initial step of the degradation of *c*DCE to glyoxal by an engineered strain (Fig. 1.2). Toluene monooxygenase evolved by site directed mutagenesis catalyzed the epoxidation of *c*DCE (7). Epoxide hydrolase or glutathione S-transferase were cloned in *E. coli* from epichlorohydrine and isopropene degrading bacteria to detoxify the epoxide intermediate. The two resulting *E. coli* clones released significantly more chloride from *c*DCE than those expressing only toluene monooxygenase. Although the *E. coli* clones are not able to grow on *c*DCE, the studies demonstrated a potential degradation pathway for *c*DCE.

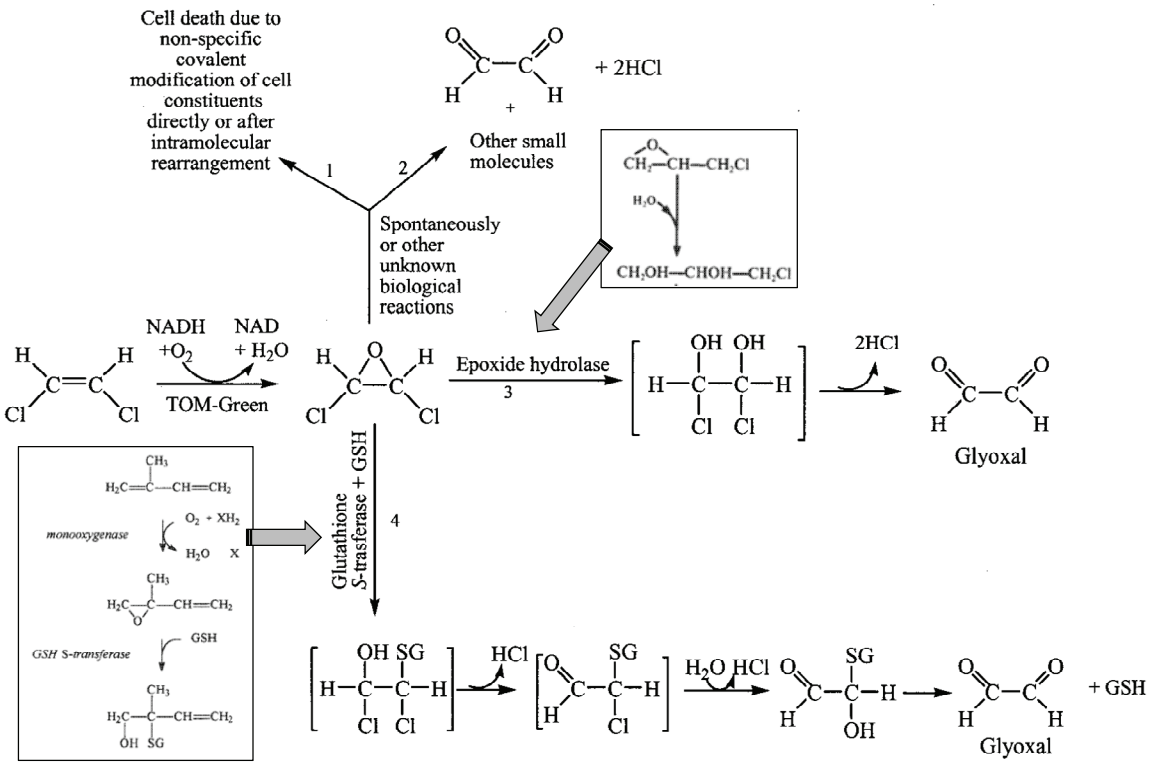


**Figure 1.2** Metabolic engineering of *c*DCE biodegradation in *E. coli*, modified from (67).

In some cases, trace amounts of chloroacetaldehyde result from intramolecular chloride migration during the oxidation of the chlorinated ethenes by methane monooxygenase (20). In mammalian systems, cytochrome P450 enzymes catalyze the initial enzymatic attack on chlorinated ethenes, similar to some of the reactions observed in bacterial systems. Non-concerted reactions of cytochrome P450 from rat liver microsomes oxidize TCE to TCE epoxide and 1,1,1-trichloroacetaldehyde (chloral), but the mechanisms controlling the partitioning to the two intermediates are not fully understood (51, 52).

### 1.2.4 Genome of *Polaromonas* sp. strain JS666

The genome of *Polaromonas* strain JS666 has been sequenced by the US Department of Energy Joint Genome Institute (DOE JGI) (47). A number of putative genes in xenobiotic metabolism are located on the circular chromosome (5.2 Mb) and two large plasmids (338 and 360 kb) but no operon for *c*DCE degradation is apparent. Similarly, putative genes for dichloroethane (DCA) degradation are annotated in the genome of JS666 even though they do not form a recognizable operon and JS666 was reported not to grow on DCA (47). Several additional genes annotated as dehalogenases were dispersed in the genome. Both the absence of a recognizable operon and the presence of many potential genes for *c*DCE degradation make it difficult to predict which genes encode enzymes involved in *c*DCE degradation in JS666.

Genes that encode the biodegradation of cyclohexanone and n-alkane are present in operonic structures, which is consistent with the growth of strain JS666 on

cyclohexanone or heptane and octane (47). The two separate operons are located on the same plasmid in JS666. The flanking regions have high G+C content and are associated with several transposase genes, which suggests that the gene clusters were recently recruited from cyclohexanone or alkane assimilating bacteria. Cyclohexanone and n-alkane degradation would be initiated by monooxygenase enzymes like cyclohexanone monooxygenase and cytochrome P450 monooxygenase found in the two separate operons, respectively. Activities of the two monooxygenases for *c*DCE are unknown.

### 1.2.5 Proteins and genes upregulated by *c*DCE in *Polaromonas* sp. strain JS666

Whole genome expression microarrays and protein expression analyses have revealed a number of genes that are upregulated by growth on *c*DCE compared to growth on glycolate (34) (Table 1.1), but the initial steps in *c*DCE biodegradation remain a mystery. Upregulation of glutathione *S*-transferase (GST), cyclohexanone monooxygenase (CMO), and haloacid dehalogenase (HAD) was revealed by protein 2-D gel electrophoresis and mass spectrometry. A mRNA microarray experiment confirmed the observation as well as identified 217 genes as upregulated during the growth of strain JS666 on *c*DCE. Collectively, the protein and cDNA microarray studies suggest a downstream pathway of *c*DCE degradation via (di)chloroacetaldehyde, (di)chloroacetic acid, and (chloro)glycolate similar to a pathway in bacteria able to grow on 1,2-dichloroethane (DCA) (27, 33). The argument is further supported by the detection of chloroacetaldehyde dehydrogenase and haloacid dehalogenase activities in cell extracts of JS666.

**Table 1.1** Selected proteins and genes upregulated during the growth of JS666 on *c*DCE versus glycolate (34).

| Gene | Protein (of 33) | mRNA (of 103) |
|---|---|---|
| Glutathione S-transferase | X | 100X |
| Pyridoxamine 5′-phosphate oxidase | X | 87X |
| Haloacid dehalogenase* | X | 53X |
| Haloacid transporter | | 41X |
| Cyclohexanone monooxygenase | X | 10X |
| Cytochrome P450 alkane hydroxylase | | 4X |
| Glutathione S-transferase, isozyme 2 | X | |
| Glyoxylate carboligase | X | |
| 2-hydroxy-3-oxopropionate reductase | X | |
| Hydroxypyruvate isomerase | X | |

* Enzyme detected in cell extracts

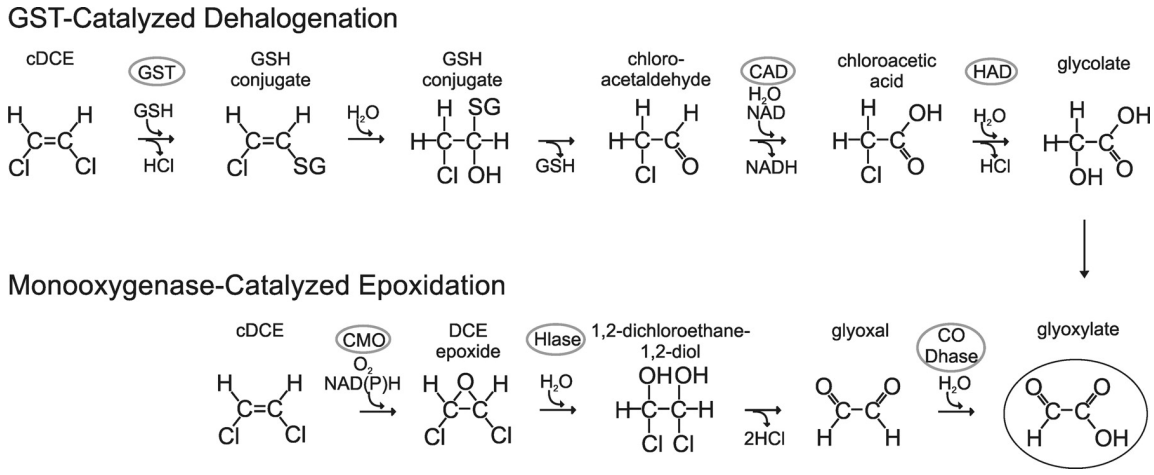


**Figure 1.3** Previously proposed *c*DCE degradation pathways (34) (GST: glutathione S-transferase, GSH: glutathione, CAD: chloroacetaldehyde dehydrogenase, HAD: haloacid dehydrogenase, CO Dhase: carbon monoxide dehydrogenase, Hlase: hydrolase, CMO: cyclohexanone monooxygenase).

Based on the expression of glutathione-S-transferase and cyclohexanone monooxygenase, the authors suggested two possible initial steps of *c*DCE degradation pathways (34) (Fig. 1.3): (i) GST-catalyzed dehalogenation of *c*DCE and (ii) monooxygenase-catalyzed expoxidation of *c*DCE. The proposed pathways of *c*DCE degradation are, however, not consistent with the other findings: (i) an *E. coli* clone expressing the GST gene catalyzed the transformation of 1-chloro-2,4-dinitrobenzene (standard substrate for GST), but did not transform *c*DCE. (ii) Cyclohexanone grown cells of strain JS666 did not show immediate *c*DCE degradation.

### 1.2.6 Hypothetical pathways of *c*DCE biodegradation by *Polaromonas* sp. strain JS666

The proteomics and transcriptomics provided some evidence of the downstream pathway of *c*DCE degradation, but the initial steps of the degradation remained to be discovered. A solid understanding of the biodegradation pathway is required before the isolate can be used in environmental remediation. Based on the possible biochemical reactions of *c*DCE and by analogy with known pathways, there are five possible reactions for the initial steps of *c*DCE biodegradation (Fig. 1.4). High levels of expression of glutathione-*S*-transferase (GST) by *c*DCE-grown cells (34) raised the question of the formation of glutathione conjugates (I) during *c*DCE biodegradation even though the GST most upregulated by *c*DCE did not directly transform *c*DCE. A reductase (II) or a hydratase (III) might channel *c*DCE into the DCA degradation pathway. Attack by a monooxygenase enzyme could produce varying amounts of an aldehyde (IV) and *c*DCE

epoxide (V) (20, 52). Chapter 2 describes experiments to test the above hypotheses to determine the initial steps of *c*DCE biodegradation and the genes that encode the enzymes involved.

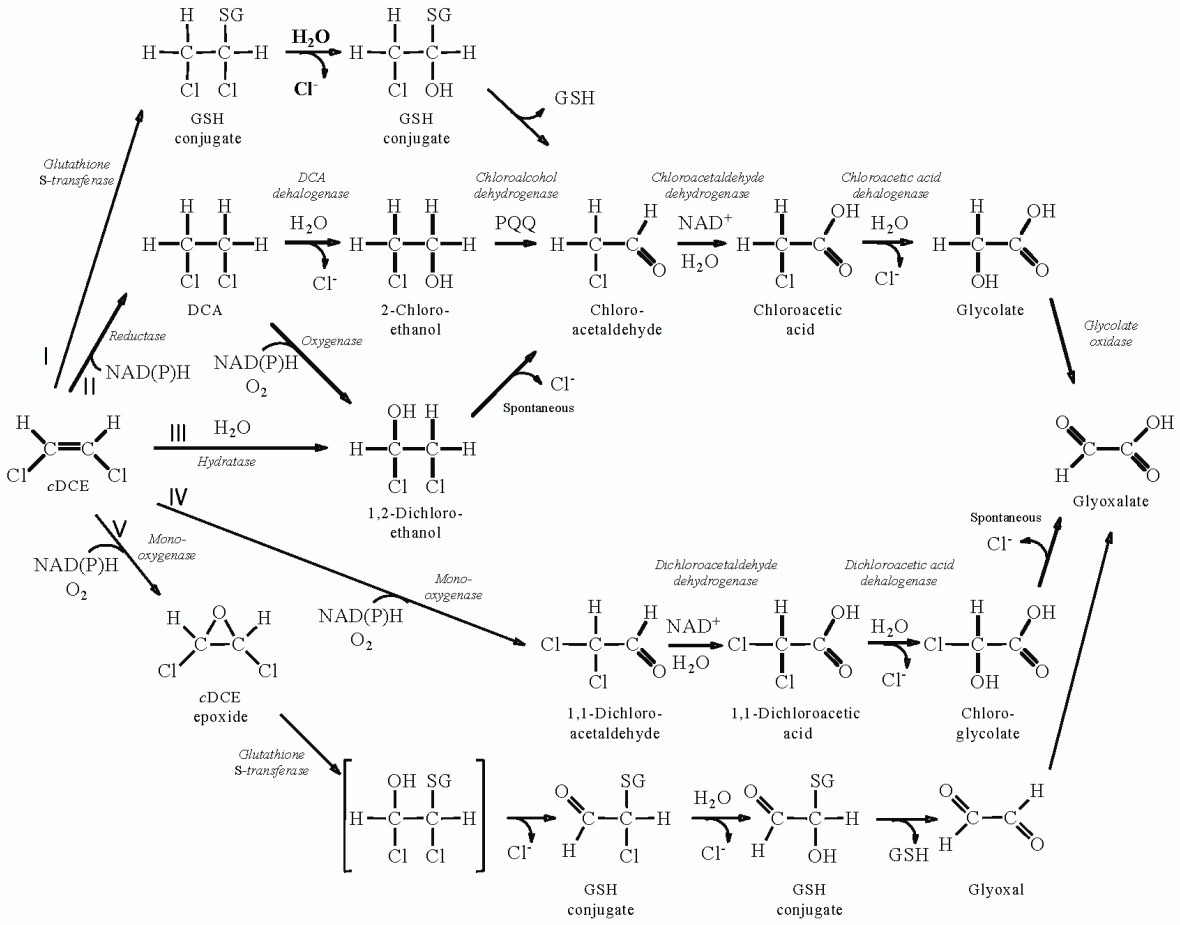


**Figure 1.4** Hypothetical pathways of *c*DCE biodegradation.

## 1.3 DIPHENYLAMINE (DPA) BIODEGRADATION

### 1.3.1 Use and occurrence of DPA

DPA has been widely used as a stabilizer for nitrocellulose-containing explosives and an antioxidant for apple scald prevention because of its ability to bind hydroxyl or nitric oxide free radicals that develop during storage (15). Reactions with the radicals result in hydroxylated and nitrated derivatives of DPA (44, 66). DPA and its derivatives are common contaminants at munitions-contaminated sites as well as in apples (39, 66). It is also used as a precursor for dyes, pesticides, pharmaceuticals, and photographic chemicals (15). The worldwide production of DPA in the 1980s was about 40,000 ton/year (15) and reported US production was 7,300 tons in the US in 2002 (73). DPA is made by the condensation of aniline and it is also formed as a byproduct during the manufacture of aniline. Operational practices associated with the production of DPA have led to substantial DPA contamination problems at many of the aniline and DPA manufacturing sites. DPA is slightly toxic to laboratory animals so that it is listed in Toxicity Category III (second lowest of four categories) (74). Ecotoxicological studies indicate that DPA and its derivatives are potentially hazardous to aquatic organisms (15, 17), but mechanisms of the toxicity are unknown. Therefore, they require remediation at contaminated sites.

DPA is also a naturally occurring compound found in onions and tea leaves (15, 38), but the synthesis and roles of DPA in the plant have not been investigated. Karawya et al (38) reported that DPA has the capability to reduce blood sugar concentration in rabbits, suggesting the potential of DPA as antihyperglycaemic agent.

### 1.3.2 Biodegradation of DPA

Little is known about the biodegradation of DPA, but there have been several reports (16, 17, 25, 63) that it is biodegraded under both aerobic and anoxic conditions. Gardner et al (25) observed the accumulation of hydroxylated DPA, indole, and aniline after aerobic incubation of activated sludge with DPA. Growth of mixed cultures on DPA was observed in DPA enrichment cultures with sediment from a DPA contaminated stream (63). Under anaerobic conditions, aniline accumulated from DPA via cometabolism by a sulfate reducing bacterium (16). The above studies, however, did not address final products, transformation mechanisms, or the organisms responsible for the biodegradation of DPA.

### 1.3.3 Biodegradation pathways of structurally similar compounds

Existing microbial metabolic diversity provides the source for evolution of catabolic pathways for synthetic chemicals (78, 79). This section describes known biochemical reactions of DPA and related compounds to provide functional insight about microbial metabolic diversity that could contribute to evolution of DPA degradation pathway.

Aromatic ring hydroxylating dioxygenases incorporate two atoms of molecular oxygen into aromatic rings (26). The dioxygenation of the aromatic ring is a prerequisite for the cleavage of the aromatic nucleus by bacterial ring-fission dioxygenases. They exhibit high diversity in substrate range (Fig. 1.5) and they are frequently involved in the

initial steps of biodegradation of aromatic hydrocarbons (77). For example, biphenyl dioxygenase catalyzes initial attack at the 2,3-position of biphenyl (24). Shindo et al.

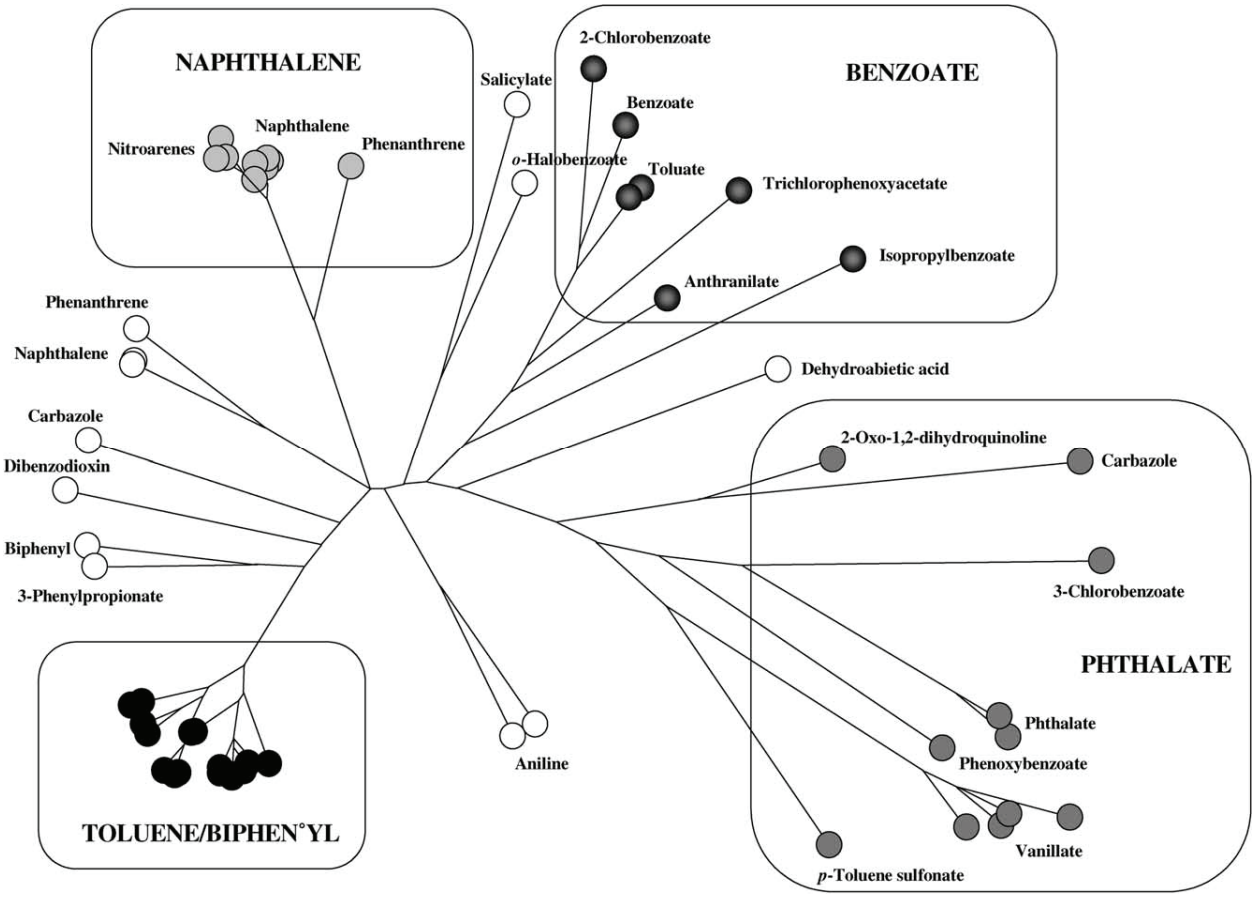


**Figure 1.5** Phylogeny of aromatic ring hydroxylating oxygenases based on sequence relatedness of the α subunits of the dioxygenase iron-sulfur protein components (77).

reported that a modified biphenyl dioxygenase transforms DPA to 2-hydroxydiphenylamine and 3-hydroxydiphenylamine (71). The authors proposed that the monohydroxylated products are generated non-enzymatically by dehydration of the 2,3-dihydrodiol as a consequence of its structural instability (Fig. 1.6). A binding model (24) suggests how biphenyl dioxygenase might acquire the ability to oxidize DPA at the 2,3-

position. Alternatively, soluble di-iron monooxygenases such as toluene and methane monooxygenases or cytochrome P450 enzymes also have the potential to hydroxylate aromatic rings (53, 69, 75), but no information is available on their capability to transform DPA.

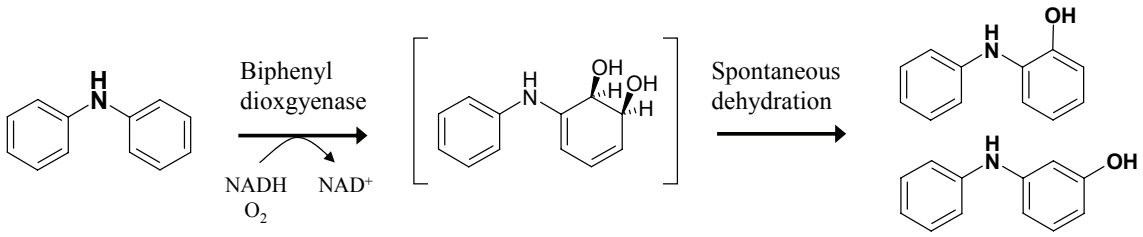


**Figure 1.6** Biotransformation of DPA by modified biphenyl dioxygenase (24, 71).

Biodegradation pathways of the structurally similar carbazole, dibenzo-*p*-dioxin, and diphenyl ether are well established (30, 70, 81) (Fig. 1.7). In all of the pathways dioxygenases catalyze the initial attack at the carbon atom that is bonded to the nitrogen or oxygen, resulting in the spontaneous cleavage of the three-ring structure or the diphenylether structure (58). The dioxygenation of carbazole and dibenzo-*p*-dioxin produces unstable hemiacetal-like intermediates that are spontaneously converted to 2′-aminobiphenyl-2,3-diol and 2,2′,3 trihydroxyldiphenyl ether (Fig. 1.7). The dihydroxylated aromatic rings of both intermediates are subject to *meta* ring cleavage and then hydrolysis, resulting in biodegradable intermediates (Fig. 1.7). Diphenyl ether is converted to phenol and catechol via dioxygenation at the 1,2 position of the aromatic

ring and spontaneous rearomatization (Fig. 1.7). Phenol and catechol are then further biodegraded by the well-established phenol degradation pathway (3).

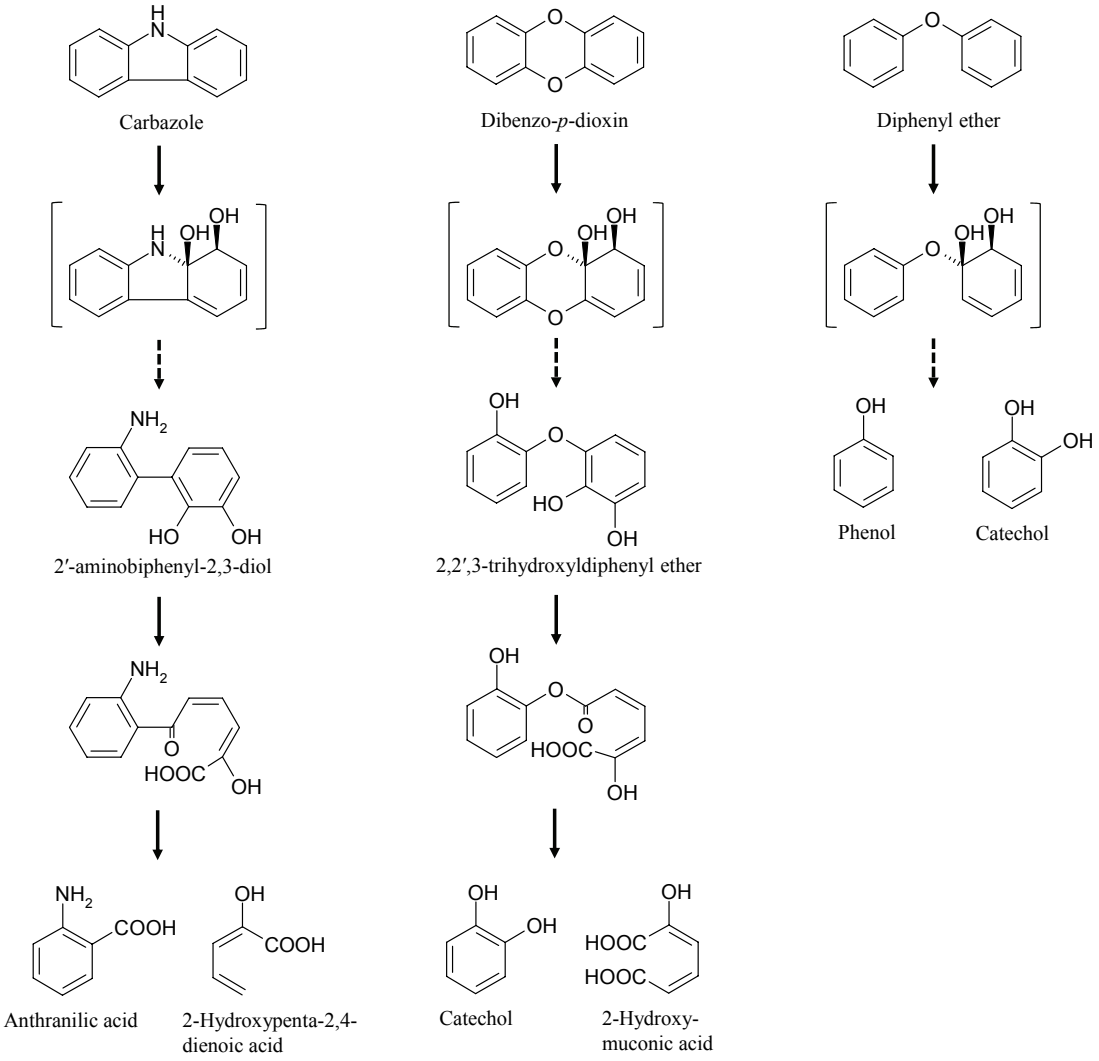


**Figure 1.7** Biodegradation pathways of carbazole, dibenzo-*p*-dioxin, and diphenyl ether (58, 60, 70, 81). The structures in brackets have not been characterized. Dashed lines indicate spontaneous reactions.

Carbazole is a naturally occurring component of coal tar. Several bacteria able to use carbazole as their growth substrate have been isolated from seawater, contaminated soil and activated sludge (31, 45, 60). Genes involved in the carbazole degradation pathway are well established (30, 32, 46). The genes are found in three separate operons: one encodes carbazole dioxygenase (CarAaAcAd), the *meta* cleavage enzyme (CarBaBb), and the hydrolase (CarC) (Fig. 1.8A). The three enzymes catalyze the conversion of carbazole to anthranilate and 2-hydroxypenta-2,4-dienoic acid (Fig. 1.7) which are also intermediates of biodegradation of tryptophan and 3-methyl catechol, respectively. Genes that encode anthranilate and 2-hydroxypenta-2,4-dienoic acid degradation are organized in two separate operons and they are widely distributed in soil bacteria.

Carbazole dioxygenases genes (*carAa*) from several carbazole degrading bacteria form a distinct clade in the family of Rieske non heme iron oxygenases (Fig. 1.5), but they varied within the clade (Fig. 1.8B). The organization of the genes that encode the dioxygenase genes is also similar, but not identical (Fig. 1.8A). The main differences are that the hydrolase (*carC*) is located between the genes that encode the oxygenase (*carAa*) and the *meta*-cleavage enzyme (*carBaBb*) in strains OC7 and IC177 and ferredoxin (*carAc*) and ferredoxin reductase (*carAd*) homologs are not found in strain OC7. The diversity in the sequences of the dioxygenases and gene organization raised questions about their possible physiological roles other than carbazole degradation. The possibility is supported by up-regulation of carbazole dioxygenase during the growth of *Lysobacter* sp. strain OC7 on naphthalene, phenanthrene, and carbazole and the broad substrate specificity of carbazole dioxygenase for aromatic hydrocarbons including naphthalene and phenanthrene (59).

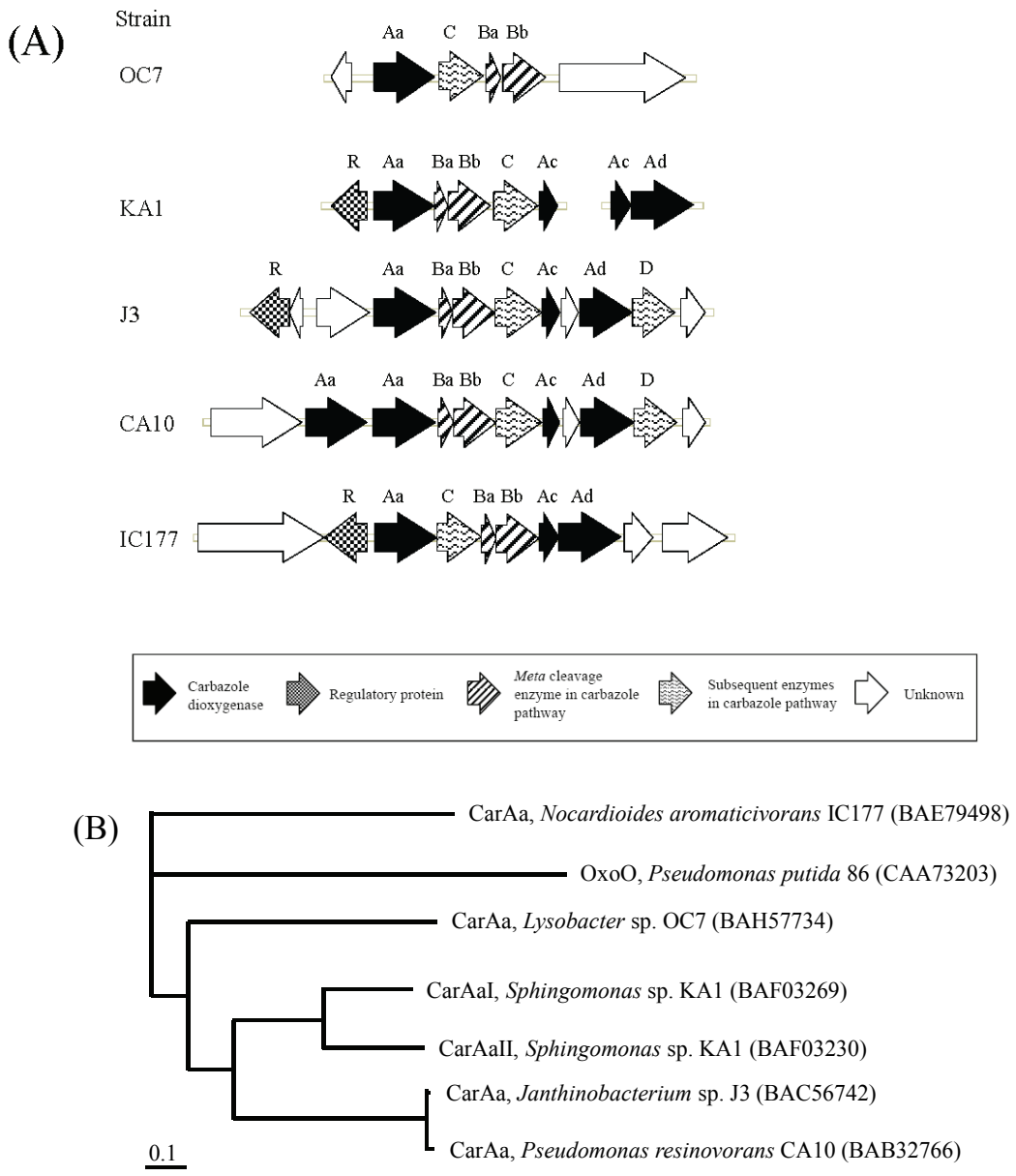


**Figure 1.8** (A) Organization of the genes that encode carbazole dioxygenases from *Lysobacter* sp. strain OC7, *Sphingomonas* sp. strain KA1, *Janthinobacterium* sp. J3, *Pseudomonas resinovorans* CA10, and *Nocardioides aromaticivorans* IC177 (30, 46). (B) Phylogenetic relationships of the terminal oxygenase component (CarAa) in carbazole dioxygenases. The scale bar denotes 0.1 amino acid substitutions per site. GenBank accession numbers are indicated after strain designations.

## 1.4 BIODEGRADATION OF NITROBENZENE AND ANILINE

The degradation mechanisms, the biochemistry, and the genes that encode the pathways are well established for both nitrobenzene and aniline (2, 56, 57) (Fig. 1.9). There are two aerobic pathways for the degradation of nitrobenzene. The most common involves the partial reduction of the nitro group to the hydroxylamine and then rearrangement to 2-aminophenol, which is mineralized (56). The final products are biomass, carbon dioxide, water and a small amount of ammonium. The alternative pathway involves an initial dioxygenase catalyzed removal of the nitro group as nitrite and the resultant catechol is mineralized (57). The process yields the same products as above except that the excess nitrogen is released as nitrite rather than ammonium.

Aniline degradation under aerobic conditions is initiated by a dioxygenase attack at the 1,2 position of the aromatic ring of aniline that leads to the formation of catechol, which is mineralized (2) (Fig. 1.9). Incorporation of both atoms of $^{18}O_2$ into aniline in *Nocardia* sp. first suggested the involvement of dioxygenase in the conversion of aniline to catechol (4). Relatively recent studies identified the genes that encode aniline dioxygenase (TdnA1A2B) in several aniline degraders (21, 23). The aniline dioxygenases form a separate clade among Rieske non heme iron oxygenases (Fig. 1.5). Association of the dioxygenase genes with an amido transferase-like gene (*tdnT*) and a glutamine synthease-like gene (*tdnQ*) is a unique feature of aniline dioxygenase. TdnQ is essential for dioxygenation of aniline (22), but its function is not known. The role of the auxiliary genes should be established to rigorously understand the mechanisms of aniline oxidation to catechol.

Under anaerobic conditions, nitrobenzene can be reduced to aniline (8, 62, 65, 72). The addition of electron donors accelerates the nitrobenzene reduction but information on the mechanism or responsible bacteria is lacking. Biodegradation of aniline under nitrate reducing and sulfate reducing conditions has been reported as well (14, 37). *Desulfobacterium anilini* Ani1, isolated from marine sediment, degrades aniline to 4-aminobenzoate via carboxylation followed by activation to 4-aminobenzoyl-CoA and reductive deamination to benzoyl-CoA, which is further metabolized. Combinations of the biological reduction of nitrobenzene and then subsequent aniline biodegradation could result in mineralization of nitrobenzene under anaerobic conditions.

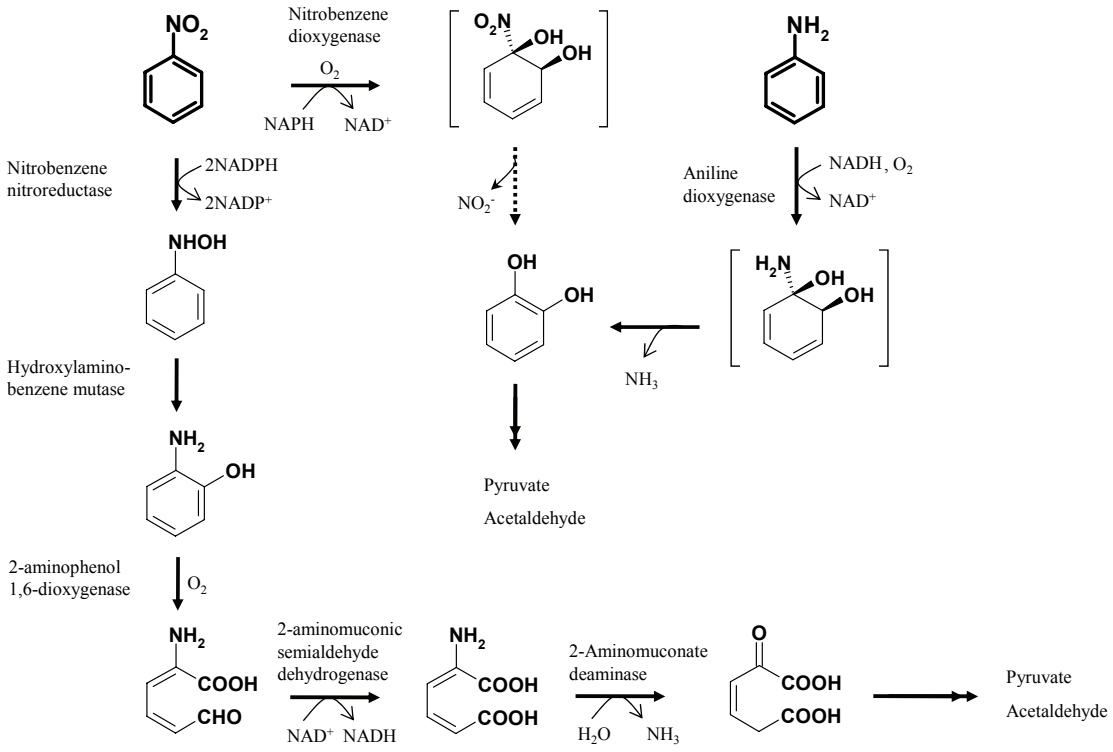


**Figure 1.9** Aerobic biodegradation pathways of nitrobenzene and aniline.

## 1.5 MONITORED NATURAL ATTENUATION AT SITES CONTAMINATED WITH NITROBENZENE, ANILINE, AND DPA

Aniline is widely used as a feedstock for a variety of dyes and other organic products. It is made by the reduction of nitrobenzene, which is often made by nitration of benzene at the manufacturing site. At many of the aniline manufacturing sites the soil and groundwater are extensively contaminated with not only nitrobenzene and aniline but also diphenylamine, a byproduct of the process. Bioremediation of the contaminated sites is potentially a cost efficient and environmentally benign approach. Prior to establish the engineered strategies for bioremediation, the potentials for natural attenuation processes should be evaluated at historically contaminated sites where the above compounds drive the risk. The primary objective of the treatability studies is to identify bottlenecks for biodegradation at sites contaminated with the above contaminants.

In some instances, it is possible to identify site-specific conditions such as temperature, pH, electron donors or acceptors, or nutrients that explain the persistence and mobility of contaminants and recommend engineered solutions to achieve remediation goals. Other cases are not as simple because of poorly understood factors influencing the biodegradation of the compounds. The most important among these factors are: 1) the degradation mechanisms and intermediates, 2) thresholds end points and final concentrations, 3) the presence and distribution of appropriate bacteria, 4) the effect of mixtures of contaminants on the processes. The following section describes the approaches to address the factors that affect the biodegradation.

As mentioned above, the degradation mechanisms and the biochemistry are well established for both nitrobenzene and aniline (2, 56, 57) (Fig. 1.9). Based on the

understanding it is relatively simple to establish appropriate conditions to isolate the bacteria responsible for the degradation. The parameters that control the degradation of nitrobenzene and aniline could be readily identified by a series of approaches such as simple microcosms with material from the contaminated sites and enumeration and isolation of bacteria responsible for the degradation. The degradation pathways can be confirmed by assay of key enzymes previously established (5, 13, 43, 61). For instance, enzyme assay for hydroxylaminobenzene mutase (13), aminophenol dioxygenase (43), and catechol dioxygenase (5, 61) can identify the degradation pathways employed by nitrobenzene degraders from contaminated sites. In contrast, the degradation mechanisms for diphenylamine and the organisms responsible are not known. The uncertainty about the degradation pathway and intermediates is a deterrent to field applications involving bioremediation of diphenylamine. Once the biodegradation mechanisms of diphenylamine and the bacteria responsible are known, the effect of mixtures of the contaminants on the biodegradation can be simply identified in pure or mixed cultures with each chemical alone and with all three chemicals in combination.

In some cases, the behavior of the contaminants is critical to evaluate the impact of biodegradation at the contaminated sites. The situation exists at two DuPont sites where a contaminated plume is intersected by a ditch. The anoxic groundwater and the sediment are extensively contaminated with nitrobenzene, aniline, and diphenylamine. The release of these compounds from contaminated sediment to the overlying water via groundwater flow increases the risk at the contaminated sites. At the same time, the transport of the contaminants provides aerobic microbial populations at the interface between sediment and water with the opportunity to degrade the contaminants. The overlying water

contains negligible concentrations of the contaminants even though there are substantial concentrations of the contaminants in the plume just before it emerges. The observation suggests the hypothesis that the sediments are anaerobic and that the lack of oxygen limits the biodegradation. As the contaminants migrate into the aerobic zone between the sediment and the overlying water there should be considerable potential for biodegradation by aerobic bacteria at the interface. Such a scenario is analogous to that in natural aquatic ecosystems where substantial populations of aerobic methane oxidizing bacteria in the sediment/water interface prevent the escape of the methane produced in underlying anoxic sediment layers (6, 12, 64). The aerobic biodegradation potential at the sediment/water interface must, therefore, be evaluated to determine whether it is sufficient to eliminate the risk to overlying water caused by the migration of the contaminants. Experiments with columns designed to simulate the field conditions and to evaluate the impact of biodegradation on the fate of the contaminants are described in Chapter 4.

## 1.6 REFERENCES


1. **Allen, J. R., D. D. Clark, J. G. Krum, and S. A. Ensign.** 1999. A role for coenzyme M (2-mercaptoethanesulfonic acid) in a bacterial pathway of aliphatic epoxide carboxylation. Proc. Natl. Acad. Sci. USA **96:**8432-8437.
2. **Aoki, K., R. Shinke, and H. Nishira.** 1983. Metabolism of aniline by *Rhodococcus erythropolis* AN-13. Agric. Biol. Chem. **47:**1611-1616.
3. **Arai, H., T. Ohishi, M. Y. Chang, and T. Kudo.** 2000. Arrangement and regulation of the genes for *meta*-pathway enzymes required for degradation of phenol in *Comamonas testosteroni* TA441. Microbiology **146** 1707-1715.
4. **Bachofer, R., F. Lingens, and W. Schafer.** 1975. Conversion of aniline into pyrocatechol by a *Nocardia* sp.: incorporation of oxygen-18. FEBS Lett. **50:**288-290.
5. **Broderick, J.** 1999. Catechol dioxygenases. Essays Biochem. **34:**173-189.
6. **Buckley, D. H., L. K. Baumgartner, and P. T. Visscher.** 2008. Vertical distribution of methane metabolism in microbial mats of the Great Sippewissett Salt Marsh. Environ. Microbiol. **10:**967-977.
7. **Canada, K. A., S. Iwashita, H. Shim, and T. K. Wood.** 2002. Directed evolution of toluene *ortho*-monooxygenase for enhanced 1-naphthol synthesis and chlorinated ethene degradation. J. Bacteriol. **184:**344-349.
8. **Cao, H.-B., Y. Li, -P, G.-F. Zhang, and Y. Zhang.** 2004. Reduction of nitrobenzene with $H_2$ using a microbial consortium. Biotech. Lett. **26:**307-310.
9. **Coleman, N. V., T. E. Mattes, J. M. Gossett, and J. C. Spain.** 2002. Biodegradation of *cis*-dichloroethene as the sole carbon source by a beta-proteobacterium. Appl. Environ. Microbiol. **68:**2726-2730.
10. **Coleman, N. V., T. E. Mattes, J. M. Gossett, and J. C. Spain.** 2002. Phylogenetic and kinetic diversity of aerobic vinyl chloride-assimilating bacteria from contaminated sites. Appl. Environ. Microbiol. **68:**6162-6171.
11. **Coleman, N. V., and J. C. Spain.** 2003. Epoxyalkane: coenzyme M transferase in the ethene and vinyl chloride biodegradation pathways of *Mycobacterium* strain JS60. J. Bacteriol. **185:**5536-5545.

12. **Costello, A. M., A. J. Auman, J. L. Macalady, K. M. Scow, and M. E. Lidstrom.** 2002. Estimation of methanotroph abundance in a freshwater lake sediment. Environ. Microbiol. **4:**443-450.

13. **Davis, J. K., G. C. Paoli, Z. He, L. J. Nadeau, C. C. Somerville, and J. C. Spain.** 2000. Sequence analysis and initial characterization of two isozymes of hydroxylaminobenzene mutase from *Pseudomonas pseudoalcaligenes* JS45. Appl. Environ. Microbiol. **66:**2965-2971.

14. **De, M. A., O. A. O'Connor, and D. S. Kosson.** 1994. Metabolism of aniline under different anaerobic electron-accepting and nutritional conditions. Environ. Toxicol. Chem. **13:**233-239.

15. **Drzyzga, O.** 2003. Diphenylamine and derivatives in the environment: a review. Chemosphere **53:**809-818.

16. **Drzyzga, O., and K. H. Blotevogel.** 1997. Microbial degradation of diphenylamine under anoxic conditions. Curr. Microbiol. **35:**343-347.

17. **Drzyzga, O., A. Schmidt, and K. Blotevogel.** 1995. Reduction of nitrated diphenylamine derivatives under anaerobic conditions. Appl. Environ. Microbiol. **61:**3282-3287.

18. **Ensign, S. A., M. R. Hyman, and D. J. Arp.** 1992. Cometabolic degradation of chlorinated alkenes by alkene monooxygenase in a propylene-grown *Xanthobacter* strain. Appl. Environ. Microbiol. **58:**3038-3046.

19. **Fennell, D. E., A. B. Carroll, J. M. Gossett, and S. H. Zinder.** 2001. Assessment of indigenous reductive dechlorinating potential at a TCE-contaminated site using microcosms, polymerase chain reaction analysis, and site data. Environ. Sci. Technol. **35:**1830-1839.

20. **Fox, B. G., J. G. Borneman, L. P. Wackett, and J. D. Lipscomb.** 1990. Haloalkene oxidation by the soluble methane monooxygenase from *Methylosinus trichosporium* OB3b: mechanistic and environmental implications. Biochemistry **29:**6419-6427.

21. **Fujii, T., M. Takeo, and Y. Maeda.** 1997. Plasmid-encoded genes specifying aniline oxidation from *Acineobacter* sp. strain YAA. Microbiology **143:**93-99.

22. **Fukumori, F., and C. P. Saint.** 1997. Nucleotide sequences and regulational analysis of genes involved in conversion of aniline to catechol in *Pseudomonas putida* UCC22(pTDN1). J. Bacteriol. **179:**399-408.

23. **Fukumori, F., and C. P. Saint.** 1997. Nucleotide sequences and regulational anlysis of genes involved in conversion of aniline to catechol in *Pseudomonas putida* UCC22(pTDN1). J. Bacteriol. **179:**399-408.

24. **Furukawa, K., H. Suenaga, and M. Goto.** 2004. Biphenyl dioxygenases: functional versatilities and directed evolution. J. Bacteriol. **186:**5189-5196.

25. **Gardner, A. M., G. H. Alvarez, and Y. Ku.** 1982. Microbial degradation of $^{14}C$-diphenylamine in a laboratory model sewage sludge system. Bull. Environ. Contam. Toxicol. **28:**91-96.

26. **Gibson, D. T., and R. E. Parales.** 2000. Aromatic hydrocarbon dioxygenases in environmental biotechnology. Curr. Opin. Biotechnol. **11:**236-243.

27. **Hage, J. C., and S. Hartmans.** 1999. Monooxygenase-mediated 1,2-dichloroethane degradation by *Pseudomonas* sp. strain DCA1. Appl. Environ. Microbiol. **65:**2466-2470.

28. **He, J., K. M. Ritalahti, K. L. Yang, S. S. Koenigsberg, and F. E. Loffler.** 2003. Detoxification of vinyl chloride to ethene coupled to growth of an anaerobic bacterium. Nature **424:**62-65.

29. **Holliger, C., D. Hahn, H. Harmsen, W. Ludwig, W. Schumacher, B. Tindall, F. Vazquez, N. Weiss, and A. J. Zehnder.** 1998. *Dehalobacter restrictus* gen. nov. and sp. nov., a strictly anaerobic bacterium that reductively dechlorinates tetra- and trichloroethene in an anaerobic respiration. Arch. Microbiol. **169:**313-321.

30. **Inoue, K., H. Habe, H. Yamane, and H. Nojiri.** 2006. Characterization of novel carbazole catabolism genes from gram-positive carbazole degrader *Nocardioides aromaticivorans* IC177. Appl. Environ. Microbiol. **72:**3321-3329.

31. **Inoue, K., H. Habe, H. Yamane, T. Omori, and H. Nojiri.** 2005. Diversity of carbazole-degrading bacteria having the *car* gene cluster: isolation of a novel gram-positive carbazole-degrading bacterium. FEMS Microbiol. Lett. **245:**145-153.

32. **Inoue, K., J. Widada, S. Nakai, T. Endoh, M. Urata, Y. Ashikawa, M. Shintani, Y. Saiki, T. Yoshida, H. Habe, T. Omori, and H. Nojiri.** 2004. Divergent structures of carbazole degradative *car* operons isolated from gram-negative bacteria. Biosci. Biotechnol. Biochem. **68:**1467-1480.

33. **Janssen, D. B., A. Scheper, L. Dijkhuizen, and B. Witholt.** 1985. Degradation of halogenated aliphatic compounds by *Xanthobacter autotrophicus* GJ10. Appl. Environ. Microbiol. **49:**673-677.

34. **Jennings, L. K., M. M. Chartrand, G. Lacrampe-Couloume, B. S. Lollar, J. C. Spain, and J. M. Gossett.** 2009. Proteomic and transcriptomic analyses reveal genes upregulated by *cis*-dichloroethene in *Polaromonas* sp. strain JS666. Appl. Environ. Microbiol. **75:**3733-3744.

35. **Johnson, G. R., R. K. Jain, and J. C. Spain.** 2002. Origins of the 2,4-dinitrotoluene pathway. J. Bacteriol. **184:**4219-4232.

36. **Johnson, G. R., and J. C. Spain.** 2003. Evolution of catabolic pathways for synthetic compounds: bacterial pathways for degradation of 2,4-dinitrotoluene and nitrobenzene. Appl. Microbiol. Biotechnol. **62:**110-123.

37. **Kahng, H.-Y., J. J. Kukor, and K.-H. Oh.** 2000. Characterization of strain HY99, a novel microorganism capable of aerobic and anaerobic degradation of aniline. FEMS Microbiol. Lett. **190:**215-221.

38. **Karawya, M. S., S. M. Abdel Wahab, M. M. El-Olemy, and N. M. Farrag.** 1984. Diphenylamine, an antihyperglycemic agent from onion and tea. J. Nat. Prod. **47:**775-780.

39. **Kim-Kang, H., R. A. Robinson, and J. Wu.** 1998. Fate of $^{14}$C-diphenylamine in stored apples. J. Agric. Food. Chem. **46:**707-717.

40. **Koziollek, P., D. Bryniok, and H. J. Knackmuss.** 1999. Ethene as an auxiliary substrate for the cooxidation of *cis*-1, 2-dichloroethene and vinyl chloride. Arch. Microbiol. **172:**240-246.

41. **Krum, J. G., and S. A. Ensign.** 2001. Evidence that a linear megaplasmid encodes enzymes of aliphatic alkene and epoxide metabolism and coenzyme M (2-mercaptoethanesulfonate) biosynthesis in *Xanthobacter* strain Py2. J. Bacteriol. **183:**2172-2177.

42. **Krum, J. G., and S. A. Ensign.** 2000. Heterologous expression of bacterial Epoxyalkane:Coenzyme M transferase and inducible coenzyme M biosynthesis in *Xanthobacter* strain Py2 and *Rhodococcus rhodochrous* B276. J. Bacteriol. **182:**2629-2634.

43. **Lendenmann, U., and J. C. Spain.** 1996. 2-aminophenol 1,6-dioxygenase: a novel aromatic ring cleavage enzyme purified from *Psedomonas pseudoalcaligenes* JS45. J. Bacteriol. **178:**6227-6232.

44. **Lussier, L. S., and H. Gagnon.** 2000. On the chemical reactions of diphenylamine and its derivatives with nitrogen dioxide at normal storage temperature. Propellants, Explosives, Pyrotechnics **25:**117-125.

45. **Maeda, R., H. Nagashima, J. Widada, K. Iwata, and T. Omori.** 2009. Novel marine carbazole-degrading bacteria. FEMS Microbiol. Lett. **292:**203-209.

46. **Maeda, R., H. Nagashima, A. B. Zulkharnain, K. Iwata, and T. Omori.** 2009. Isolation and characterization of a *car* gene cluster from the naphthalene, phenanthrene, and carbazole-degrading marine isolate *Lysobacter* sp. strain OC7. Curr. Microbiol. **59:**154-159.

47. **Mattes, T. E., A. K. Alexander, P. M. Richardson, A. C. Munk, C. S. Han, P. Stothard, and N. V. Coleman.** 2008. The genome of *Polaromonas* sp. strain JS666: insights into the evolution of a hydrocarbon- and xenobiotic-degrading bacterium, and features of relevance to biotechnology. Appl. Environ. Microbiol. **74:**6405-6416.

48. **Mattes, T. E., N. V. Coleman, A. S. Chuang, A. J. Rogers, J. C. Spain, and J. M. Gossett.** 2007. Mechanism controlling the extended lag period associated with vinyl chloride starvation in *Nocardioides* sp. strain JS614. Arch. Microbiol. **187:**217-226.

49. **Mattes, T. E., N. V. Coleman, J. C. Spain, and J. M. Gossett.** 2005. Physiological and molecular genetic analyses of vinyl chloride and ethene biodegradation in *Nocardioides* sp. strain JS614. Arch. Microbiol. **183:**95-106.

50. **Maymo-Gatell, X., Y. Chien, J. M. Gossett, and S. H. Zinder.** 1997. Isolation of a bacterium that reductively dechlorinates tetrachloroethene to ethene. Science **276:**1568-1571.

51. **Meunier, B., S. P. de Visser, and S. Shaik.** 2004. Mechanism of oxidation reactions catalyzed by cytochrome P450 enzymes. Chem. Rev. **104:**3947-3980.

52. **Miller, R. E., and F. P. Guengerich.** 1982. Oxidation of trichloroethylene by liver microsomal cytochrome P450: evidence for chlorine migration in a transition state not involving trichloroethylene oxide. Biochemistry **21:**1090-1097.

53. **Mitchell, K. H., C. E. Rogge, T. Gierahn, and B. G. Fox.** 2003. Insight into the mechanism of aromatic hydroxylation by toluene 4-monooxygenase by use of specifically deuterated toluene and *p*-xylene. Proc. Natl. Acad. Sci. USA **100:**3784-3789.

54. **Mohn, W. W., and J. M. Tiedje.** 1992. Microbial reductive dehalogenation. Microbiol. Rev. **56:**482-507.

55. **Muller, T. A., C. Werlen, J. Spain, and J. R. Van Der Meer.** 2003. Evolution of a chlorobenzene degradative pathway among bacteria in a contaminated groundwater mediated by a genomic island in *Ralstonia*. Environ. Microbiol. **5:**163-173.

56. **Nishino, S. F., and J. C. Spain.** 1993. Degradation of nitrobenzene by a *Pseudomonas pseudoalcaligenes*. Appl. Environ. Microbiol. **59:**2520-2525.

57. **Nishino, S. F., and J. C. Spain.** 1995. Oxidative pathway for the biodegradation of nitrobenzene by *Comamonas* sp. stranin JS765. Appl. Environ. Microbiol. **61:**2308-2313.

58. **Nojiri, H., H. Habe, and T. Omori.** 2001. Bacterial degradation of aromatic compounds via angular dioxygenation. J. Gen. Appl. Microbiol. **47:**279-305.

59. **Nojiri, H., J. W. Nam, M. Kosaka, K. I. Morii, T. Takemura, K. Furihata, H. Yamane, and T. Omori.** 1999. Diverse oxygenations catalyzed by carbazole 1,9a-dioxygenase from *Pseudomonas* sp. Strain CA10. J. Bacteriol. **181:**3105-3113.

60. **Ouchiyama, N., Y. Zhang, T. Omori, and T. Kodama.** 1993. Biodegradation of carbazole by *Pseudomonas* spp. CA06 and CA10. Biosci. Biotech. Biochem. **57:**455-460.

61. **Parales, R. E., T. A. Ontl, and D. T. Gibson.** 1997. Cloning and sequence analysis of a catechol 2,3-dioxygenase gene from the nitrobenzene-degradaing strain Comamonas sp. JS765. J. Ind. Microbio. Biotechnol. **19:**385-391.

62. **Peres, C. M., H. Naveau, and S. N. Agathos.** 1998. Biodegradation of nitrobenzene by its simultaneous reduction into aniline and mineralization of the aniline formed. Appl. Microbiol. Biotechnol. **49:**343-349.

63. **Perkins, R. E., C. M. Swindoll, and M. A. Troy.** 1997. Bioremediation evaluation of nitroaromatic and aromatic amine contaminated sediment, p. 399-403. *In* B. C. Alleman and A. Leeson (ed.), In situ and on-site bioremediation: papers from the Fourth International In Situ and On-Site Bioremediation Symposium, vol. vol. 5. . Battelle Press, Columbus, OH.

64. **Rahalkar, M., J. Deutzmann, B. Schink, and I. Bussmann.** 2009. Abundance and activity of methanotrophic bacteria in littoral and profundal sediments of lake constance (Germany). Appl. Environ. Microbiol. **75:**119-126.

65. **Razo-Flores, E., G. Lettinga, and J. A. Field.** 1999. Biotransformation and biodegradation of selected nitroaromatics under anaerobic conditions. Biotechnol. Prog. **1999:**358-365.

66. **Rudell, D. R., J. P. Mattheis, and J. K. Fellman.** 2005. Evaluation of diphenylamine derivatives in apple peel using gradient reversed-phase liquid chromatography with ultraviolet-visible absorption and atmospheric pressure chemical ionization mass selective detection. J. Chromatogr. A **1081:**202-209.

67. **Rui, L., L. Cao, W. Chen, K. F. Reardon, and T. K. Wood.** 2004. Active site engineering of the epoxide hydrolase from *Agrobacterium radiobacter* AD1 to enhance aerobic mineralization of *cis*-1,2-dichloroethylene in cells expressing an evolved toluene *ortho*-monooxygenase. J. Biol. Chem. **279:**46810-46817.

68. **Rui, L., Y. M. Kwon, K. F. Reardon, and T. K. Wood.** 2004. Metabolic pathway engineering to enhance aerobic degradation of chlorinated ethenes and to reduce their toxicity by cloning a novel glutathione S-transferase, an evolved toluene *o*-monooxygenase, and gamma-glutamylcysteine synthetase. Environ. Microbiol. **6:**491-500.

69. **Sarabia, S. F., B. T. Zhu, T. Kurosawa, M. Tohma, and J. G. Liehr.** 1997. Mechanism of cytochrome P450-catalyzed aromatic hydroxylation of estrogens. Chem. Res. Toxicol. **10:**767-771.

70. **Schmidt, S., R. M. Wittich, D. Erdmann, H. Wilkes, W. Francke, and P. Fortnagel.** 1992. Biodegradation of diphenyl ether and its monohalogenated derivatives by *Sphingomonas* sp. strain SS3. Appl. Environ. Microbiol. **58:**2744-2750.

71. **Shindo, K., R. Nakamura, I. Chinda, Y. Ohnishi, S. Horinouchi, H. Takahashi, K. Iguchi, S. Harayama, K. Furukawa, and N. Misawa.** 2003. Hydroxylation of ionized aromatics including carboxylic acid or amine using recombinant *Streptomyces lividans* cells expressing modified biphenyl dioxygenase genes. Tetrahedron **59:**1895-1900.

72. **Swindoll, C. M., R. E. Perkins, J. T. Gannon, M. Holmes, and G. A. Fisher.** 1993. Assessment of bioremediation of a contaminated wetland, p. 163-169. *In* R. E. Hinchee, J. T. Wilson, and D. C. Downey (ed.), Intrinsic Bioremediation. Battelle Press, Columbus.

73. **USEPA.** 2002. EPA office of compliance sector notebook project: Profile of the Organic Chemical Industry 2nd Edition http://www.epa.gov/compliance/resources/publications/assistance/sectors/notebooks/organic.pdf.

74. **USEPA.** 1998. Reregistration eligibility decision: Diphenylamine http://www.epa.gov/oppsrrd1/REDs/2210red.pdf.

75. **Valentine, A. M., S. S. Stahl, and S. J. Lippard.** 1999. Mechanistic studies of the reaction of reduced methane monooxygenase hydroxylase with dioxygen and substrates. J. Am. Chem. Soc. **121:**3876-3887.

76. **Vogel, T. M., C. S. Criddle, and P. L. McCarty.** 1987. Transformations of halogenated aliphatic compounds. Environ. Sci. Technol. **21:**722-736.

77. **Wackett, L. P.** 2002. Mechanism and applications of Rieske non-heme iron dioxygenases. Enzym. Microb. Tech. **31:**577-587.

78. **Wackett, L. P.** 2007. Pathways to discovering new microbial metabolism for functional genomics and biotechnology. Adv. Appl. Microbiol. **61:**219-232.

79. **Wackett, L. P.** 2009. Questioning our perceptions about evolution of biodegradative enzymes. Curr. Opin. Microbiol. **12:**244-251.

80. **Wackett, L. P., M. J. Sadowsky, L. M. Newman, H. G. Hur, and S. Li.** 1994. Metabolism of polyhalogenated compounds by a genetically engineered bacterium. Nature **368:**627-629.

81. **Wittich, R. M., H. Wilkes, V. Sinnwell, W. Francke, and P. Fortnagel.** 1992. Metabolism of dibenzo-*p*-dioxin by *Sphingomonas* sp. strain RW1. Appl. Environ. Microbiol. **58:**1005-1010.

# CHAPTER 2

# Initial Steps of *cis*-Dichloroethene Biodegradation by *Polaromonas* sp. JS666

## 2.1 ABSTRACT

*Polaromonas* sp. strain JS666 is the only bacterium known to grow on *cis*-dichloroethene (*c*DCE) as the sole carbon and energy source under aerobic conditions. Whole genome expression microarrays and protein expression analysis have been conducted during the growth of JS666 on *c*DCE (Jennings et al 2009 Appl. Environ. Microbiol. 75:3733-3744), but the pathway for *c*DCE biodegradation and the enzymes involved are unknown. In this study, we established the initial reaction in *c*DCE degradation by using heterologous gene expression, inhibition studies, enzyme assays, and analysis of intermediates. The requirement of oxygen for *c*DCE degradation and inhibition of *c*DCE degradation by cytochrome P450 specific inhibitors suggested that cytochrome P450 monooxygenase catalyzes the initial steps of *c*DCE degradation. The finding was supported by the observation that an *E. coli* recombinant expressing cytochrome P450 monooxygenase catalyzes the transformation of *c*DCE to dichloroacetaldehyde and small amounts of the epoxide. Both the transient accumulation of dichloroacetaldehyde in cDCE degrading cultures and dichloroacetaldehyde dehydrogenase activities in cell extracts of JS666 further support a pathway involving the degradation of *c*DCE through dichloroacetaldehyde. Molecular phylogeny of the cytochrome P450 gene and organization of neighboring genes suggest that the *c*DCE

degradation pathway evolved in a progenitor capable of degrading dichloroacetaldehyde by the recruitment of the cytochrome P450 monooxygenase gene from alkane assimilating bacteria.

## 2.2 INTRODUCTION

Chlorinated ethenes such as perchloroethene and trichloroethene have been widely used as de-greasing agents and solvents, resulting in soil and groundwater contamination throughout the world (48). Reductive dechlorination by anaerobic bacteria is a major route to detoxify the chlorinated solvents by converting them to ethene (18, 19, 31). Incomplete reduction, however, frequently increases the risk by accumulating the suspected carcinogens *cis*-dichloroethene (*c*DCE) and vinyl chloride (VC) in the field (13, 35). Once the toxic intermediates migrate into aerobic zones reductive dehalogenation ceases.

Bacteria able to use VC as their growth substrates under aerobic conditions are widely distributed in the environment (9). The VC-assimilation occurs via monooxygenase-catalyzed epoxidation of VC and the subsequent reaction catalyzed by epoxyalkane coenzyme M transferase followed by spontaneous chloride elimination, which produces 2-hydroxyethyl-CoM, an intermediate in ethene assimilation pathway (2, 10). The degradation mechanism, the biochemistry, and the genes that encode the pathway are analogous to those for aerobic ethene-assimilation which suggests adaptation of ethene-assimilating bacteria to VC (10, 26, 30). In contrast, *Polaromonas* sp. strain JS666 is the only isolate able to grow on *c*DCE as the sole carbon and energy source under aerobic conditions. The pathway for *c*DCE biodegradation and the enzymes

involved are unknown.

Coleman et al (8) suggested an epoxidation reaction as the first step in *c*DCE degradation based on the induction of monooxygenase activities for ethene during the growth of strain JS666 on *c*DCE. The epoxidation of chlorinated ethenes by oxygenases is a widespread mechanism in bacteria (12, 15, 25, 49), but it is cometabolism and accumulates a toxic and highly reactive epoxide intermediate except in the case of VC biodegradation (10). Rui et al (38, 39) exploited the epoxide formation in conjunction with toluene monooxygenase and epoxide hydrolase or glutathione S-transferase to construct engineered pathways in *E. coli* for transformation of *c*DCE to glyoxal. Although the engineered strains could not grow on *c*DCE the results suggested that the engineered pathway could be feasible. In some cases, trace amounts of chloroacetaldehyde side product result from intramolecular chloride migration during the oxidation of the chlorinated ethenes by methane monooxygenase (15). In mammalian systems, cytochrome P450 enzymes catalyze the initial enzymatic attack on chlorinated ethenes, similar to some reactions observed in bacterial systems. Non-concerted reactions of cytochrome P450s from rat liver microsomes oxidize TCE to TCE epoxide and 1,1,1-trichloroacetaldehyde (chloral), but the mechanisms controlling the partitioning to the two different intermediates are not fully understood (33, 34).

The genome of *Polaromonas* sp. strain JS666 has been sequenced by the US Department of Energy Joint Genome Institute (DOE JGI) (29). Whole genome expression microarrays and protein expression analysis have been conducted during the growth of JS666 on *c*DCE (23), but the initial steps in *c*DCE biodegradation were not evident. A number of putative genes related to metabolism of xenobiotic compounds are located on

the circular chromosome (5.2 Mb) and two large plasmids (338 and 360 kb) but the genes that encode the *c*DCE degradation pathway are not apparent.

Putative genes for 1,2-dichloroethane (DCA) degradation are annotated in JS666 even though they do not form a recognizable operon and JS666 was reported not to grow on DCA (29). Proteomics and transcriptomics suggest a downstream pathway of *c*DCE degradation via (di)chloroacetaldehyde, (di)chloroacetic acid, and (chloro)glycolate similar to a pathway in bacteria able to grow on 1,2-dichloroethane (DCA) (16, 22). The above observations suggested the possibility of *c*DCE degradation via part of the DCA pathway.

Here, we describe the initial steps of *c*DCE biodegradation and genes that encode the enzymes involved. The understanding of the *c*DCE degradation pathway will provide the basis to predict and enhance *c*DCE degradation at contaminated sites as well as increase our understanding of bacterial evolution of catabolic pathways for synthetic chemicals.

## 2.3 MATERIALS AND METHODS

### 2.3.1 Growth conditions

*Polaromonas* sp. JS666 was routinely grown with *c*DCE as the sole carbon and energy source in a 4-L bioreactor. Minimal salt medium (MSB) (42) was modified as follows: the phosphate buffer concentration was 10 mM; all other nutrients were supplied at half-strength. *c*DCE was supplied continuously by a syringe pump. Portions of the culture (1-2 L) were harvested by centrifugation, and suspended in the same mineral medium for use in experiments. Fresh minimal medium was added to the bioreactor to maintain the volume. Trypticase soy at one-quarter strength (1/4-TSA) solidified with 15

g agar/L was used as a purity check. Strain JS666 was also grown in mineral medium with cyclohexanone (5 mM), glycolate (10 mM), succinate (10 mM), or DCA (0.25 mM) as carbon sources in 160 mL serum bottles. Inocula were prepared from single colonies grown on agar plates containing cyclohexanone (5 mM) or cells actively growing on *c*DCE.

### 2.3.2 Substrate transformation by whole cells

Cells were suspended to an appropriate density in the mineral medium in 160 mL serum bottles sealed with teflon-coated butyl rubber stoppers. Reactions were initiated by the addition of substrates and cultures were incubated at 25 °C with shaking (150 rpm). Substrate disappearance and/or product formation was monitored by GC.

### 2.3.3 Respirometry

Cells grown on various substrates were harvested by centrifugation, washed with potassium phosphate buffer (pH 7.2; 20 mM), and suspended in the same buffer. Oxygen uptake was measured polargraphically at 25 °C with a Clark-type oxygen electrode connected to YSI Model 5300 Biological Oxygen Monitor.

### 2.3.4 Cloning and expression of putative cytochrome P450 monooxygenase

Genomic DNA was extracted with a Genomic DNA purification system (Promega, Madison, WI). A 3.5 kb fragment containing genes encoding the putative cytochrome P450, ferredoxin reductase, and ferredoxin (BPro5299-5301) was amplified by PCR using 017F (CACCACGCTGCACCGT G TTATGTTT CAC) and 017R

(TCAGTGCTGGCCGA GCGGCG) primers. The PCR reaction mixture (20 μL) contained genomic DNA (50 ng), primers (0.25 μM each), dNTPs (0.4 mM each), and Promega GoTaq Hot Start polymerase (2U) and 1X buffer (Madison, WI). Amplifications (30 cycles) were carried out as follows: 95°C for 1 min, 56 °C for 30 s, and 72°C for 1 min, after initial denaturation at 95°C for 10 min. The PCR products were treated with Klenow Fragment of DNA Polymerase I (New England Biolabs, MA), then cloned into the pET101/D-TOPO vector (Novagen, Gibbstown, NJ). The resulting plasmid was designated pJS593. pJS593 was transformed into *E. coli* BL21 Star (DE3) for expression. *E. coli* BL21 pJS593 was grown in 30 ml of TB media containing Overnight Express Autoinduction Systems I (Novagen) at 37 °C. When the $OD_{600}$ reached 0.8~0.9, the temperature was reduced to 25 °C and the cultures were incubated an additional 14.5 h. Cells were harvested by centrifugation, washed twice with phosphate buffer (20 mM, pH 7.5) and stored on ice until used.

**2.3.5 Enzyme assays**

Cell extracts were prepared by passing cells twice through a French pressure cell at 20,000 $lb/in^2$ and centrifugation at 160,000 ×g to remove intact cells and cell debris. Cytochrome P450 monooxygenase was assayed by monitoring substrate disappearance and/or product formation by GC/electron capture detector (ECD). Reaction mixtures (1 mL) consisted of cell extracts (1 – 4 mg protein) and substrates (80 – 160 nmol) in phosphate buffer (50 mM, pH 7.2) in 4 mL bottles sealed with Teflon-coated butyl rubber stoppers. Reactions were started by addition of NADH or NADPH (2.5 mM) and the bottles were incubated at 25°C. At appropriate intervals, the reactions were stopped by

the addition of $ZnSO_4$ (30 mM) and the mixtures were extracted with ethyl ether. Dichloroacetaldehyde dehydrogenase (45) was measured by following the reduction of NAD to NADH at 365 nm in the presence of substrates, cell extract (0.5 – 1 mg protein), and NAD (1 mM). Chloroacetate dehalogenase (22) was measured by chloride release in the presence of substrates and cell extract (0.5 – 1 mg protein).

### 2.3.6 Analytical methods

*c*DCE and DCA were monitored by GC using an Agilent 6890N GC equipped with a flame ionization detector (FID) and a Supelco 60/80 Carbopack B column (6 feet by 1/8 inched). The method (7) was used with the following modification. The oven temperature was ramped at 20 °C/min from 100 °C to 150 °C, then at 10 °C/min to a maximum of 175 °C and held until all compounds eluted. *c*DCE epoxide, dichloroacetaldehyde, and chloroacetaldehyde were analyzed with an HP6890 GC equipped with either an electron capture detector (ECD) or a 5973 mass detector. Compounds were separated on a DB-5MS column (30 m × 0.25 mm, 0.25 μm film thickness; J&W scientific, CA) (27). The oven temperature was initially held at 35 °C for 10 min, ramped at 20 °C/min to 175 °C, and held at the final temperature for 3 min. Headspace samples (50 μL) were analyzed directly. Aqueous samples were spiked with TCE as an internal standard, mixed with equal volumes of ethyl ether and shaken for 10 min. The phases were separated by centrifugation and the ether extracts were analyzed by GC/ECD or GC/MS. Protein was measured with a Pierce Bicinchonninic acid protein assay kit (Rockford, IL). Chloride was measured by the method of Bergmann (3).

### 2.3.7 Chemicals

*cis*-1,2-Dichloroethene (*c*DCE) (97%) was obtained from Sigma-Aldrich. All other chemicals were reagent grade. Dichloroacetaldehyde hydrate was converted to dichloroacetaldehyde by heating at 90 °C for 30 min then cooling on ice. *c*DCE epoxide was synthesized chemically (47) and biologically (15) by transformation of *c*DCE by *E. coli* BL21 pJS593 expressing cytochrome P450 monooxygenase. Products produced by both methods had the same GC retention times and parent masses [$M^+$] at *m/z* 112, 114, and 116 which corresponds to those of *c*DCE epoxide (21). Concentrations of *c*DCE epoxide were estimated by measuring $A_{530}$ in extracts after derivatization with 4-(*p*-nitrobenzyl)pyridine (15, 17, 34).

## 2.4 RESULTS

### 2.4.1 Hypothetical initial steps of *c*DCE degradation

Based on the findings from related studies (8, 23, 29), the potential biochemical reactions of *c*DCE, and analogy with known pathways, we investigated five possible reactions for the initial steps of *c*DCE biodegradation (Fig. 2.1). I) A reductase or II) hydratase might channel *c*DCE into the DCA degradation pathway (16, 22). III) High levels of expression of glutathione-*S*-transferase (GST) by *c*DCE-grown cells (23) raised the possibility of the formation of glutathione conjugates during *c*DCE biodegradation. Attack by a monooxygenase enzyme could produce IV) varying amounts of an aldehyde and V) *c*DCE epoxide (15, 34).

### 2.4.2 Stimulation of oxygen uptake by potential intermediates of *c*DCE degradation

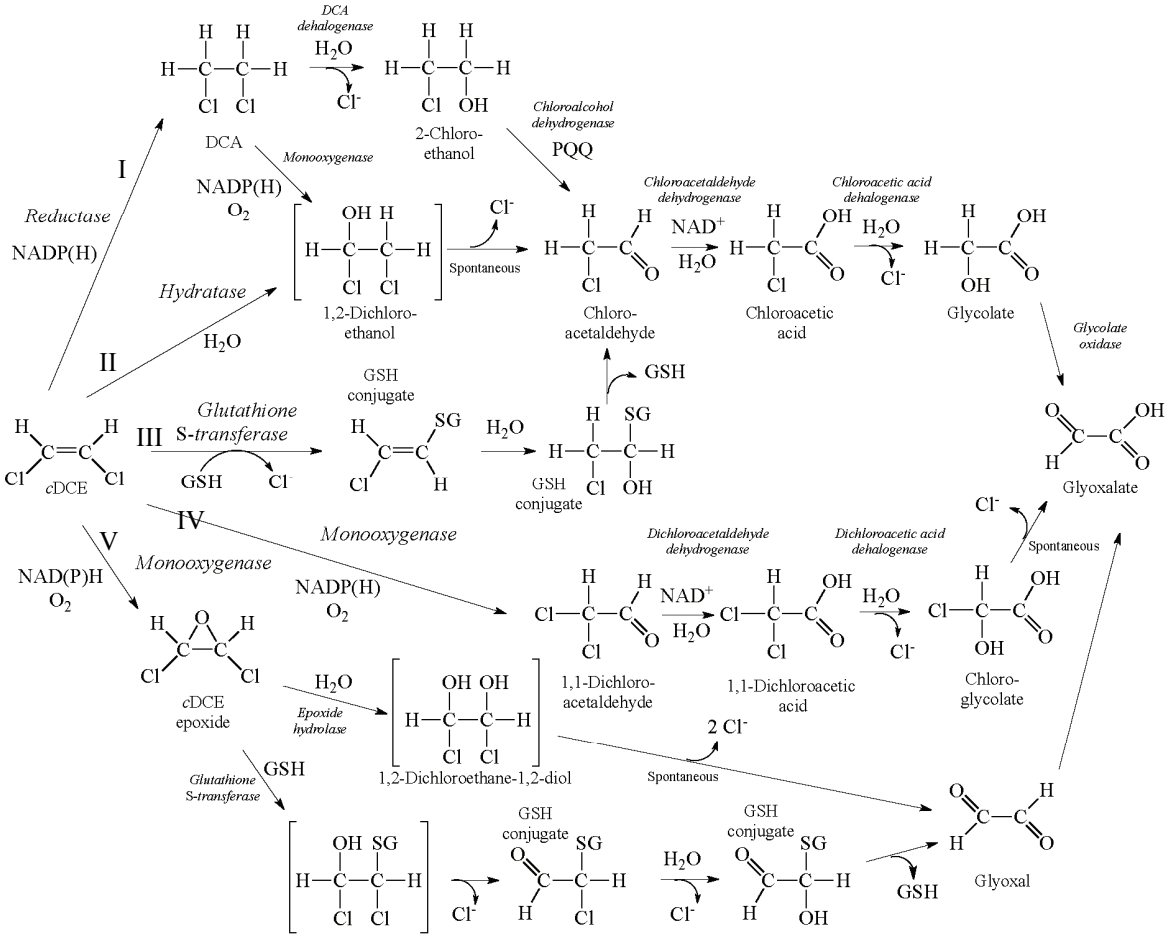


**Figure 2.1** Hypothetical pathways of *c*DCE biodegradation.

*c*DCE, DCA, and the intermediates of the DCA degradation pathway stimulated high oxygen uptake rates by *c*DCE grown cells of JS666 (Table 2.1). The induction of enzymes involved in DCA biodegradation in *c*DCE grown cells of JS666 suggests that *c*DCE is degraded via DCA or its degradation intermediates. Alternatively, cyclohexanone monooxygenase or cytochrome P450 monooxygenase induced by *c*DCE (23) could transform DCA into chloroacetaldehyde as is the case during oxidative DCA degradation (16). Chloroacetaldehyde would be further degraded by an enzyme that is constitutive and moderately upregulated during growth on *c*DCE, DCA, or cyclohexanone (Table 2.1). Lack of detectable oxygen uptake with DCA and *c*DCE by cyclohexanone grown cells seems to argue against the involvement of cyclohexanone monooxygenase in the transformation of both compounds in JS666.

### 2.4.3 Involvement of oxygen in the initial steps of *c*DCE biodegradation

In preliminary experiments the oxygen requirement for the initial step in *c*DCE degradation by JS666 was tested with *c*DCE grown cells (Fig. 2.2). Aerobic cultures rapidly degraded *c*DCE, but no degradation was observed without oxygen. The observation is not consistent with the hypothetical initial steps catalyzed by reductase or hydratase enzymes leading to the conversion of *c*DCE to DCA. The results, taken with the immediate resumption of *c*DCE degradation upon addition of air (Fig. 2.2) suggest that an oxygenase enzyme catalyzes the initial steps in *c*DCE degradation.

### 2.4.4 Metyrapone and phenylhydrazine inhibition of *c*DCE biodegradation

Cytochrome P450 enzymes catalyze a wide variety of oxygenation reactions

**Table 2.1** Oxygen uptake (nmol $O_2 \cdot min^{-1} \cdot mg\ protein^{-1}$) by resting cells of JS666 grown with various substrates.

| Test Substrate (Conc, mM) | Growth Substrate | | | | |
|---|---|---|---|---|---|
| | *c*DCE | DCA | Cyclohexanone | Glycolate | Succinate |
| *c*DCE (1) | 13 ± 0 | 6 ± 2 | < 1 | < 1 | < 1 |
| 1,2-DCA (1) | 11 ± 0 | 23 ± 6 | < 1 | < 1 | < 1 |
| 2-Chloroethanol (1) | 7 ± 2 | 13 ± 0 | < 1 | < 1 | < 1 |
| Chloroacetaldehyde (0.5) | 55 ± 1 | 47 ± 0 | 81 ± 6 | 39 ± 2 | 27 ± 5 |
| Dichloroacetaldehyde hydrate (0.5) | 18 ± 2 | 12 ± 0 | 6 ± 4 | 7 ± 1 | 3 ± 0 |
| Cyclohexanone (0.5) | 10 ± 1 | 1 ± 2 | 276 ± 36 | < 1 | < 1 |
| Ethanol (1) | 15 ± 1 | 10 ± 3 | < 1 | < 1 | 4 ± 1 |
| Chloroacetate (1) | 2 ± 0 | 26 ± 8 | < 1 | 7 ± 2 | 2 ± 1 |
| Dichloroacetate (1) | *- | 10 ± 3 | - | - | - |
| Glycolate (1) | 7 ± 2 | 14 ± 2 | < 1 | 95 ± 1 | 6 ± 2 |
| Acetate (1) | - | 8 ± 0 | 29 ± 3 | - | - |
| Succinate (1) | - | 7 ± 1 | 32 ± 1 | - | 41 ± 1 |

Reaction mixtures contained substrate, cells (0.29 – 0.31 mg of protein), and air-saturated phosphate buffer (20 mM, pH 7.2) to a final volume of 1.85 ml. *c*DCE, 1,2-DCA, and cyclohexanone were added from a 1.0 M stock in acetone and the other substrates were dissolved in water. Acetone did not interfere with the rates of oxygen uptake. Data represent means and variability from at least two measurements.

*Not determined

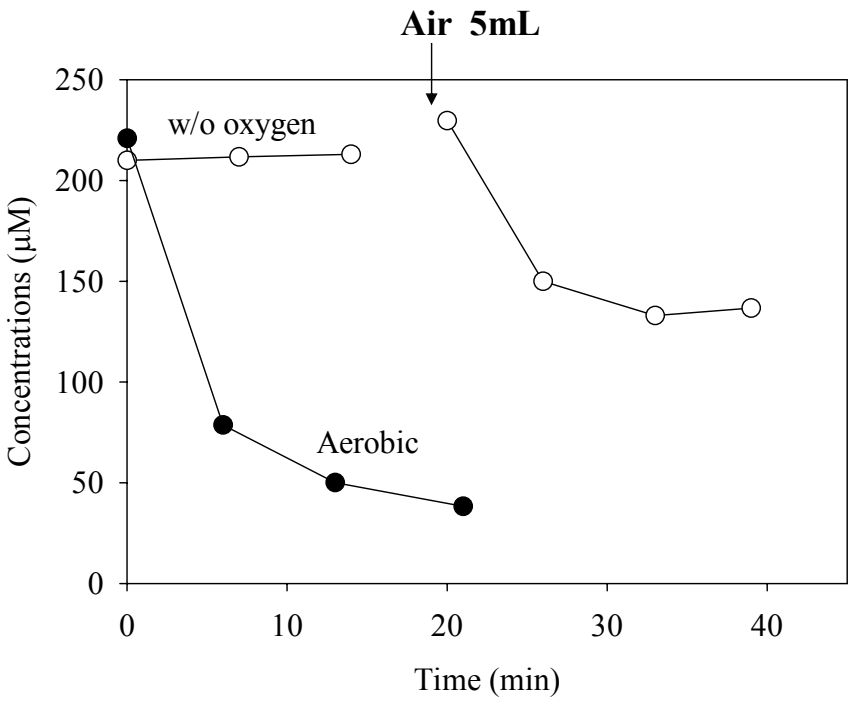


**Figure 2.2** Biodegradation of *c*DCE with (●) and without oxygen (○). *c*DCE-grown cells (30 mL, OD 6.5) were sealed in 35 mL serum bottles. Oxygen in the headsapce was removed by sparging with $N_2$. After 5 min incubation, oxygen in the liquid was depleted due to respiration. Reactions were initiated by adding *c*DCE to yield a final concentration of 210 μM in the aqueous phase. The aerobic control was prepared without sparging.

including the epoxidation of double bonds and the hydroxylation of alkanes. The enzymes are inhibited by metyrapone and phenylhydrazine (37, 50). The inhibitors also prevent cytochrome P450 mediated reactions in intact cells (4, 40). Both *c*DCE and DCA degradation were inhibited over 90% in intact cells of JS666 by 200 μM metyrapone or phenylhydrazine as measured by stimulation of oxygen uptake. The oxygen uptake rates with chloroacetaldehyde and cyclohexanone were unchanged. The degree of inhibition of the initial rates of *c*DCE and DCA degradation were proportional to the concentrations of metyrapone (Fig. 2.3). The same results were obtained when the experiment was replicated with cells grown on DCA (data not shown). The results indicate that a cytochrome P450 catalyzes early steps in *c*DCE and DCA biodegradation in JS666.

### 2.4.5 Cloning and expression of cytochrome P450 monooxygenase

Four genes annotated as cytochrome P450 are in the genome of JS666. Bpro5301, which was upregulated 3.5 fold by growth on *c*DCE (23), showed 76% amino acid identity to alkane hydroxylase (CYP153A6) from *Mycobacterium* sp. HXN-1500 (44). The gene was on one of the large plasmids of JS666 and adjacent to the genes similar to the ones that encode ferredoxin reductase (Bpro5300) and ferredoxin (Bpro5299). The three components were cloned together into *E. coli* and the expression of each component was confirmed by SDS-PAGE (data not shown). The *E. coli* recombinant expressing cytochrome P450 monooxygenase catalyzed the transformation of DCA and *c*DCE at 4.1 and 2.3 nmol/min, respectively**.** No transformation was observed in the absence of oxygen, but transformation was immediate upon the addition of oxygen (data not shown). *E. coli* containing the vector alone did not catalyze transformation of *c*DCE. The results

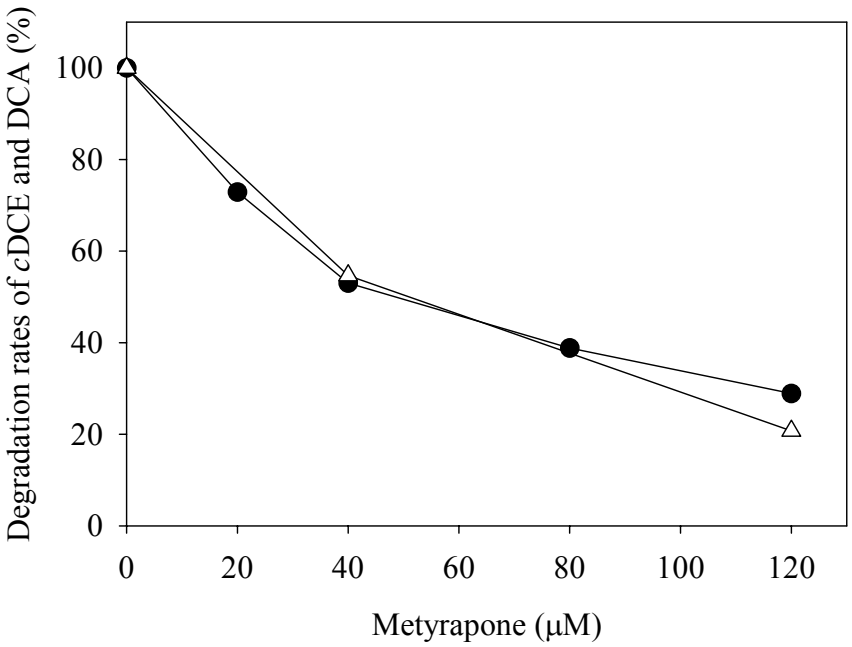


**Figure 2.3** Metyrapone inhibition of *c*DCE and DCA degradation.
*c*DCE (●) ($OD_{600}$ = 0.7, 100 μM *c*DCE), DCA (Δ) ($OD_{600}$ = 0.9, 100 μM DCA)

support the hypothesis that the cytochrome P450 monooxygenase catalyzes the initial steps of *c*DCE biodegradation in JS666.

### 2.4.6 Products of the transformation of *c*DCE by cytochrome P450 monooxygenase

Dichloroacetaldehyde (60%) and *c*DCE epoxide (5%) were produced during *c*DCE transformation by dialyzed extracts prepared from cells of the *E. coli* recombinant expressing cytochrome P450 monooxygenase only when NADH or NADPH was present in the reaction mixture (Fig. 2.4). Both products were stable under the reaction conditions. When DCA was the substrate, chloroacetaldehyde was produced in the presence of NADH. The results indicate that the cytochrome P450 monooxygenase catalyzes the transformation of both *c*DCE and DCA to chloroacetaldehydes which can be further degraded in JS666.

### 2.4.7 *c*DCE degradation kinetics

Coleman et al (8) reported the growth of JS666 on *c*DCE with stoichiometric accumulation of chloride. Chloride release was slightly delayed during the early stages of growth of JS666, which suggested a transient accumulation of degradation intermediates. During *c*DCE degradation by JS666 in the present study, dichloroacetaldehyde transiently accumulated and then disappeared (Fig. 2.5), which suggested strongly that dichloroacetaldehyde is an intermediate of *c*DCE degradation. Small amounts of *c*DCE epoxide also accumulated in the *c*DCE degrading cultures. The detection of dichloroacetaldehyde and *c*DCE epoxide in *c*DCE degrading cultures is consistent with

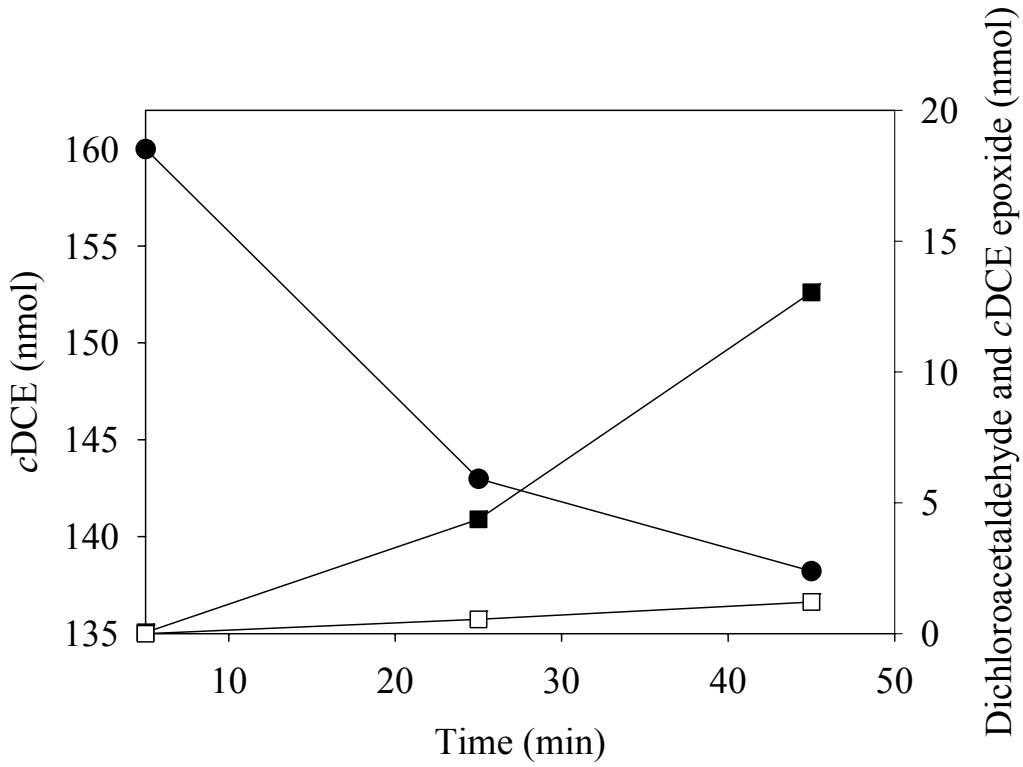


**Figure 2.4** Biotransformation of *c*DCE in cell extracts of an *E. coli* BL21 pJS593 expressing cytochrome P450 monooxygenase. *c*DCE (●), dichloroacetaldehyde (■), and *c*DCE epoxide (□)

5 min was allowed for equilibration of cDCE in reaction bottles and then reactions were initiated by adding NADH. There was no detectable *c*DCE degradation without NADH.

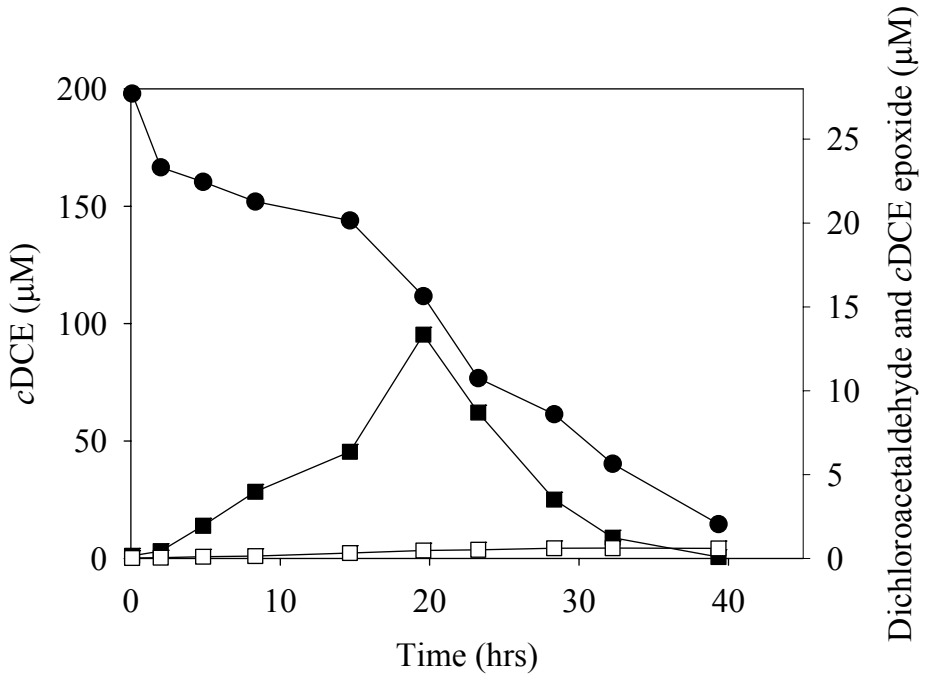


**Figure 2.5** *c*DCE degradation kinetics during the growth of JS666. *c*DCE (●), dichloroacetaldehyde (■), and *c*DCE epoxide (□)

the involvement of the cytochrome P450 monooxygenase in the initial steps of *c*DCE degradation in JS666.

When all of the added *c*DCE was degraded, the rates of *c*DCE epoxide disappearance in the cultures were similar to those of cell free culture fluids prepared by filtration. The decomposition rate was similar to the reported 72 hr half life of the compound in liquid medium (21). When *c*DCE was added sequentially to a total of 5.2 mM over 74 hrs, the *c*DCE epoxide accumulated in the cultures to approximately 0.14% of the *c*DCE degraded. The results suggest that the *c*DCE epoxide is a side product that decomposes spontaneously in the cultures, but that it is not degraded by JS666.

### 2.4.8 Dichloroacetaldehyde degradation in cell extracts of JS666

Dichloroacetaldehyde was degraded at a rate of 16 nmol/min/mg protein in extracts of cells grown on *c*DCE, which is consistent with the rate of *c*DCE degradation by whole cells (17 nmol/min/mg protein). The Km of the dichloroacetaldehyde dehydrogenase was 120 ± 12 μM. The small accumulation of dichloroacetaldehyde (Fig. 2.5) may result from the high Km value of dichloroacetaldehyde dehydrogenase. The results indicate that *c*DCE degradation through dichloroacetaldehyde is the productive pathway in JS666 and that the dichloroacetaldehyde dehydrogenase step might be a bottleneck.

## 2.5 DISCUSSION

Several lines of evidence indicate that cytochrome P450 monooxygenase (Bpro5301) is responsible for the initial steps in *c*DCE biodegradation in JS666. *c*DCE grown cells degraded *c*DCE only in the presence of oxygen, *c*DCE degradation was inhibited by

cytochrome P450 specific inhibitors, cytochrome P450 monooxygenase catalyzes the transformation of *c*DCE to dichloroacetaldehyde and small amounts of the epoxide, and Bpro5301 is upregulated by *c*DCE (23). Both the transient accumulation of dichloroacetaldehyde in *c*DCE degrading cultures and dichloroacetaldehyde dehydrogenase activities in cell extracts of JS666 further support the flux of *c*DCE through the proposed pathway (Fig. 2.6).

The cytochrome P450 catalyzed oxidation of the chlorinated ethenes can yield multiple products. The formation of chloroacetaldehyde side products has been reported during the oxidation of 1,1-dichloroethene (33) and trichloroethene (34) by cytochrome P450s from rat liver microsomes. A transient intermediate between an unsaturated carbon of the chlorinated ethenes and highly electron-deficient oxygen of a heme bound oxo-$Fe^{IV}$ in the cytochrome P450 can be partitioned to epoxide, a chloroacetaldehyde side product as a consequence of a chloride migration, and a dead end product due to an irreversible porphyrin *N*-alkylation with one carbon atom of the ethenes (11, 28, 34). The portion of the suicide complex ranged from 2~24% of 1,1-dichlroethelyene transformation by different cytochrome P450s (28). Theoretical studies on terminal olefin oxidation by cytochrome P450 further suggest that different environments in the protein pocket of the enzyme may lead to different product ratios of epoxides, aldehydes, and suicide products (11). The cytochrome P450 monooxygenase in JS666 appears to be specialized for dichloroacetaldehyde rather than epoxide production from *c*DCE, which channels the carbon into a productive pathway to prevent accumulation of the toxic and reactive product.

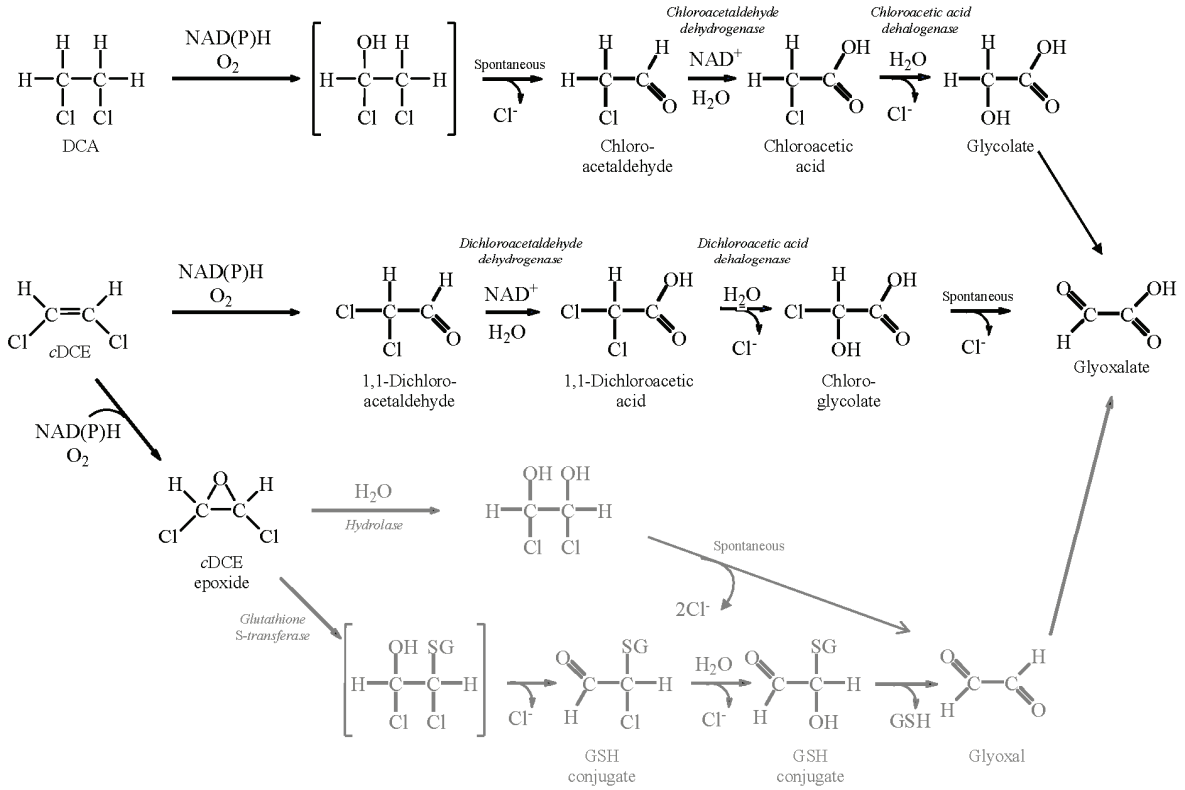


**Figure 2.6** Proposed *c*DCE and DCA degradation pathways. Pathways in black are supported by results of this study.

The cleavage of a C-Cl bond was suggested as the initial step of *c*DCE degradation by JS666 based on the large carbon isotope fractionation (-17.4 to -22.4‰) during *c*DCE degradation (23). The observation is consistent with the conversion of *c*DCE to dichloroacetaldehyde under the assumption that the chloride migration of the transient intermediate ($Fe^{IV}O$ -CClHCHCl•) between *c*DCE and $Fe^{IV}O$ in cytochrome P450 monooxygenase is a rate-limiting step. Considering the small amounts of *c*DCE epoxide produced, isotope effects caused by the formation of *c*DCE epoxide may be negligible. In contrast, Abe et al (1) suggested the epoxidation of *c*DCE as the initial step of *c*DCE degradation by JS666 based on the typical carbon isotope fractionation (-8.5‰) for epoxidation and a small chloride isotope fractionation (-0.3‰) during *c*DCE degradation by JS666. The results make sense if the formation of $Fe^{IV}O$ -CClHCHCl• in cytochrome P450 monooxygenase is the rate-limiting step. Alternatively, if an electron transfer from reduced ferredoxin to *c*DCE bound cytochrome P450 is rate limiting, the extent of isotope fractionation will be smaller than would be expected from the cleavage of a C-Cl bond. The hypothesis should be tested in future work by measuring isotope fractionation during *c*DCE transformation by cytochrome P450 monooxygenase with sufficient or limited amounts of ferredoxin and ferredoxin reductase.

The loss of 35% of the mass of *c*DCE during degradation by cytochrome P450 monooxygenase could be explained by the formation of a suicide complex between cytochrome P450 and *c*DCE and the decomposition of *c*DCE epoxide. The occurrence of the suicide complex is under investigation. Alternatively, Miller and Guengerich suggested that a transient intermediate between TCE and the oxygen of a heme bound oxo-$Fe^{IV}$ ($Fe^{IV}O$-$CCl_2CHCl$•) in cytochrome P450 enzymes from rat liver can be

hydrolyzed to form glyoxylic acid, CO, and formic acid. By the analogous reactions, glyoxal could be produced from the hydrolysis and spontaneous chloride release from a transient intermediate ($Fe^{IV}O$ -CClHCHCl•) between *c*DCE and $Fe^{IV}O$ in cytochrome P450 monooxygenase. Glyoxal was not detected during *c*DCE degradation by cytochrome P450 monooxygenase but it is a highly reactive intermediate that forms various protein-bound adducts.

The low (0.1%) accumulation of *c*DCE epoxide in cells of JS666 is not consistent with the higher (5%) accumulation in extracts of the *E. coli* recombinant expressing cytochrome P450 monooxygenase. Both the detection of glutathione inside cells of JS666 and upregulation of glutathione *S*-transferase by *c*DCE (23) suggest that glutathione conjugates could be formed between *c*DCE epoxide and glutathione by spontaneous or enzymatic reactions (14, 46). Alternatively, *c*DCE epoxide might be transformed to 1,2-dichloroethane-1,2-diol by hydrolases upregulated by *c*DCE (23). The lack of *c*DCE epoxide biodegradation by resting cells of JS666 does not preclude the two possibilities of the degradation of *c*DCE epoxide in actively growing cells.

Growth of strain JS666 on DCA contrasts with the previous findings of Mattes et al (29). The authors reported that JS666 was not able to grow on DCA even though potential genes for the hydrolytic DCA degradation pathway (22) are present in JS666 and *c*DCE grown cells of JS666 degraded DCA. In our hands DCA degradation was slow but stable for a month. Both the inhibition of DCA degradation by metyrapone in cells grown on DCA and the transformation of DCA to chloroacetaldehyde by cytochrome P450 monooxygenase support the hypothesis that strain JS666 degrades DCA by the oxidative pathway (16). The monooxygenation of DCA has been demonstrated

previously in crude extracts of DCA degrading bacteria in the presence of NADH and oxygen, but the enzymes involved were not identified (16). The ability of cytochrome P450 monooxygenase to transform both *c*DCE and DCA further explains why DCA and its degradation intermediates stimulate oxygen uptake by *c*DCE grown cells of JS666 as well as why *c*DCE degradation is induced in DCA grown cells. The regulation of the system, however, is currently not understood.

Based on amino acid sequence identity, the cytochrome P450 monooxygenase (Bpro_5301) belongs to the CYP153A subfamily (43). Several enzymes in the group were identified in alkane degrading bacteria lacking membrane bound alkane hydroxylases (AlkB) (43). The cytochrome P450 alkane hydroxylases catalyze the transformation of medium-chain-length alkanes (C6-C10) to alkanols which are further degraded to fatty acids by alcohol dehydrogenase (AlkJ), aldehyde dehydrogenase (AlkH), and acyl-CoA synthetase (AlkK). The cytochrome P450 alkane hydroxylases also catalyze the epoxidation of styrene, cyclohexene, and 1-octene. A few amino acid substitutions can enhance the activity of the enzyme toward small alkanes (24). In JS666, putative *alkKJH* genes and PQQ dependent dehydrogenase are located upstream of cytochrome P450 monooxygenase genes, which is consistent with the growth of JS666 on heptane and octane (29). Mattes et al suggest that the gene cluster was recruited from alkane assimilating bacteria based on the high G+C content, the association with several transposase genes, and the gene organization (29).

The recruitment and expression of the genes encoding the cytochrome P450 monooxygenase could allow the relatively common chloroacetaldehyde degrading bacteria to grow with *c*DCE as a sole source of carbon and energy. Instability and rapid

loss by JS666 of the ability to degrade *c*DCE under non selective conditions suggests that the system was recently assembled and sustained at the field site in response to contamination by *c*DCE. Such a scenario was strongly supported for assembly of chlorobenzene and diphenylamine degradation pathways (36, 41). We are currently testing the hypothesis by introducing the cytochrome P450 monooxygenase genes into chloroacetaldehyde degrading bacteria, which will provide more insight about the evolution of the *c*DCE degradation pathway.

*c*DCE degradation is a rate limiting step in natural attenuation processes for the chlorinated ethenes at many contaminated sites (13, 20, 32, 51). *Polaromonas* sp. strain JS666 is the only isolate able to grow on *c*DCE as the sole carbon and energy source under aerobic condition (8) although disappearance of *c*DCE under aerobic conditions has been reported (5, 6, 47). Bioaugmentation with strain JS666 would be a promising strategy to clean up *c*DCE-contaminated plumes, but uncertainty about the degradation pathway and intermediates has been a deterrent to the use of the strategy in practical applications. The determination of the *c*DCE degradation pathway and genes that encode the enzymes involved provides the basis to predict and enhance *c*DCE degradation at contaminated sites.

## 2.6 REFERENCES


1. **Abe, Y., R. Aravena, J. Zopfi, O. Shouakar-Stash, E. Cox, J. D. Roberts, and D. Hunkeler.** 2009. Carbon and chlorine isotope fractionation during aerobic oxidation and reductive dechlorination of vinyl chloride and *cis*-1,2-dichloroethene. Environ. Sci. Technol. **43:**101-107.
2. **Allen, J. R., D. D. Clark, J. G. Krum, and S. A. Ensign.** 1999. A role for coenzyme M (2-mercaptoethanesulfonic acid) in a bacterial pathway of aliphatic epoxide carboxylation. Proc. Natl. Acad. Sci. USA **96:**8432-8437.
3. **Bergmann, J. G., and J. Sanik.** 1957. Determination of trace amounts of chlorine in naphtha. Anal. Chem. **29:**241-242.
4. **Bhushan, B., S. Trott, J. C. Spain, A. Halasz, L. Paquet, and J. Hawari.** 2003. Biotransformation of hexahydro-1,3,5-trinitro-1,3,5-triazine (RDX) by a rabbit liver cytochrome P450: insight into the mechanism of RDX biodegradation by *Rhodococcus* sp. strain DN22. Appl. Environ. Microbiol. **69:**1347-1351.
5. **Bradley, P. M., and F. H. Chapelle.** 2000. Aerobic microbial mineralization of dichloroethene as sole carbon substrate. Environ. Sci. Technol. **34:**221-223.
6. **Bradley, P. M., and F. H. Chapelle.** 1998. Effect of contaminant concentration on aerobic microbial mineralization of DCE and VC in stream-bed sediments. Environ. Sci. Technol. **32:**553-557.
7. **Carr, C. S., and J. B. Hughes.** 1998. Enrichment of high-rate PCE dechlorination and comparative study of lactate, methanol, and hydrogen as electron donors to sustain activity. Environ. Sci. Technol. **32:**1817-1824.
8. **Coleman, N. V., T. E. Mattes, J. M. Gossett, and J. C. Spain.** 2002. Biodegradation of *cis*-dichloroethene as the sole carbon source by a beta-proteobacterium. Appl. Environ. Microbiol. **68:**2726-2730.
9. **Coleman, N. V., T. E. Mattes, J. M. Gossett, and J. C. Spain.** 2002. Phylogenetic and kinetic diversity of aerobic vinyl chloride-assimilating bacteria from contaminated sites. Appl. Environ. Microbiol. **68:**6162-6171.
10. **Coleman, N. V., and J. C. Spain.** 2003. Epoxyalkane: coenzyme M transferase in the ethene and vinyl chloride biodegradation pathways of *Mycobacterium* strain

JS60. J. Bacteriol. **185:**5536-5545.

11. **de Visser, S. P., D. Kumar, and S. Shaik.** 2004. How do aldehyde side products occur during alkene epoxidation by cytochrome P450? Theory reveals a state-specific multi-state scenario where the high-spin component leads to all side products. J. Inorg. Biochem. **98:**1183-1193.
12. **Ensign, S. A., M. R. Hyman, and D. J. Arp.** 1992. Cometabolic degradation of chlorinated alkenes by alkene monooxygenase in a propylene-grown *Xanthobacter* strain. Appl. Environ. Microbiol. **58:**3038-3046.
13. **Fennell, D. E., A. B. Carroll, J. M. Gossett, and S. H. Zinder.** 2001. Assessment of indigenous reductive dechlorinating potential at a TCE-contaminated site using microcosms, polymerase chain reaction analysis, and site data. Environ. Sci. Technol. **35:**1830-1839.
14. **Forkert, P. G.** 1999. In vivo formation and localization of 1,1-dichloroethylene epoxide in murine liver: identification of its glutathione conjugate 2-S-glutathionyl acetate. J. Pharmacol. Exp. Ther. **290:**1299-1306.
15. **Fox, B. G., J. G. Borneman, L. P. Wackett, and J. D. Lipscomb.** 1990. Haloalkene oxidation by the soluble methane monooxygenase from *Methylosinus trichosporium* OB3b: mechanistic and environmental implications. Biochemistry **29:**6419-6427.
16. **Hage, J. C., and S. Hartmans.** 1999. Monooxygenase-mediated 1,2-dichloroethane degradation by *Pseudomonas* sp. strain DCA1. Appl. Environ. Microbiol. **65:**2466-2470.
17. **Halsey, K. H., L. A. Sayavedra-Soto, P. J. Bottomley, and D. J. Arp.** 2006. Site-directed amino acid substitutions in the hydroxylase alpha subunit of butane monooxygenase from *Pseudomonas butanovora*: Implications for substrates knocking at the gate. J. Bacteriol. **188:**4962-4969.
18. **He, J., K. M. Ritalahti, K. L. Yang, S. S. Koenigsberg, and F. E. Loffler.** 2003. Detoxification of vinyl chloride to ethene coupled to growth of an anaerobic bacterium. Nature **424:**62-65.
19. **Holliger, C., D. Hahn, H. Harmsen, W. Ludwig, W. Schumacher, B. Tindall, F. Vazquez, N. Weiss, and A. J. Zehnder.** 1998. *Dehalobacter restrictus* gen. nov.

and sp. nov., a strictly anaerobic bacterium that reductively dechlorinates tetra- and trichloroethene in an anaerobic respiration. Arch. Microbiol. **169:**313-321.

20. **Hughes, J. B., and N. Cope.** 2001. Biologically-enhanced removal of PCE from NAPL sourve zones. Environ. Sci. Technol. **35:**2014-2021.
21. **Janssen, D. B., G. Grobben, R. Hoekstra, R. Oldenhuis, and B. Witholt.** 1988. Degradation of *trans*-1,2-dichloroethene by mixed and pure cultures of methanotrophic bacteria. Appl. Microbiol. Biotechnol. **29:**392-399.
22. **Janssen, D. B., A. Scheper, L. Dijkhuizen, and B. Witholt.** 1985. Degradation of halogenated aliphatic compounds by *Xanthobacter autotrophicus* GJ10. Appl. Environ. Microbiol. **49:**673-677.
23. **Jennings, L. K., M. M. Chartrand, G. Lacrampe-Couloume, B. S. Lollar, J. C. Spain, and J. M. Gossett.** 2009. Proteomic and transcriptomic analyses reveal genes upregulated by *cis*-dichloroethene in *Polaromonas* sp. strain JS666. Appl. Environ. Microbiol. **75:**3733-3744.
24. **Koch, D. J., M. M. Chen, J. B. van Beilen, and F. H. Arnold.** 2009. In vivo evolution of butane oxidation by terminal alkane hydroxylases AlkB and CYP153A6. Appl. Environ. Microbiol. **75:**337-344.
25. **Koziollek, P., D. Bryniok, and H. J. Knackmuss.** 1999. Ethene as an auxiliary substrate for the cooxidation of *cis*-1, 2-dichloroethene and vinyl chloride. Arch. Microbiol. **172:**240-246.
26. **Krum, J. G., and S. A. Ensign.** 2001. Evidence that a linear megaplasmid encodes enzymes of aliphatic alkene and epoxide metabolism and coenzyme M (2-mercaptoethanesulfonate) biosynthesis in *Xanthobacter* strain Py2. J. Bacteriol. **183:**2172-2177.
27. **Lessner, D. J., G. R. Johnson, R. E. Parales, J. C. Spain, and D. T. Gibson.** 2002. Molecular characterization and substrate specificity of nitrobenzene dioxygenase from *Comamonas* sp. strain JS765. Appl. Environ. Microbiol. **68:**634-641.
28. **Liebler, D. C., and F. P. Guengerich.** 1983. Olefin oxidation by cytochrome P450: evidence for group migration in catalytic intermediates formed with vinylidene chloride and *trans*-1-phenyl-1-butene. Biochemistry **22:**5482-5489.

29. **Mattes, T. E., A. K. Alexander, P. M. Richardson, A. C. Munk, C. S. Han, P. Stothard, and N. V. Coleman.** 2008. The genome of *Polaromonas* sp. strain JS666: insights into the evolution of a hydrocarbon- and xenobiotic-degrading bacterium, and features of relevance to biotechnology. Appl. Environ. Microbiol. **74:**6405-6416.

30. **Mattes, T. E., N. V. Coleman, J. C. Spain, and J. M. Gossett.** 2005. Physiological and molecular genetic analyses of vinyl chloride and ethene biodegradation in *Nocardioides* sp. strain JS614. Arch. Microbiol. **183:**95-106.

31. **Maymo-Gatell, X., Y. Chien, J. M. Gossett, and S. H. Zinder.** 1997. Isolation of a bacterium that reductively dechlorinates tetrachloroethene to ethene. Science **276:**1568-1571.

32. **McCarty, P. L.** 1993. In situ bioremediation of chlorinated solvents. Curr. Opin. Biotechnol. **4:**323-330.

33. **Meunier, B., S. P. de Visser, and S. Shaik.** 2004. Mechanism of oxidation reactions catalyzed by cytochrome P450 enzymes. Chem. Rev. **104:**3947-3980.

34. **Miller, R. E., and F. P. Guengerich.** 1982. Oxidation of trichloroethylene by liver microsomal cytochrome P450: evidence for chlorine migration in a transition state not involving trichloroethylene oxide. Biochemistry **21:**1090-1097.

35. **Mohn, W. W., and J. M. Tiedje.** 1992. Microbial reductive dehalogenation. Microbiol. Rev. **56:**482-507.

36. **Muller, T. A., C. Werlen, J. Spain, and J. R. Van Der Meer.** 2003. Evolution of a chlorobenzene degradative pathway among bacteria in a contaminated groundwater mediated by a genomic island in *Ralstonia*. Environ. Microbiol. **5:**163-173.

37. **Raag, R., B. A. Swanson, T. L. Poulos, and P. R. Ortiz de Montellano.** 1990. Formation, crystal structure, and rearrangement of a cytochrome P450cam iron-phenyl complex. Biochemistry **29:**8119-8126.

38. **Rui, L., L. Cao, W. Chen, K. F. Reardon, and T. K. Wood.** 2004. Active site engineering of the epoxide hydrolase from *Agrobacterium radiobacter* AD1 to enhance aerobic mineralization of *cis*-1,2-dichloroethylene in cells expressing an evolved toluene *ortho*-monooxygenase. J. Biol. Chem. **279:**46810-46817.

39. **Rui, L., Y. M. Kwon, K. F. Reardon, and T. K. Wood.** 2004. Metabolic pathway engineering to enhance aerobic degradation of chlorinated ethenes and to reduce their toxicity by cloning a novel glutathione S-transferase, an evolved toluene *o*-monooxygenase, and gamma-glutamylcysteine synthetase. Environ. Microbiol. **6:**491-500.

40. **Seth-Smith, H. M., J. Edwards, S. J. Rosser, D. A. Rathbone, and N. C. Bruce.** 2008. The explosive-degrading cytochrome P450 system is highly conserved among strains of *Rhodococcus* spp. Appl. Environ. Microbiol. **74:**4550-4552.

41. **Shin, K. A., and J. C. Spain.** 2009. Pathway and evolutionary implications of diphenylamine biodegradation by *Burkholderia* sp. strain JS667. Appl. Environ. Microbiol. **75:**2694-2704.

42. **Stanier, R. Y., N. J. Palleroni, and M. Doudoroff.** 1966. The aerobic pseudomonads: a taxonomic study. J. Gen. Microbiol. **43:**159-271.

43. **van Beilen, J. B., E. G. Funhoff, A. van Loon, A. Just, L. Kaysser, M. Bouza, R. Holtackers, M. Rothlisberger, Z. Li, and B. Witholt.** 2006. Cytochrome P450 alkane hydroxylases of the CYP153 family are common in alkane-degrading eubacteria lacking integral membrane alkane hydroxylases. Appl. Environ. Microbiol. **72:**59-65.

44. **van Beilen, J. B., R. Holtackers, D. Luscher, U. Bauer, B. Witholt, and W. A. Duetz.** 2005. Biocatalytic production of perillyl alcohol from limonene by using a novel *Mycobacterium* sp. cytochrome P450 alkane hydroxylase expressed in *Pseudomonas putida*. Appl. Environ. Microbiol. **71:**1737-1744.

45. **van der Ploeg, J., M. P. Smidt, A. S. Landa, and D. B. Janssen.** 1994. Identification of chloroacetaldehyde dehydrogenase involved in 1,2-Dichloroethane degradation. Appl. Environ. Microbiol. **60:**1599-1605.

46. **van Hylckama Vlieg, J. E., J. Kingma, A. J. van den Wijngaard, and D. B. Janssen.** 1998. A glutathione S-transferase with activity towards *cis*-1, 2-dichloroepoxyethane is involved in isoprene utilization by *Rhodococcus* sp. strain AD45. Appl. Environ. Microbiol. **64:**2800-2805.

47. **Verce, M. F., C. K. Gunsch, A. S. Danko, and D. L. Freedman.** 2002. Cometabolism of *cis*-1,2-dichloroethene by aerobic cultures grown on vinyl

chloride as the primary substrate. Environ. Sci. Technol. **36:**2171-2177.

48. **Vogel, T. M., C. S. Criddle, and P. L. McCarty.** 1987. Transformations of halogenated aliphatic compounds. Environ. Sci. Technol. **21:**722-736.

49. **Wackett, L. P., M. J. Sadowsky, L. M. Newman, H. G. Hur, and S. Li.** 1994. Metabolism of polyhalogenated compounds by a genetically engineered bacterium. Nature **368:**627-629.

50. **Williams, P. A., J. Cosme, D. M. Vinkovic, A. Ward, H. C. Angove, P. J. Day, C. Vonrhein, I. J. Tickle, and H. Jhoti.** 2004. Crystal structures of human cytochrome P450 3A4 bound to metyrapone and progesterone. Science **305:**683-686.

51. **Yang, Y., and P. L. McCarty.** 2002. Comparison between donor substrates for biologically enhanced tetrachloroethene DNAPL dissolution. Environ. Sci. Technol. **36:**3400-3404.

# CHAPTER 3

# Pathway and Evolutionary Implications of Diphenylamine Biodegradation by *Burkholderia* sp. Strain JS667



## 3.1 ABSTRACT

Diphenylamine (DPA) is a common contaminant at munitions-contaminated sites as well as at aniline manufacturing sites. Little is known about the biodegradation of the compound and bacteria able to use DPA as the growth substrate have not been reported. *Burkholderia* sp. strain JS667 and *Ralstonia* sp. strain JS668 were isolated by selective enrichment from DPA-contaminated sediment. The isolates grew aerobically with DPA as the sole carbon, nitrogen, and energy source. During induction of DPA degradation, stoichiometric amounts of aniline accumulated and then disappeared, which suggested that aniline is on the DPA degradation pathway. Genes encoding the enzymes that catalyze the initial steps in DPA degradation were cloned from the genomic DNA of strain JS667. The *E. coli* clone catalyzed stoichiometric transformation of DPA to aniline and catechol. Transposon mutagenesis, the sequence similarity of putative open reading

frames to those of well characterized dioxygenases, and $^{18}O_2$ experiments support the conclusion that the initial reaction in DPA degradation is catalyzed by a multi-component ring-hydroxylating dioxygenase. DPA is converted to aniline and catechol via dioxygenation at the 1,2 position of the aromatic ring and spontaneous rearomatization. Aniline and catechol are further biodegraded by the well established aniline degradation pathway. Genes that encode the complete aniline degradation pathway were found 12 kb downstream of the genes that encode the initial dioxygenase. Expression of the relevant dioxygenases was confirmed by reverse transcriptional PCR analysis. Both the sequence similarity and the gene organization suggest that the DPA degradation pathway evolved by the recruitment of two gene clusters that encode the DPA dioxygenase and the aniline degradation pathway.

## 3.2 INTRODUCTION

Diphenylamine (DPA) has been widely used as a precursor of dyes, pesticides, pharmaceuticals, photographic chemicals, and as a stabilizer for explosives (7). A significant amount of DPA is formed as a byproduct during the manufacture of aniline. DPA also reacts with nitric oxides to form nitrated derivatives of DPA (25). DPA and its nitrated derivatives are common contaminants at munitions-contaminated sites as well as at manufacturing sites. It is also a naturally occurring compound found in onions and tea leaves (20). Ecotoxicological studies indicate that DPA and its derivatives are potentially hazardous to aquatic organisms (9). Little is known about the biodegradation of the compound, but there have been several reports (7, 8, 14) that it is biodegraded under both

aerobic and anoxic conditions. The previous studies, however, did not address the mechanisms and the organisms responsible for the biodegradation of DPA. Shindo et al. reported that a modified biphenyl dioxygenase transforms DPA to 2-hydroxydiphenylamine and 3-hydroxydiphenylamine (40). The authors proposed that the monohydroxylated products are generated non-enzymatically by dehydration of the 2,3-dihydrodiol as a consequence of its structural instability. Biodegradation pathways of the structurally similar carbazole, dibenzo-*p*-dioxin, dibenzofuran, and diphenylether are well established (17, 39, 51). In all of the pathways dioxygenases catalyze the initial attack on the aromatic ring resulting in the spontaneous cleavage of the three-ring structure or the diphenylether structure (31).

We have isolated aerobic bacteria able to use DPA as the growth substrate through selective enrichment with samples from DPA contaminated sites. Here we describe the degradation pathway of DPA and the genes that encode the enzymes involved. The understanding of the DPA degradation pathway will provide the basis to predict and enhance DPA biodegradation at contaminated sites.

## 3.3 MATERIALS AND METHODS

### 3.3.1 Isolation and growth of DPA degraders

Samples from the surface of the sediment in a DPA contaminated stream near Repauno, NJ were suspended in nitrogen-free minimal medium (BLK) (6) containing DPA (100 μM). The culture was incubated under aerobic conditions at room temperature.

When DPA disappeared from the culture, portions (10%, vol/vol) were transferred into fresh BLK containing DPA crystals (0.85 g/l). After several serial transfers samples were spread on BLK agar (1.8%) plates containing DPA (500 μM). Individual colonies were transferred into 5 ml of BLK containing DPA (500 μM) as the carbon and nitrogen source. DPA concentrations in the culture fluids were measured by high performance liquid chromatography (HPLC) at appropriate intervals. Isolated DPA degraders were routinely grown in BLK liquid medium or agar plates containing DPA (1 mM).

### 3.3.2 Analytical methods

DPA and its degradation intermediates were separated by paired ion chromatography on a Merck Chromolith RP18e column (4.6 mm x 100 mm) with a Varian HPLC system equipped with photodiode array detector. The mobile phase consisted of part A (5 mM PIC A low-UV reagent (Waters, MA) in 30% methanol-70% water) and part B (70% methanol-30% water). The flow rate was 3 ml/min. The mobile phase was changed from 100% part A to 100% part B over a 2-min period, and then held at 100% part B for 2 min. DPA, aniline, and catechol were monitored at 280, 230, and 275 nm, respectively. Alternatively, catechol was analyzed on a Phenomenex Synergi Polar-RP column (4 μm, 2.0 mm x 150 mm) with an isocratic mobile phase composed of 10% methanol-90% water (23). The flow rate was 1.5 ml/min. Aniline, catechol, and DPA were also analyzed by gas chromatography mass spectrometry (GC/MS) (23). The compounds were separated on a capillary column Equity-1701 (30 m by 0.25 mm, 0.25 μm film thickness, Supelco, PA). Helium was used as the carrier gas at a constant flow rate of 1 ml/min. The

chromatography program was as follows: initial column temperature of 55 °C for 1 min, temperature increase of 20 °C/min to 280°C, and isothermal for 5 min. Protein was measured with a Pierce (Rockford, IL) BCA protein assay reagent kit.

### 3.3.3 Respirometry

Cells grown on DPA were harvested by centrifugation, washed with potassium phosphate buffer (pH 7.2, 20 mM), and suspended in the same buffer. Oxygen uptake was measured polarographically at 25°C with a Clark-type oxygen electrode connected to a YSI model 5300 biological oxygen monitor (29). Succinate grown cells served as negative controls.

### 3.3.4 Enzyme assays

Cells were harvested by centrifugation, washed with potassium phosphate buffer (pH 7.2, 20 mM), and broken by two passages through a French pressure cell at 20,000 lb/in$^2$. Catechol 1,2-dioxygenase, catechol 2,3-dioxygenase, and 2,3-dihydroxybiphenyl-1,2-dioxygenase activities were measured spectrophotometrically as described previously (5, 41).

### 3.3.5 Bacterial identification

Genomic DNA was extracted with a Genomic DNA purification system (Promega, Madison, WI). The 16S rDNA was PCR amplified with fD1 and rD1 universal primers (49). PCR products were purified with Wizard® SV Gel clean-up system (Promega, Madison, WI) and sequenced by Nevada Genomics Center (Reno, NV). The resulting 16S rDNA sequences (600 bp) were compared with the sequences in GenBank (http://www.ncbi.nlm.nih.gov/Genbank/index.html) using BLAST.

### 3.3.6 Gene library construction and screening

A recombinant fosmid library of DNA from *Burkholderia* sp. JS667 was created according to the manufacturer's directions (CopyControl$^{TM}$ Fosmid Library Production Kit, Epicentre Biotechnologies, WI). Total DNA from DPA grown cells was randomly sheared by vortexing. DNA fragments were ligated into the fosmid vector pCC1FOS. Fosmids harboring 40 kb DNA fragments were transfected into *E. coli* strain EPI300. Approximately 2,000 clones of the *E. coli* recombinant library were spread on LB agar plates containing chloramphenicol (12.5 μg/ml). For preliminary screening an ether solution of catechol (0.1%) was sprayed onto colonies on plates to screen for *meta* cleavage of catechol (21). Several presumptive catechol dioxygenase clones were selected for further characterization based on the formation of a faint yellow color. For confirmation of phenotypes the clones were grown in LB containing chloramphenicol (12.5 μg/ml) and Fosmid Induction Solution (Epicentre), harvested by centrifugation, washed and suspended in phosphate buffer (20 mM, pH 7.2). Yellow color formation from catechol was tested visually and the ability to transform DPA was monitored by

HPLC analysis of the culture fluid. The clone designated pJS702 had the ability to transform either catechol or DPA (Table 3.1). Clone pJS701 transformed DPA but not catechol.

### 3.3.7 Generation of transposon mutants

Fosmid pJS702 was purified from recombinant *E. coli* strain EPI300 using the FosmidMAX DNA purification kit (Epicentre Biotechnologies, WI) and then randomly mutated *in vitro* with a modified miniTn*5* transposon carrying the kanamycin resistance cassette (Ez-Tn*5* <KAN-2>) according to the manufacturer's directions (Ez-Tn5$^{TM}$ <KAN2> Insertion Kit, Epicentre Biotechnologies, WI). The resulting fosmids were then reintroduced into *E. coli* strain EPI300 by electroporation. Transposon insertion mutants were selected by growth on LB medium supplemented with chloramphenicol (20 g/ml) and kanamycin (25 g/ml). The kanamycin-resistant transposon mutants were then screened as above for the ability to transform DPA or catechol. Clones pJS7021 and pJS7022 are transposon insertion mutant of pJS702 (Table 3.1).

### 3.3.8 DNA sequencing and sequence analysis

The fosmids that lost the ability to transform DPA or catechol due to transposon insertion were sequenced using Ez-Tn5 <KAN2> specific outward reading primers by Nevada Genomics Center (Reno, NV). The flanking regions were sequenced by primer walking (19). The sequences were analyzed with BioEdit 7.0.4. Sequence Alignment

Editor (Ibis Therapeutics, Carlsbad, CA). Sequence databases were searched using the BLAST programs via the National Center for Biotechnology Information website. Multiple-sequence alignments were done using ClustalW (45) and phylogenetic analysis was performed by using the neighbor-joining algorithm found in BioEdit. Phylogenetic trees were drawn using the TreeView program (33).

### 3.3.9 Biotransformation of substrates by fosmid clones.

Cells were incubated in 50 ml of LB (12.5 µg/ml chloramphenicol) at 25 ºC. When the $OD_{600}$ reached 0.9, Fosmid Induction Solution (Epicentre) was added to the cultures and they were incubated for another 4 h. Cells were harvested by centrifugation, washed twice with sterile BLK medium, and suspended to an $OD_{600}$ of 6 in BLK medium. The cell suspensions (1 ml) were transferred to individual test tubes. The reaction was initiated by the addition of substrates and suspensions were incubated at 25 ºC with shaking at 250 rpm. At appropriate intervals samples were mixed with equal volumes of acidified acetonitrile (pH 1.5), centrifuged at 16,100 ×g for 1 min, and analyzed by HPLC. Cloned carbazole dioxygenase from *Pseudomonas* sp. CA10 in intact cells of *E. coli* was tested for transformation of DPA analogues as above. Cells were grown and induced as described previously (37).

### 3.3.10 $^{18}O_2$ incorporation

Cells of *E. coli* EPI300 pJS7021 ($DPA^+$, $catechol^-$) were prepared as indicated above. The cell suspensions were transferred to a 50 ml round bottom flask and incubated with DPA (400 μM) in the presence of $^{18}O_2$ as previously described (42). After 2 hrs, the metabolites were extracted from the culture fluid and analyzed by GC/MS.

### 3.3.11 Total RNA extraction and reverse transcription PCR (RT-PCR)

Total RNA was isolated from DPA or succinate grown cells at mid-exponential phase (SV Total RNA Isolation System, Promega, WI). cDNA was synthesized from total RNA (340 ng) (High Capacity cDNA Reverse Transcription Kits, Applied Biosystems, CA). Samples of the reverse transcription reaction mixtures (1 μl) were subjected to PCR amplification by the primer pairs: DPADO-F and DPADO-R, ANDO-F and ANDO-R, and CatDO-F and CatDO-R (Table 3.1). The 30 cycles of amplification were carried out as follows: 95 °C for 1 min, 56.5 °C for 30 s, and 72 °C for 30 s after initial denaturation at 95 °C for 10 min. The predicted sizes of the PCR products were 218, 205, and 164 bp, respectively.

### 3.3.12 Chemicals

Diphenylamine, 3- and 4-hydroxydiphenylamines, naphthalene, biphenyl, aniline, catechol, and 2,3-dihydroxybiphenyl were from Sigma-Aldrich (Milwaukee, WI). Carbazole and dibenzofuran were from Chem Service (West Chester, PA).

### 3.3.13 Extraction of hydroxydiphenylamine

Cells were removed from the DPA degrading cultures by centrifugation and the supernatant was passed through a C18 solid phase extraction (SPE) column (Waters, MA). The cartridge was washed with 50% methanol and then metabolites were eluted with 60% methanol. The putative 2-hydroxydiphenylamine was purified on a Merck Chromolith RP18e column (4.6 mm X 100 mm) with 60% methanol as the mobile phase.

### 3.3.14 Nucleotide sequence accession numbers

Nucleotide sequences of *Burkholderia* sp. JS667 and *Ralstonia* sp. JS668 were deposited in GenBank under accession numbers FJ708484 to FJ708486.

**Table 3.1** Bacterial strains, plasmids, and PCR primers used in this study.

| Strain and plasmid | Description | Source or reference |
|---|---|---|
| Strains | | |
| *Burkholderia* sp. JS667 | Diphenylamine degrader | This study |
| *Ralstonia* sp. JS668 | Diphenylamine degrader | This study |
| Plasmid | | |
| pCC1FOS | $Cm^r$, Fosmid used for genomic library construction of JS667 | Epicentre (Madison,WI) |
| pJS700 | $Cm^r$, pCC1FOS containing genomic fragment of JS667 ($DPA^-$, $Catechol^+$) | This study |
| pJS701 | $Cm^r$, pCC1FOS containing genomic fragment of JS667 ($DPA^+$, $Catechol^-$) | This study |
| pJS702 | $Cm^r$, pCC1FOS containing genomic fragment of JS667 ($DPA^+$, $Catechol^+$) | This study |
| pJS7021 | $Cm^r$ and $Km^r$, Transposon (Ez-Tn*5* <KAN-2>) insertion mutant into *tdnC* of pJS702 ($DPA^+$, $Catechol^-$) | This study |
| pJS7022 | $Cm^r$ and $Km^r$, Transposon (Ez-Tn*5* <KAN-2>) insertion mutant into *dpaAa* of pJS702 ($DPA^-$, $Catechol^+$) | This study |
| pUCARA | $Ap^r$, pUC119 with 5.6-kb EcoRI insert that encodes carbazole dioxygenase from *P. resinovorans* CA10 | (37) |
| PCR primers | | |
| DPADO-F | PCR amplification of gene fragment (218 bp) of *dpaAa*; ATACGAAGTGGTACGTGCCCGATT | This study |
| DPADO-R | PCR amplification of gene fragment (218 bp) of *dpaAa*; TCTCATTGATCCAGCCACGGTCAT | This study |
| ANDO-F | PCR amplification of gene fragment (205 bp) of *tdnA1*; ACATCTTTCCCAACCTGGCACTGA | This study |
| ANDO-R | PCR amplification of gene fragment (205 bp) of *tdnA1*; CATTCCTCGAAATTGGCTGCGTCA | This study |

**Table 3.1 (Continued)** Bacterial strains, plasmids, and PCR primers used in this study.

| | | |
|---|---|---|
| CatDO-F | PCR amplification of gene fragment (164 bp) of *tdnC*; GGGTGTGATGCGTATTGGTCATGT | This study |
| CatDO-R | PCR amplification of gene fragment (164 bp) of *tdnC*; ACAGGATCAGCGAATACTTGTCCC | This study |
| Primer4-F | PCR amplification of gene fragment (370 bp) of *tdnQ* ; GGCTGGATGCTGGCAGATCT | (47) |
| Primer5R-R | PCR amplification of gene fragment (370 bp) of *tdnQ* ; AAGGTGGTTTCCATCTGGCT | (47) |
| TdnQ-F | PCR amplification of gene fragment (5 kbp) of *tdnQTA1A2B*; ATTTGGACGAGGTTGAGCCCATCA | This study |
| TdnR-R | PCR amplification of gene fragment (5 kbp) of *tdnQTA1A2B*; TCCATCACGCTGATTCGGATGACA | This study |

## 3.4 RESULTS

### 3.4.1 Isolation of DPA degraders

From the DPA enrichment culture, we isolated *Burkholderia* sp. strain JS667 and *Ralstonia* sp. strain JS668 able to use DPA as the sole carbon, nitrogen, and energy source. Both strains can utilize aniline, anthranilate, and catechol but not carbazole as growth substrates. DPA was completely biodegraded (Fig. 3.1) and no UV absorbing products were detected in the culture fluid by HPLC. The growth was slow (about 15 hrs doubling time). HPLC analysis indicated that no UV absorbing intermediates of DPA accumulated in actively growing cultures. A typical DPA degradation rate was 39 nmol DPA/mg protein/min during exponential growth (Fig. 3.1). The growth yield was 0.23 mg of total protein per mg of DPA, which is similar to those of the dibenzo-*p*-dioxin degrader, *Sphingomonas* sp. RW1 (51) and the biphenyl degrader, *Burkholderia xenovorans* LB400 (34). The capability of JS667 and JS668 to grow on DPA was relatively stable. After 7 transfers in 0.75% (wt/vol) tryptic soy broth, a small portion of JS667 (20.8%) and JS668 (5.5%) lost the ability to degrade DPA.

### 3.4.2 DPA degradation kinetics during induction

When succinate-grown cells of JS667 were transferred to media containing DPA, substantial amounts of aniline accumulated and then disappeared (Fig. 3.2). Transient accumulation of aniline suggested strongly that it is an intermediate of DPA degradation. The lack of an induction period before DPA disappearance and aniline accumulation in

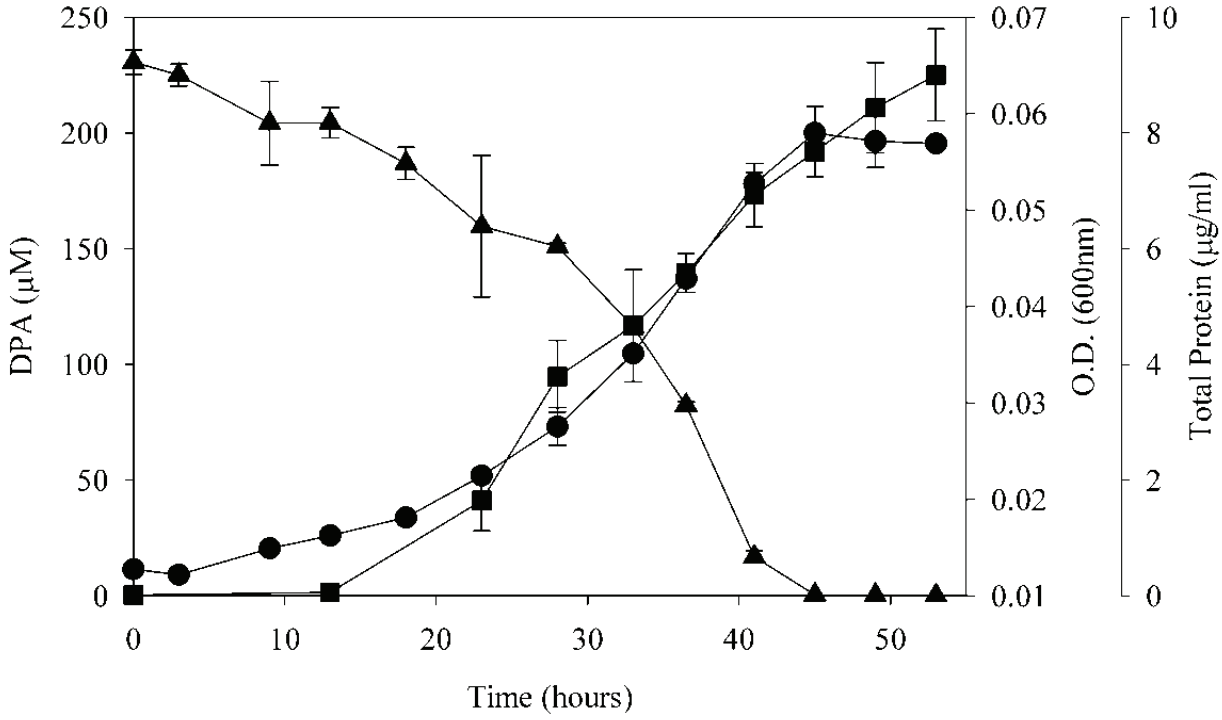


**Figure 3.1** Growth of *Burkholderia* sp. JS667 on DPA as sole carbon and nitrogen source (▲: Concentration of DPA, ●: Optical density at 600 nm, ■: Total protein).

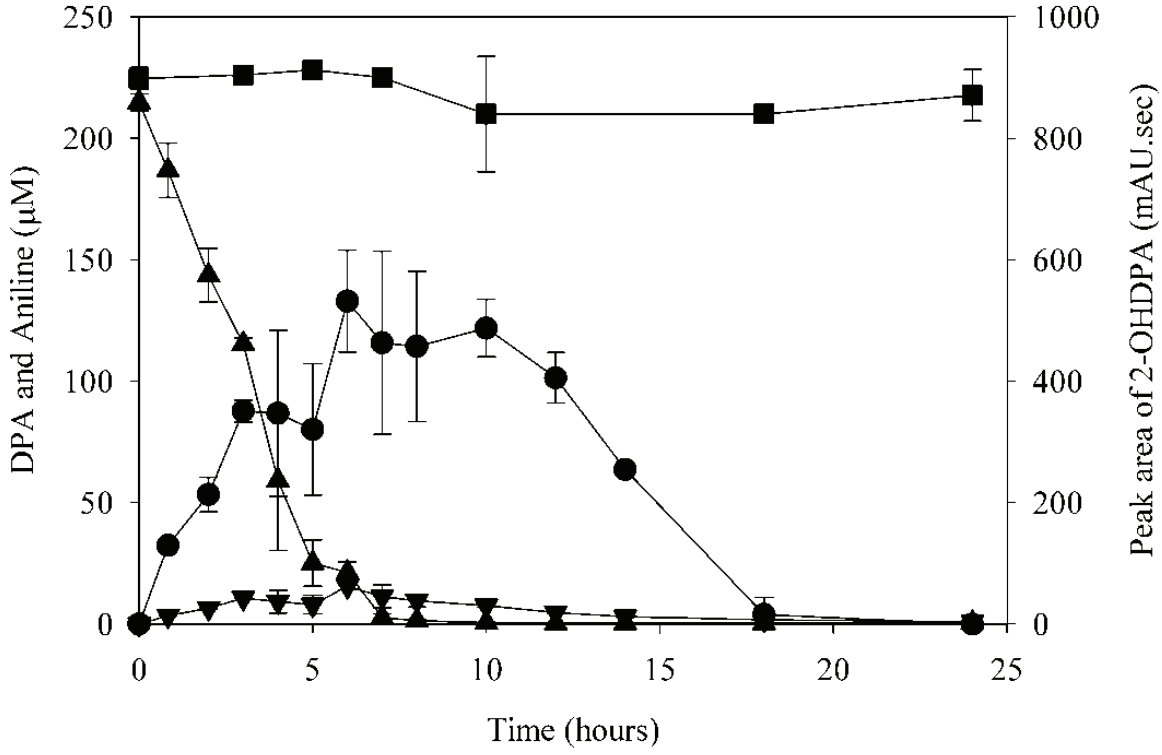


**Figure 3.2** DPA degradation kinetics during induction of *Burkholderia* sp. JS667 (▲: DPA, ●: Aniline, ▼: 2-hydroxydiphenylamine, ■: DPA in abiotic control). Cells grown on succinate were suspended to $OD_{600}$ = 0.2.

the first phase indicate that the initial enzymes of the pathway are at least partially constitutive, whereas enzymes that catalyze aniline degradation are inducible.

Small amounts of an unknown intermediate were also detected by HPLC. GC/MS analysis of the unknown compound extracted from the culture fluids after growth of JS667 on 1 mM DPA revealed a characteristic mass fragment [$M^+$] at *m/z* 185 with major fragment ions at *m/z* 168, 156, and 139 which are similar to those of 3- and 4-hydroxydiphenylamines (36). The unknown compound was tentatively identified as 2-hydroxydiphenylamine based on the difference in HPLC retention time and UV spectrum from those of 3- and 4-hydroxydiphenylamines. The compound might be generated non-enzymatically by dehydration of a dihydrodiol intermediate as a consequence of its structural instability (40) or enzymatically by a monooxygenase mechanism (15). Similar results were obtained when the above experiments were repeated with strain JS668, which suggest that the two strains employ a similar DPA degradation pathway. Further studies to determine the DPA biodegradation pathway were carried out with strain JS667.

### 3.4.3 Oxygen uptake rates

Catechol, DPA, monohydroxylated-DPA isomers, and aniline stimulated immediate and rapid oxygen uptake by DPA grown cells (Table 3.2). The results suggest that enzymes involved in DPA degradation are induced during growth on DPA and that some of the above compounds are on the degradation pathway. Slight stimulation of oxygen uptake by DPA in succinate grown cells supports the observation that the initial enzymes of the pathway have a moderate constitutive activity. The oxidation of aniline and

**Table 3.2** Oxygen uptake (nmoles/min/mg of protein) by DPA and succinate grown cells.

| Substrate | DPA grown cells (nmoles/min/mg of protein) | Succinate grown cells (nmoles/min/mg of protein) |
|---|---|---|
| DPA | 81 ± 21 | 28 ± 2 |
| Aniline | 50 ± 5 | 3 ± 0 |
| Catechol | 351 ± 5 | 13 ± 5 |
| 2-HydroxyDPA | 48 ± 12 | 8 ± 2 |
| 3-HydroxyDPA | 63 ± 9 | 10 ± 5 |
| 4-HydroxyDPA | 15 ± 2 | 10 ± 0 |

Reaction mixtures contained substrate (20 μM), cells (0.14 mg of protein), and air-saturated phosphate buffer (20 mM, pH 7.2) to a final volume of 1.85 ml. Data represent means of at least 2 experiments. 2-Nitrodiphenylamine, 4-nitrodiphenylamine, *N*-nitrosodiphenylamine, biphenyl, toluene, and phenol did not stimulate oxygen uptake.

catechol required 3.1 ± 0.28 and 1.85 ± 0.13 mol of $O_2$ per mol of substrate, respectively. The result is consistent with conversion of aniline to catechol by a dioxygenase (30).

### 3.4.4 Enzyme assays

Catechol was oxidized by a catechol 2,3-dioxygenase detected in extracts prepared from cells of JS667 grown on DPA. The specific activity for catechol 2,3-dioxygenase was 75.5 ± 0.2 nmol/min/mg protein when the cell extracts were incubated for 10 min at 40 °C before the assay. Catechol 1,2-dioxygenase and 2,3-dihydroxybiphenyl-1,2-dioxygenase activities were not detectable in the cell extracts.

### 3.4.5 Cloning and *in silico* analysis of the genes involved in DPA degradation

In order to determine the initial reaction in the DPA degradation pathway, a fosmid library of total genomic DNA from strain JS667 was constructed and transposon mutagenesis was carried out with pJS702 ($DPA^+$ and $catechol^+$). Some clones lost the ability to transform DPA or catechol and the regions flanking the insertions were sequenced via primer walking outward from the transposon. When the transposon was inserted in ORF4 or ORF7 the clones lost the ability to transform DPA (Fig. 3.3A). Transposon insertion in ORF29 abolished the catechol dioxygenase activity.

The remainder of the genes that encode the DPA degradation pathway were identified by primer walking and PCR amplification (Fig. 3.3A). The nucleotide sequences of ORFs 1-31 that encode DPA and catechol dioxygenases were identified by

primer walking in pJS702. ORF 31 was identical to the regulator (*tdnR*) in aniline dioxygenase (24) and was located at the end of pJS702. The nucleotide sequences of ORFs 32-36 were obtained by PCR amplification from the genomic DNA of JS667. Primers were designed based on ORF31 and the conserved region in the glutamine synthetase-like gene (*tdnQ*) of aniline dioxygenase (Table 3.1) (47).

The assembled sequence formed a 30,579 bp segment of DNA. The segment contained 35 complete ORFs and one partial ORF (ORF36) (Fig. 3.3A). Variability of GC content and nucleotide sequence similarities reveal the patchwork-like structure of the DNA segment. The abrupt increase in GC content downstream of ORF18 suggests that the DNA fragment was assembled from at least two different origins. The presence of several transposon remnants (ORFs 11-12 and 15-18) is further support for the hypothesis. On the other hand, the nucleotide sequences in ORFs 12-14 (2.4 kb) and in ORFs 22-29 (6.8 kb) were 94% and 90% identical to the homologous sequences in *R. eutropha* JMP134 and those of the hypothetical catechol degradative operon of *Burkholderia* sp. 383, respectively. ORFs 15, 18-21 and 30-36 were approximately 90% identical to nucleotide sequences in the genes that encode aniline degradation in *D. tsuruhatensis* AD9 (24) and *P. putida* UCC22 (11). It appears that ORFs 15 and 18 were divided by the insertion of ORFs 16 and 17, insertion elements first reported in *Burkholderia multivorans* (32). The results suggest that the gene cluster that encodes the DPA degradation pathway was assembled by horizontal gene transfer.

The deduced amino acid sequence of ORF4 showed 67% identity to CarAaI, the terminal oxygenase component of carbazole 1,9a-dioxygenase, from *Sphingomonas* sp.

(A)

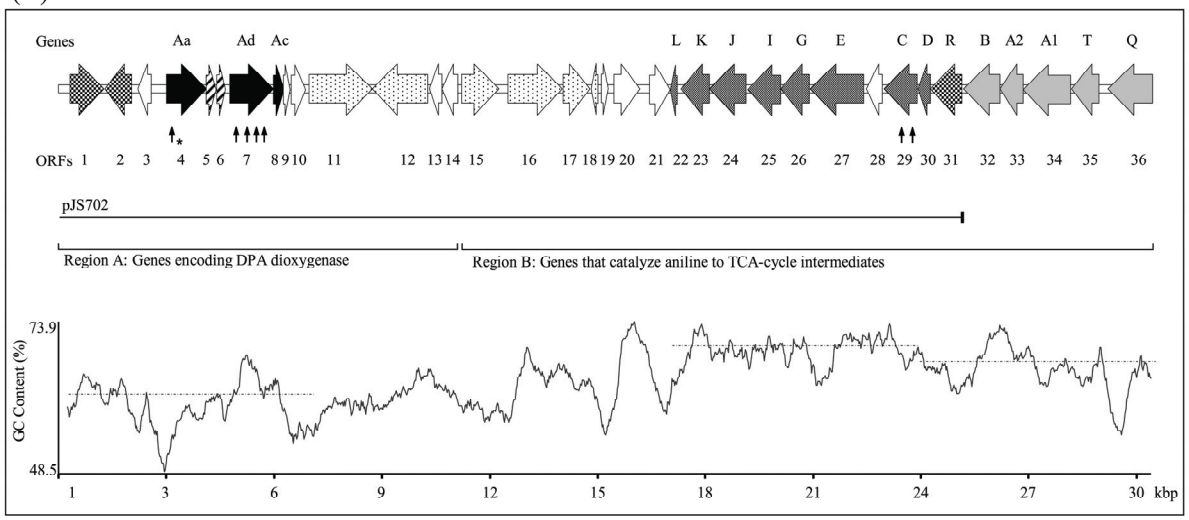
Genes
Aa
Ad
Ac
L K J I G E
C D R B A2 A1 T Q
ORFs 1 2 3 4 5 6 7 8 9 10 11 12 13 14 15 16 17 18 19 20 21 22 23 24 25 26 27 28 29 30 31 32 33 34 35 36
pJS702
Region A: Genes encoding DPA dioxygenase
Region B: Genes that catalyze aniline to TCA-cycle intermediates
GC Content (%)
73.9
48.5
1 3 6 9 12 15 18 21 24 27 30 kbp

(B)

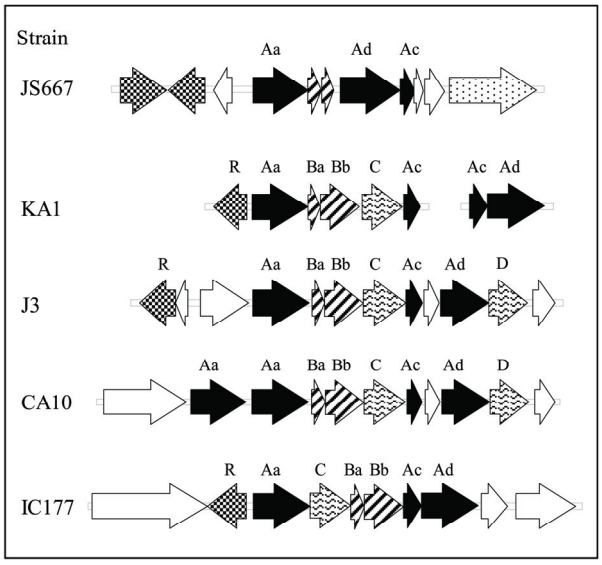
Strain
JS667
Aa Ad Ac
KA1
R Aa Ba Bb C Ac Ac Ad
J3
R Aa Ba Bb C Ac Ad D
CA10
Aa Aa Ba Bb C Ac Ad D
IC177
R Aa C Ba Bb Ac Ad

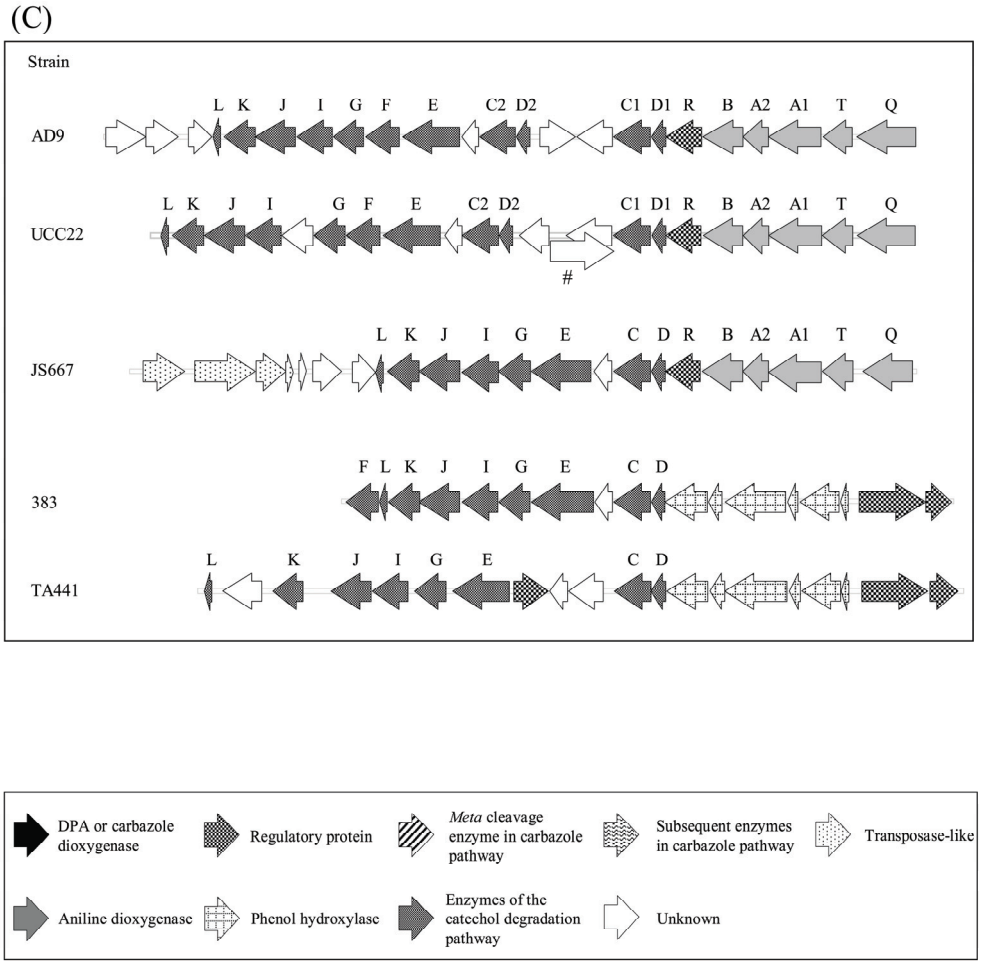


**Figure 3.3** Comparative analysis of the genes encoding DPA degradation in strain JS667. (A) Genes and G+C content of the gene cluster (30,579 bp) encoding the complete degradation of DPA from JS667. Transposon insertion sites in pJS702 are indicated by *. (B) The organization of the genes that encode DPA dioxygenase and carbazole dioxygenases from *Sphingomonas* sp. KA1, *Janthinobacterium* sp. J3, *P. resinovorans* CA10, and *N. aromaticivorans* IC177. (C) The organization of genes that encode the aniline degradation pathway from strain JS667, *Delftia tsuruhatensis* AD9, and *P. putida* UCC22 and that encode the phenol degradation pathway from *Burkholderia* sp. 383 and *Comamonas testosteroni* TA441. # Possible open reading frame in reverse orientation.

**Table 3.3** Identity of ORFs from gene cluster responsible for DPA degradation to selected genes.

| ORF; Gene | Length (aa)[a] | Putative Function | Most similar gene; Putative function; Source | % Identity | Accession no. |
|---|---|---|---|---|---|
| 1 | 323 | Regulatory protein (AraC-type) | Transcriptional regulator, AraC family; *Burkholderia* sp. 383 | 43 | YP_366764 |
| 2 | 252 (-)[b] | Regulatory protein (GntR-type) | *carRI*; Transcriptional regulator of the *car* operon; *Sphingomonas* sp. KA1 | 40 | YP_717982 |
| 3 | 128 (-) | Unknown | | | |
| 4; *dpaAa* | 382 | DPA dioxygenase | *carAa*; Carbazole 1,9a-dioxygenase; *Sphingomonas* sp. KA1 | 67 | YP_717981 |
| 5 | 89 | None | *carBaII*; 2'-Aminobiphenyl-2,3-diol 1,2-dioxygenase, subunit; *Sphingomonas* sp. KA1 | 57 | YP_717943 |
| 6 | 72 | None (Truncated) | *carBbI*; 2'-Aminobiphenyl-2,3-diol 1,2-dioxygenase, subunit; *Sphingomonas* sp. KA1 | 54 | YP_717979 |
| 7; *dpaAd* | 413 | Ferredoxin reductase | Ferredoxin reductase; *Phenylobacterium zucineum* HLK1 | 45 | YP_002129057 |
| 8; *dpaAc* | 106 | Ferredoxin | Ferredoxin; *Sphingomonas wittichii* RW1 | 49 | YP_001260794 |
| 9 | 79 | Unknown | | | |
| 10 | 117 | Unknown | *meta* pathway phenol degradation-like; *Burkholderia* sp. 383 | 27 | YP_373710 |
| 11 | 592 | None | Transposase, IS1071 family; *Comamonas sp*. CNB-1 | 99 | YP_001967728 |
| 12 | 529 (-) | None | Transposase, IS66 family; *R. eutropha* JMP134 | 95 | YP_293538 |
| 13 | 116 (-) | Unknown | Hypothetical protein; *R. eutropha* JMP134 | 99 | YP_293537 |
| 14 | 154 (-) | Unknown | Helix-turn-helix, Fis-type; *R. eutropha* JMP134 | 85 | YP_293536 |
| 15 | 358 | None | *tnpA-L1*; Transposase; *D. tsuruhatensis* AD9 | 100 | AAX47238 |
| 16 | 516 | Transposase | *istA*; Transposase, ISBmu3 family; *B. multivorans* ATCC17616 | 98 | YP_001945435 |
| 17 | 747 | Transposase | *istB*; Transposase, ISBmu3 family; *B. multivorans* ATCC17616 | 98 | YP_001945434 |
| 18 | 61 (-) | None | *tnpA-L1*; Transposase ; *D. tsuruhatensis* AD9 | 100 | AAX47238 |
| 19 | 73 | Unknown | *orfZ*; Muconate cycloisomerase; *D. tsuruhatensis* AD9 | 97 | AAX47261 |
| 20 | 243 | Unknown | *orfY*; Hydrolase/acyltransferase; *D. tsuruhatensis* AD9 | 94 | AAX47260 |
| 21 | 194 | Unknown | *orfX*; Transcriptional regulator, MarR family; *D. tsuruhatensis* AD9 | 99 | AAX47259 |

**Table 3.3 (Continued)** Identity of ORFs from gene cluster responsible for DPA degradation to selected genes.

| | | | | | |
|---|---|---|---|---|---|
| 22; *tdnL* | 63 (-) | 4-Oxalocrotonate tautomerase | *tadL*; 4-Oxalocrotonate tautomerase; *D. tsuruhatensis* AD9 | 96 | AAX47258 |
| 23; *tdnK* | 262 (-) | 4-Oxalocrotonate decarboxylase | *tadK*; 4-Oxalocrotonate decarboxylase; *D. tsuruhatensis* AD9 | 90 | AAX47257 |
| 24; *tdnJ* | 344 (-) | 4-Hydroxy-2-oxovalerate aldolase | *tadJ*; 4-Hydroxy-2-oxovalerate aldolase; *D. tsuruhatensis* AD9 | 86 | AAX47256 |
| 25; *tdnI* | 307 (-) | CoA-acylating acetaldehyde dehydrogenase | *cdoI*; Acetaldehyde dehydrogenase; *Comamonas* sp. JS765 | 83 | AAG17136 |
| 26; *tdnG* | 275 (-) | 2-Oxopent-4-dienoate hydratase | *btxK*; 2-Oxopent-4-dienoate hydratase; *Ralstonia sp. PHS1* | 75 | ABG82176 |
| 27; *tdnE* | 503 (-) | 2-Hydroxymuconic semialdehyde dehydrogenase | *btxJ*; 2-Hydroxymuconic semialdehyde dehydrogenase; *Ralstonia* sp. PHS1 | 83 | ABG82175 |
| 28 | 154 (-) | Unknown | Unknown; *Burkholderia* sp. 383 | 90 | YP_373718 |
| 29; *tdnC* | 314 (-) | Catechol 2,3-dioxygenase | Catechol 2,3-dioxygenase; *Burkholderia* sp. 383 | 95 | YP_373719 |
| 30; *tdnD* | 119 (-) | Ferredoxin | *tadD*; Plant-type ferredoxin; *D. tsuruhatensis* AD9 | 82 | AAX47245 |
| 31; *tdnR* | 295 (-) | Regulatory protein (LysR-type) | *tadR*; LysR-type regulator; *D. tsuruhatensis* AD9 | 99 | AAX47244 |
| 32; *tdnB* | 338 (-) | Reductase | *tdnB*; Electron transfer protein; *P. putida* UCC22 | 89 | BAA12809 |
| 33; *tdnA2* | 217 (-) | Aniline dioxygenase, small subunit | *tdnA2*; Aniline dioxygenase, small unit; *Frateuria* sp. ANA18 | 76 | BAC82527 |
| 34; *tdnA1* | 448 (-) | Aniline dioxygenase, large subunit | *tdnA1*; Aniline dioxygenase, large subunit; *P. putida* UCC22 | 87 | BAA12807 |
| 35; *tdnT* | 259 (-) | Unknown | *tdnT*; Unknown; *P. putida* UCC22 | 78 | BAA12806 |
| 36; Partial | 370 (-) | Unknown | *tadQ*; Unknown; *D. tsuruhatensis* AD9 | 84 | AAX47239 |

[a]aa, amino acids [b](-), reversed orientation

KA1 (Table 3.3). The consensus sequence for the binding of a [2Fe-2S] cluster in Rieske-type iron-sulfur proteins (35) and the mononuclear iron-binding residues (18) were conserved in ORF4 in the pattern $CXHX_{18}CX_2H$ from the 70$^{th}$ amino acid and $GX_2AXHX_3H$ from the 179$^{th}$ amino acid, respectively. The deduced amino acid sequences indicate that ORF7 and ORF8 are related to the ferredoxin reductase from *Phenylobacterium zucineum* HLK1 (45% identity) and the ferredoxin from *Sphingomonas wittichii* RW1 (49% identity), respectively. Conserved motifs for FAD-binding and NADH-binding sites (4) are found in ORF7. ORF8 contains four cysteine residues in the pattern $CX_5CX_2CX_{37}C$ from the 40$^{th}$ amino acid, typical of putidaredoxin-type [2Fe-2S] cluster ligands (3). ORF4, ORF7, and ORF8 are, therefore, designated *dpaAa*, *dpaAd*, and *dpaAc*, respectively.

### 3.4.6 Biotransformation of DPA by the fosmid clones

In order to determine the initial reaction in the DPA degradation pathway, cells of *E. coli* EPI300 harboring pJS7021 or pJS702 were tested for the ability to transform DPA. When DPA was transformed by *E. coli* EPI300 pJS7021 ($DPA^+$ and $catechol^-$), stoichiometric amounts of catechol and aniline accumulated (Fig. 3.4). Similar results (not shown) were obtained with pJS701 which has the same phenotype as pJS7021. When the experiment was repeated with *E. coli* EPI300 pJS702 ($DPA^+$ and $catechol^+$), only aniline accumulated (data not shown). The results clearly indicate that DPA is initially transformed to catechol and aniline, and then catechol is degraded without

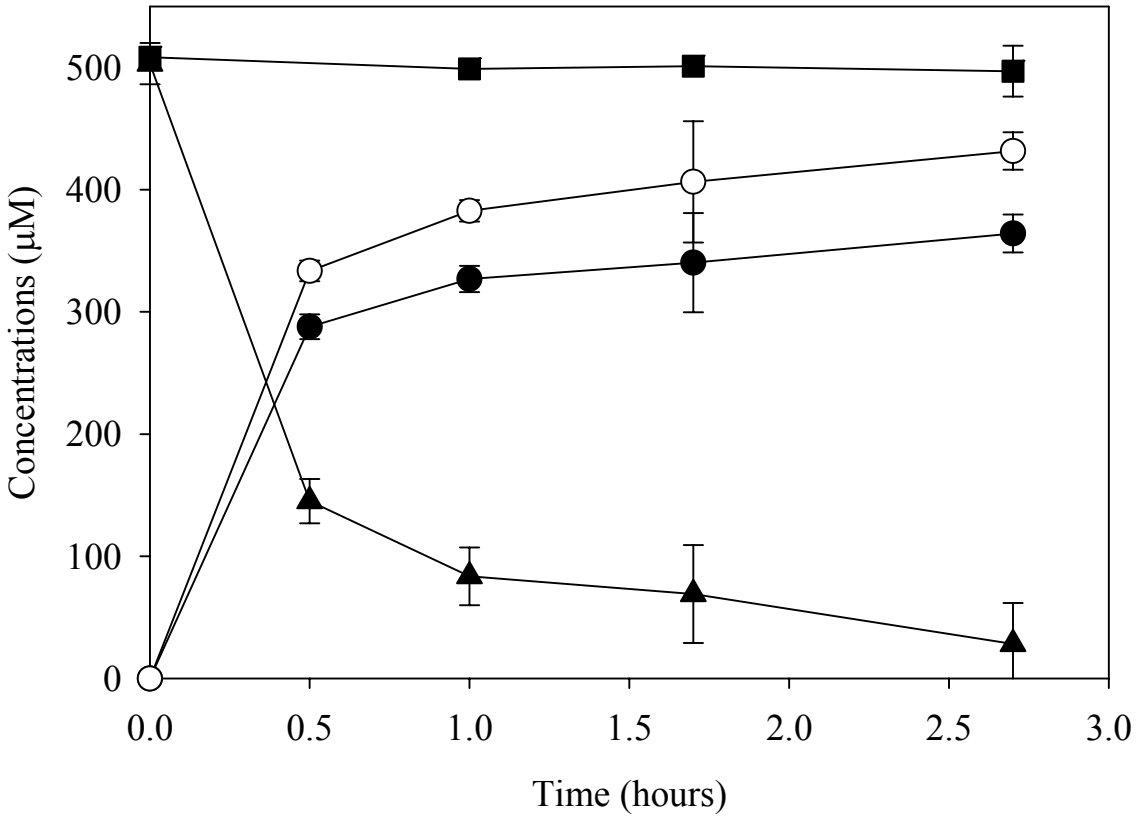


**Figure 3.4** DPA biotransformation by *E. coli* EPI300 pJS7021 ($DPA^+$ and $Cat^-$) (▲: DPA, ●: Aniline, ○: Catechol, ■: DPA in negative control). *E. coli* EPI300 pJS7022 ($DPA^-$ and $Cat^+$) served as a control. Cell suspensions (1 ml) were transferred to individual tubes and the reaction was initiated by the addition of DPA (500 μM). The cultures were incubated at 25°C with shaking.

accumulation in pJS702. The results are consistent with our failure to detect catechol in the medium of DPA degrading cultures.

### 3.4.7 Incorporation of $^{18}O_2$ into catechol

The reaction mechanism of DPA dioxygenase was rigorously determined by measuring $^{18}O_2/^{16}O_2$ incorporation. Cells of *E. coli* EPI300 pJS7021 ($DPA^+$, $catechol^-$) were incubated as above with DPA in an atmosphere that contained $^{18}O_2$ (56%) and $^{16}O_2$ (44%). At the end of the incubation period, the catechol that accumulated was a mixture of $^{18}O$-$^{18}O$ (52%) and $^{16}O$-$^{16}O$ (48%) with no detectable $^{16}O$-$^{18}O$ catechol (Fig. 3.5). The results clearly indicate that the initial enzyme functions as a dioxygenase by the incorporation of one molecule of oxygen into DPA to form an unstable intermediate that is converted to catechol and aniline.

### 3.4.8 Substrate specificities

The substrate specificity of the DPA dioxygenase encoded on pJS701 ($DPA^+$ and $catechol^-$) was compared with that of carbazole dioxygenase from *Pseudomonas* sp. CA10. The lack of transformation of DPA by carbazole dioxygenase and the preference of DPA dioxygenase for DPA indicates that DPA dioxygenase is specialized for DPA (Table 3.4). In a separate experiment, cells expressing DPA dioxygenase transformed 3-hydroxydiphenylamine (27%) and 4-hydroxydiphenlamine (30%) of the rate of DPA

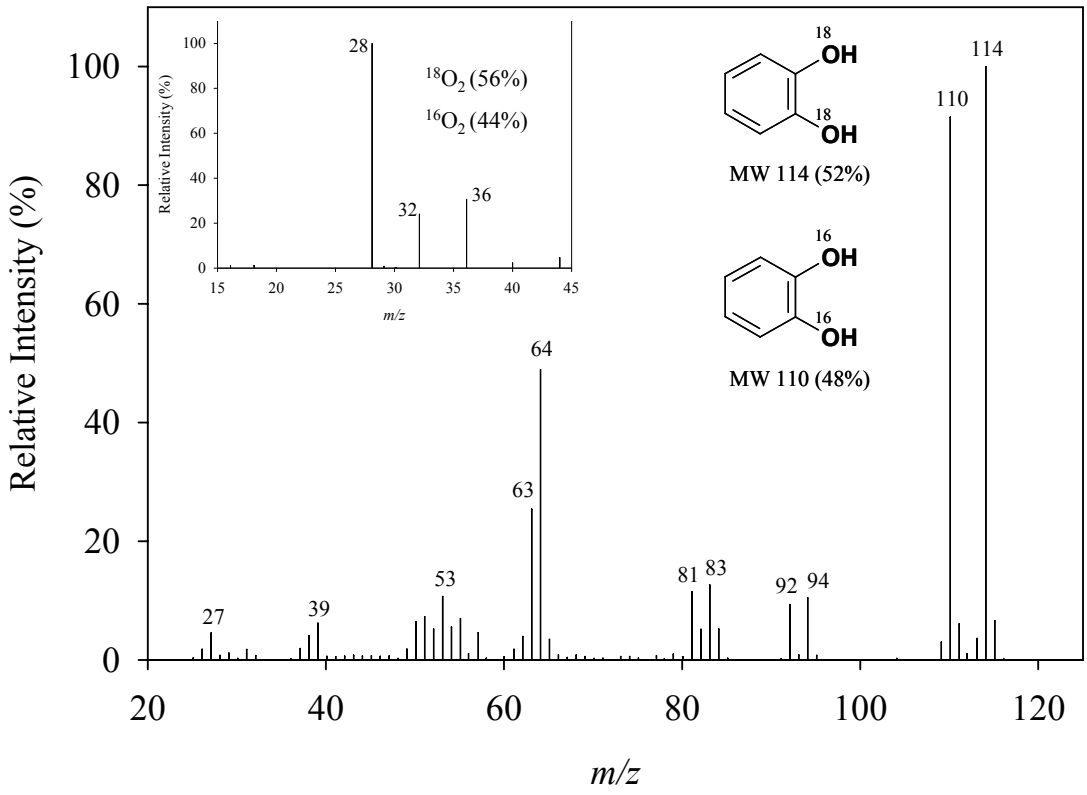


**Figure 3.5** Mass spectrum of catechol produced from DPA by cells of *E. coli* EPI300 pJS7021 ($DPA^+$, $Catechol^-$). Mass spectrum of gas phase (Inset). Incubation conditions were similar to Fig. 3.4 except that the headspace of the reaction vessel contained a mixture of $^{18}O_2$ in air.

**Table 3.4** Substrate specificities of carbazole dioxygenase from *Pseudomonas* sp. CA10 and DPA dioxygenase from JS667.

| Substrate | Substrate degraded (%)[a] | |
|---|---|---|
| | Carbazole dioxygenase | DPA dioxygenase |
| Diphenylamine | 0.0 ± 0.7 | 53.3 ± 0.0 |
| Carbazole | 45.1 ± 1.5 | 20.3 ± 1.8 |
| Biphenyl[b] | 36.4 ± 0.8 | 15.8 ± 3.0 |
| Dibenzofuran | 16.5 ± 0.9 | 5.9 ± 4.6 |
| Naphthalene[b] | 38.5 ± 0.2 | 23.0 ± 2.2 |

Suspensions (1 ml) of *E.coli* clones expressing the indicated dioxygenase enzymes were incubated at 25 ºC with shaking. Cell density was adjusted to $OD_{600}$ of 6 in BLK medium.

[a] Substrate degraded (%) = 100 × (concentration in abiotic control – concentration in active culture)/(concentration in abiotic control). The values were obtained after 90 min incubation. Initial substrate concentration was 300 μM. The experiments were done in duplicate.

[b] Volatilization losses in abiotic controls after 90 min were 27% (naphthalene) and 5% (biphenyl).

transformation, which accounts for the stimulation of oxygen uptake by the two compounds (Table 3.2). The products of the transformation were not identified.

### 3.4.9 RT-PCR amplification

The results from RT-PCR clearly indicate that DPA, aniline, and catechol dioxygenases are expressed in JS667 during growth on DPA (Fig. 3.6). The amplification of *dpaAa* in succinate grown cells of JS667 further supports the moderate constitutive expression of DPA dioxygenase. The *tdnC* encoding catechol 2,3-dioxygenase was not transcribed in succinate grown cells of JS667, which does not correspond to the moderate constitutive activities of catechol dioxygenase (Fig. 3.2 and Table 3.2). The presence of an additional catechol 2,3-dioxygenase encoded outside the region studied here would explain the observation (44). Negative results on PCR amplification of *tdnC* from pJS700 ($DPA^-$, $Catechol^+$) possessing a 40 kb genomic fragment of JS667 support the presence of the other catechol 2,3-dioxygenase (Data not shown).

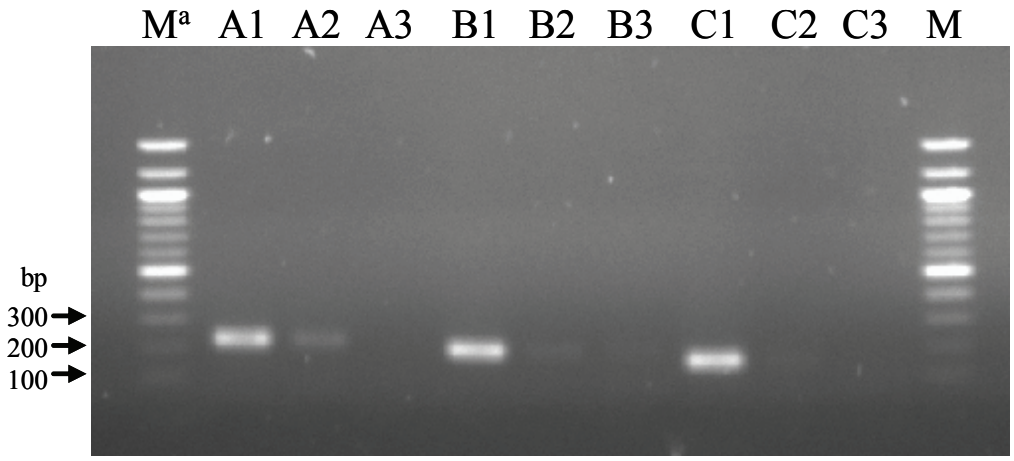


**Figure 3.6** RT-PCR amplifications of the genes that encode DPA (A), aniline (B), and catechol (C) dioxygenases from *Burkholderia* sp. JS667 grown on DPA (1) or succinate (2). RT-PCR without reverse transcriptase served as negative controls (3). M lanes contain the molecular size marker (Quick-Load 100 bp DNA ladder, New England Biolabs, Ipswich, MA).

## 3.5 DISCUSSION

Based on the stoichiometric aniline production and by analogy with related pathways, there are two possible DPA degradation pathways (Fig. 3.7). Attack by a dioxygenase at the 1,2 position would lead to the spontaneous conversion of the resulting compound to aniline and catechol (Fig. 3.7A). The initial reaction would be analogous to those catalyzed by aniline, diphenyl ether-, dibenzofuran-, and carbazole dioxygenases (2, 12, 37, 39). Alternatively, DPA dioxygenase could initially catalyze attack at the 2,3 position of the aromatic ring. The resulting *cis*-dihydrodiol intermediate would be converted to aniline and 2-hydroxymuconate via dehydrogenation, *meta* ring cleavage, and hydrolysis (Fig. 3.7B). The previous observation (40) that a modified biphenyl dioxygenase transforms DPA to the corresponding 2,3-dihydrodiol is consistent with pathway B. A binding model (13) suggests how biphenyl dioxygenase might acquire the ability to oxidize DPA at the 2,3-positon. The results with DPA dioxygenase (Fig. 3.4) indicate clearly, however, that DPA is initially converted to aniline and catechol (pathway A) which are then completely degraded via the common aniline degradation pathway (Fig. 3.7C).

Detection of hydroxydiphenylamine in culture supernatants and stimulation of oxygen uptake in DPA grown cells by hydroxydiphenylamine could be interpreted as evidence for sequential monooxygenase reactions or decomposition of a dihydrodiol intermediate. The $^{18}O_2$ experiment, however, precludes the possibility that sequential monooxygenations play a significant role in the degradation pathway. 2-

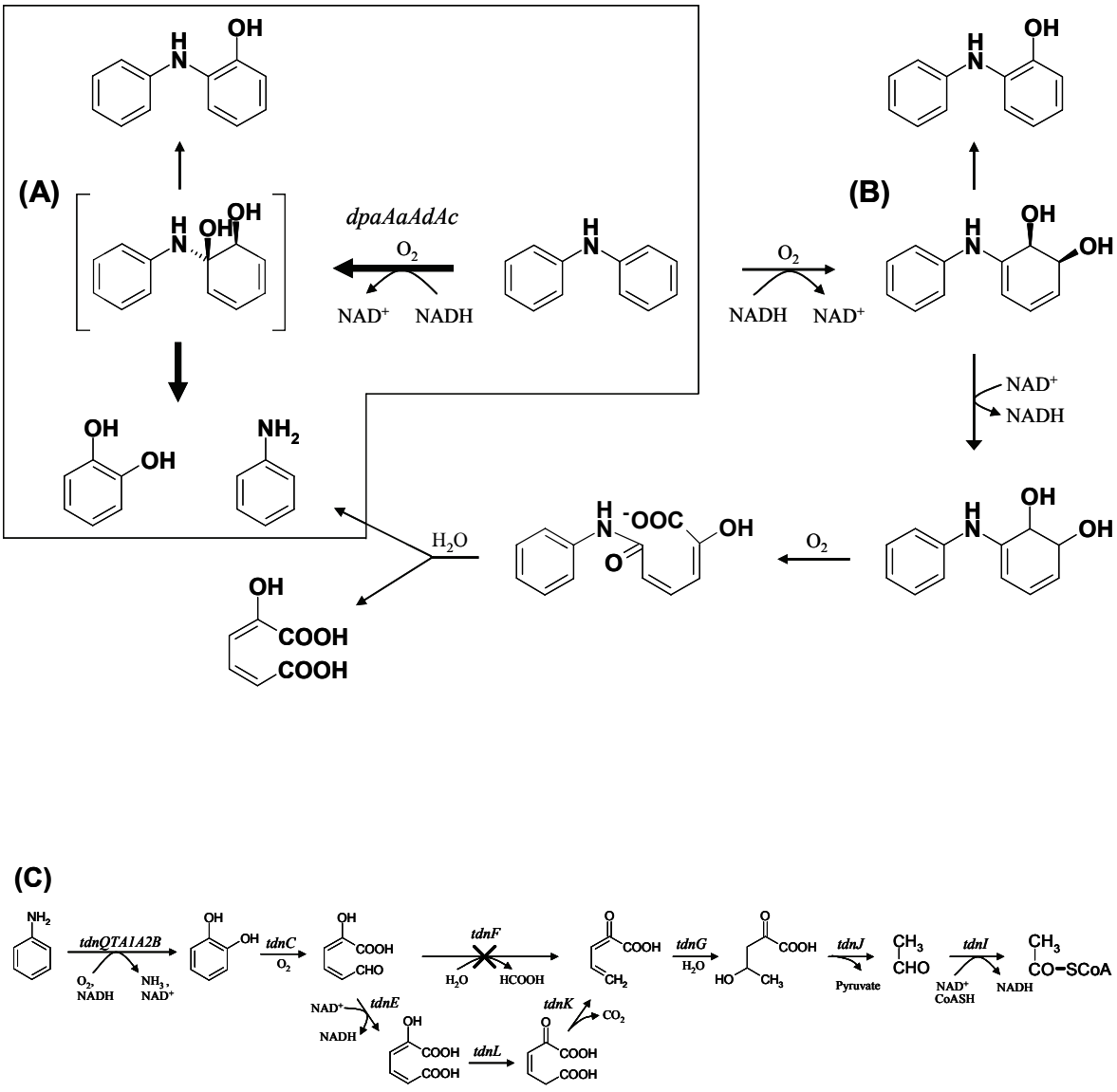


**Figure 3.7** Alternative DPA degradation pathways (A and B) and the subsequent aniline/catechol degradation pathway (C) (Pathways A and C are supported by results of this study).

X: The hydrolytic branch in the *meta* cleavage pathway is not predicted in JS667.

hydroxydiphenylamine appears to be a minor side product. The role and extent of participation of the hydroxydiphenylamines are currently under investigation.

The DPA dioxygenase system comprising a terminal dioxygenase component (*dpaAa*), ferredoxin reductase (*dpaAd*), and ferredoxin (*dpaAc*) is not readily classified by the previous classification systems for Rieske non-heme iron oxygenases that hydroxylate aromatic rings (22, 28). The *dpaAa* is phylogenetically related to *carAa* of carbazole 1,9a-dioxygenases that catalyze attack at the angular position of carbazole (Fig. 3.8). The oxygenase components listed in Fig. 3.8 have a single subunit and they form a clade distinct from the multicomponent dioxygenases composed of large (α) and small (β) oxygenase subunits including: aromatic acid dioxygenases, benzenoid dioxygenases, and naphthalene dioxygenases (28). The ferredoxin and ferredoxin reductase components of the electron transfer system of DPA dioxygenase (*dpaAdAc*) are closely related to those of Type IV dioxygenases including: dioxin dioxygenase (*Sphingomonas* sp. RW1), biphenyl dioxygenase (*Rhodococcus* sp. RHA1), and toluene dioxygenase (*P. putida* F1) (22).

The organization of the genes that encode the DPA dioxygenase enzyme system is similar, but not identical to that of the well conserved *car* degradative operons (Fig. 3.3B). The main differences are that the order of ferredoxin (*carAc*) and ferredoxin reductase (*carAd*) is reversed in JS667 and that the hydrolase gene (*carC*) is not found in JS667. CarC catalyzes the hydrolysis of the *meta* cleavage product of 2'-aminobiphenyl-2,3-diol to anthranilate and 2-hydroxypenta-2,4-dienoate. The hydrolysis is not necessary in pathway A (Fig. 3.7). The differences raise questions about how the two dioxygenase

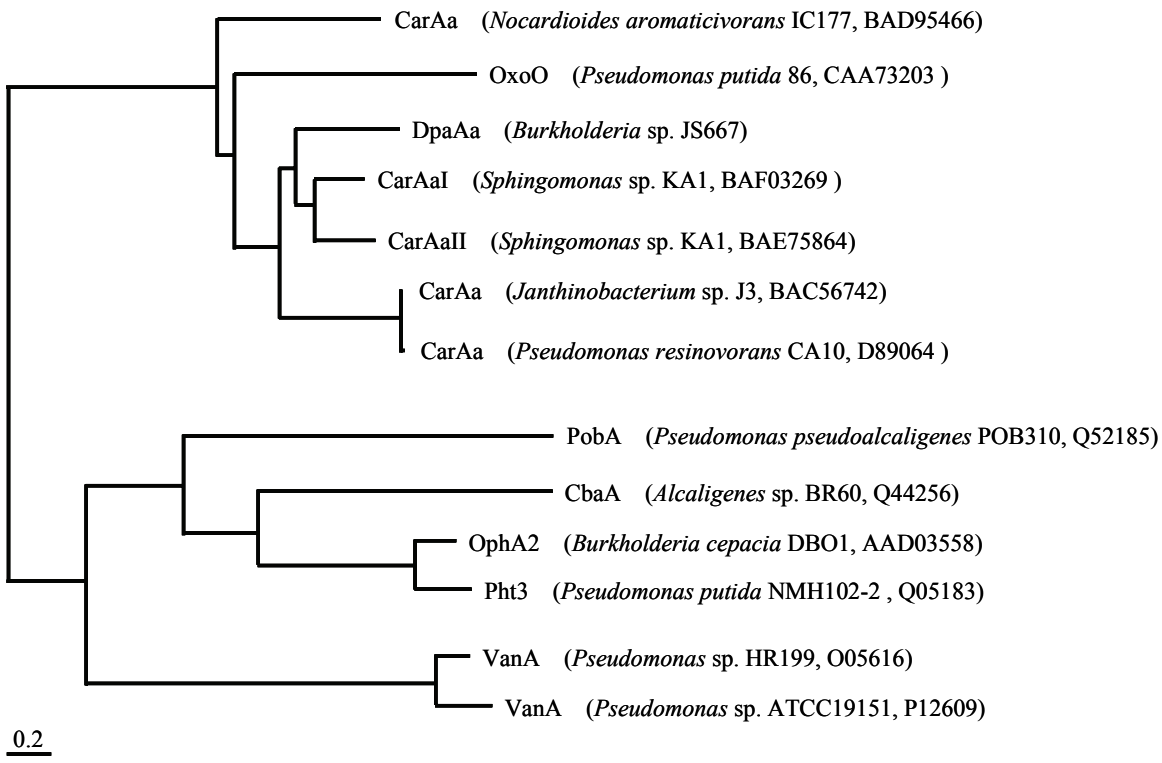


**Figure 3.8** Phylogenetic relationships of the terminal oxygenase component (DpaAa) in DPA degradation and homologs selected from results of protein BLAST (BLASTP) search. BphA1 from *Pseudomonas* sp. B4, AAB88813 was used as an outgroup. The scale bar denotes 0.2 amino acid substitution per site. The tree was constructed by the neighbor-joining method. GenBank accession numbers are indicated after strain designations.

systems divergently evolved from a common ancestor. The presence of three vestigial genes (ORFs 3, 9, and 10) and transposon remnants suggest relatively recent evolution of the DPA dioxygenase system in JS667.

ORF5 and ORF6 showed substantial amino acid identity to CarBa (57%) and CarBb (54%), the two subunits of the 2,3-dihydroxybiphenyl *meta* cleavage enzyme from *Sphingomonas* sp. KA1. CarB has about 20 times higher activity for 2,3-dihydroxybiphenyl than for catechol (38). The size of the product of ORF6, however, is about one third the size of CarBb (catalytic subunit) from carbazole degraders. Approximately 170 amino acids in the N-terminal region of CarBb including the active site histidine residues are missing in ORF6 (43). The observation explains the absence of 2,3-dihydroxybiphenyl-1,2-dioxygenase activity in extracts prepared from cells of JS667. The truncation of the *meta* cleavage enzyme in JS667 might help to avoid misrouting of the metabolites produced from DPA or structurally similar compounds. The inactivation of an extraneous *meta* cleavage gene was previously proposed as a step in the evolution of chlorobenzene-degrading bacteria, where it seems to prevent misrouting of chlorocatechol (27, 50). The presence of the truncated CarBb that functions in carbazole degradation, but not in DPA degradation provides strong evidence for the origin of the gene cluster that encodes DPA dioxygenase. The argument is analogous to the truncated salicylate hydroxylase that revealed the evolutionary origins of the nitroarene dioxygenase in 2,4-DNT degrading bacteria (10, 19).

Constitutive expression of DPA dioxygenase in JS667 is reminiscent of the expression of carbazole dioxygenases (26). In that system two different promoters located upstream of the gene that encodes the terminal dioxygenase component cause constitutive

and inducible expression of the *car* operon. The regulatory protein (CarR) negatively controls the inducible expression. 2-Hydroxy-6-oxo-6-(2'-aminophenyl)hexa-2,4-dienoate, an intermediate in carbazole degradation functions as the inducer of the expression of the *car* operon (26). The inducer is not an intermediate in DPA biodegradation. The presence of a *carR*-like gene (ORF2) and two different putative promoter sequences 204- and 323-bp upstream of *dpaAa* suggest a similar regulation pattern in JS667. The promoter sequences, however, seem unrelated to those of the *car* operon, perhaps due to the different evolutionary history of the two dioxygenase systems. ORF1 belongs to the AraC/XylS family of transcriptional regulators that function as transcriptional activators in catabolic operons (46). We are currently investigating how the two different regulatory proteins are involved in the expression of DPA dioxygenase.

Genes that encode the aniline degradation pathway in JS667 are compactly organized without extraneous elements (Fig. 3.3C and Table 3.3), which suggests that evolution of the aniline degradative operon preceded recruitment of the gene cluster that encodes DPA dioxygenase. Gene duplication (*tdnC1D1* and *tdnC2D2*) and unknown ORFs between the duplications are present in the other aniline degraders, strain AD9 and UCC22 but not in JS667. The extraneous elements are considered evolutionary remnants resulting from the recombination of two different gene clusters that encode aniline dioxygenase and the *meta* pathway enzymes (11). Highly identical unknown ORFs 15 and 18-21 among the aniline degraders suggests that similar evolutionary processes have been occurring during the development of the aniline degradative operon and that some of the unknown orfs perform an important function. On the other hand, the organization of genes that encode the *meta* cleavage pathway in JS667 is identical to that of the hypothetical phenol

degradative operon in *Burkholderia* sp. 383, the phylogenetically closest relative to JS667 in the database. The only difference is that the gene (*tdnF*) that encodes 2-hydroxymuconic semialdehyde hydrolase is absent in JS667, which suggests that catechol is degraded via the 4-oxalocrotonate branch in JS667 (Fig. 3.7C) (1, 16).

The recruitment of the genes encoding DPA dioxygenase would be sufficient to allow the relatively common aniline degrading bacteria to grow with DPA as a sole source of carbon, nitrogen, and energy. The hypothesis is supported by several lines of evidence: the significant differences in GC content between the gene clusters that encode DPA dioxygenase and the aniline degradation pathway, several transposon remnants (ORFs 11, 12, and 15-18) between the gene clusters, and the relatively well organized aniline degradative operon without superfluous genetic material compared to the genes that encode DPA dioxygenase. The immature organization seems to contradict the expectation that the genes encoding the degradation pathways of naturally occurring compounds are often linked in operons without superfluous genetic material. It seems reasonable to speculate that the system was assembled in response to contamination by DPA. Such a scenario was strongly supported for assembly of a chlorobenzene degradation pathway in response to chlorobenzene contamination (27, 48). We are currently isolating new DPA degraders to determine their distribution in the environment and the organization of the genes that encode DPA degradation, which will provide additional insight about the evolution of the DPA degradation pathway.

## 3.6 REFRENCES


1. **Arai, H., T. Ohishi, M. Y. Chang, and T. Kudo.** 2000. Arrangement and regulation of the genes for *meta*-pathway enzymes required for degradation of phenol in *Comamonas testosteroni* TA441. Microbiology **146:**1707-1715.
2. **Armengaud, J., B. Happe, and K. N. Timmis.** 1998. Genetic analysis of dioxin dioxygenase of *Sphingomonas* sp. strain RW1: catabolic genes dispersed on the genome. J. Bacteriol. **180:**3954-3966.
3. **Armengaud, J., and K. N. Timmis.** 1997. Molecular characterization of Fdx1, a putidaredoxin-type [2Fe-2S] ferredoxin able to transfer electrons to the dioxin dioxygenase of *Sphingomonas* sp. RW1. Eur. J. Biochem. **247:**833-842.
4. **Armengaud, J., and K. N. Timmis.** 1998. The reductase RedA2 of the multi-component dioxin dioxygenase system of *Sphingomonas* sp. RW1 is related to class-I cytochrome $P_{450}$-type reductases. Eur. J. Biochem. **253:**437-444.
5. **Asturias, J. A., and K. N. Timmis.** 1993. Three different 2,3-dihydroxybiphenyl-1,2-dioxygenase genes in the gram-positive polychlorobiphenyl-degrading bacterium *Rhodococcus globerulus* P6. J. Bacteriol. **175:**4631-4640.
6. **Bruhn, C., H. Lenke, and H. J. Knackmuss.** 1987. Nitrosubstituted aromatic compounds as nitrogen source for bacteria. Appl. Environ. Microbiol. **53:**208-210.
7. **Drzyzga, O.** 2003. Diphenylamine and derivatives in the environment: a review. Chemosphere **53:**809-818.
8. **Drzyzga, O., and K. H. Blotevogel.** 1997. Microbial degradation of diphenylamine under anoxic conditions. Curr. Microbiol. **35:**343-347.
9. **Drzyzga, O., S. Jannsen, and K. H. Blotevogel.** 1995. Toxicity of diphenylamine and some of its nitrated and aminated derivatives to the luminescent bacterium *Vibrio fischeri*. Ecotoxicol. Environ. Saf. **31:**149-152.
10. **Fuenmayor, S. L., M. Wild, A. L. Boyes, and P. A. Williams.** 1998. A gene cluster encoding steps in conversion of naphthalene to gentisate in *Pseudomonas* sp. strain U2. J. Bacteriol. **180:**2522-2530.

11. **Fukumori, F., and C. P. Saint.** 2001. Complete nucleotide sequence of the catechol metabolic region of plasmid pTDN1. J. Gen. Appl. Microbiol. **47:**329-333.

12. **Fukumori, F., and C. P. Saint.** 1997. Nucleotide sequences and regulational analysis of genes involved in conversion of aniline to catechol in *Pseudomonas putida* UCC22(pTDN1). J. Bacteriol. **179:**399-408.

13. **Furukawa, K., H. Suenaga, and M. Goto.** 2004. Biphenyl dioxygenases: functional versatilities and directed evolution. J. Bacteriol. **186:**5189-5196.

14. **Gardner, A. M., G. H. Alvarez, and Y. Ku.** 1982. Microbial degradation of $^{14}$C-diphenylamine in a laboratory model sewage sludge system. Bull. Environ. Contam. Toxicol. **28:**91-96.

15. **Haigler, B. E., W. C. Suen, and J. C. Spain.** 1996. Purification and sequence analysis of 4-methyl-5-nitrocatechol oxygenase from *Burkholderia* sp. strain DNT. J. Bacteriol. **178:**6019-6024.

16. **He, Z., R. E. Parales, J. C. Spain, and G. R. Johnson.** 2007. Novel organization of catechol *meta* pathway genes in the nitrobenzene degrader *Comamonas* sp. JS765 and its evolutionary implication. J. Ind. Microbiol. Biotechnol. **34:**99-104.

17. **Inoue, K., H. Habe, H. Yamane, and H. Nojiri.** 2006. Characterization of novel carbazole catabolism genes from gram-positive carbazole degrader *Nocardioides aromaticivorans* IC177. Appl. Environ. Microbiol. **72:**3321-3329.

18. **Jiang, H., R. E. Parales, N. A. Lynch, and D. T. Gibson.** 1996. Site-directed mutagenesis of conserved amino acids in the alpha subunit of toluene dioxygenase: Potential mononuclear non-heme iron coordination sites. J. Bacteriol. **178:**3133-3139.

19. **Johnson, G. R., R. K. Jain, and J. C. Spain.** 2002. Origins of the 2,4-dinitrotoluene pathway. J. Bacteriol. **184:**4219-4232.

20. **Karawya, M. S., S. M. Abdel Wahab, M. M. El-Olemy, and N. M. Farrag.** 1984. Diphenylamine, an antihyperglycemic agent from onion and tea. J. Nat. Prod. **47:**775-780.

21. **Kim, E., and G. J. Zylstra.** 1995. Molecular and biochemical characterization of two *meta*-cleavage dioxygenases involved in biphenyl and *m*-xylene degradation by *Beijerinckia* sp. strain B1. J. Bacteriol. **177:**3095-3103.

22. **Kweon, O., S. J. Kim, S. Baek, J. C. Chae, M. D. Adjei, D. H. Baek, Y. C. Kim, and C. E. Cerniglia.** 2008. A new classification system for bacterial Rieske non-heme iron aromatic ring-hydroxylating oxygenases. BMC Biochem. **9:**11.

23. **Lessner, D. J., G. R. Johnson, R. E. Parales, J. C. Spain, and D. T. Gibson.** 2002. Molecular characterization and substrate specificity of nitrobenzene dioxygenase from *Comamonas* sp. strain JS765. Appl. Environ. Microbiol. **68:**634-641.

24. **Liang, Q., M. Takeo, M. Chen, W. Zhang, Y. Xu, and M. Lin.** 2005. Chromosome-encoded gene cluster for the metabolic pathway that converts aniline to TCA-cycle intermediates in *Delftia tsuruhatensis* AD9. Microbiology **151:**3435-3446.

25. **Lussier, L. S., and H. Gagnon.** 2000. On the chemical reactions of diphenylamine and its derivatives with nitrogen dioxide at normal storage temperature. Propellants, Explosives, Pyrotechnics **25:**117-125.

26. **Miyakoshi, M., M. Urata, H. Habe, T. Omori, H. Yamane, and H. Nojiri.** 2006. Differentiation of carbazole catabolic operons by replacement of the regulated promoter via transposition of an insertion sequence. J. Biol. Chem. **281:**8450-8457.

27. **Muller, T. A., C. Werlen, J. Spain, and J. R. Van Der Meer.** 2003. Evolution of a chlorobenzene degradative pathway among bacteria in a contaminated groundwater mediated by a genomic island in *Ralstonia*. Environ. Microbiol. **5:**163-173.

28. **Nam, J. W., H. Nojiri, T. Yoshida, H. Habe, H. Yamane, and T. Omori.** 2001. New classification system for oxygenase components involved in ring-hydroxylating oxygenations. Biosci. Biotechnol. Biochem. **65:**254-263.

29. **Nishino, S. F., G. C. Paoli, and J. C. Spain.** 2000. Aerobic degradation of dinitrotoluenes and pathway for bacterial degradation of 2,6-dinitrotoluene. Appl. Environ. Microbiol. **66:**2139.

30. **Nishino, S. F., and J. C. Spain.** 1995. Oxidative pathway for the biodegradation of nitrobenzene by *Comamonas* sp. stranin JS765. Appl. Environ. Microbiol. **61:**2308-2313.

31. **Nojiri, H., H. Habe, and T. Omori.** 2001. Bacterial degradation of aromatic compounds via angular dioxygenation. J. Gen. Appl. Microbiol. **47:**279-305.

32. **Ohtsubo, Y., H. Genka, H. Komatsu, Y. Nagata, and M. Tsuda.** 2005. High-temperature-induced transposition of insertion elements in *Burkholderia multivorans* ATCC 17616. Appl. Environ. Microbiol. **71:**1822-1828.

33. **Page, R. D.** 1996. TreeView: an application to display phylogenetic trees on personal computers. Comput. Appl. Biosci. **12:**357-358.

34. **Rehmann, L., and A. J. Daugulis.** 2006. Biphenyl degradation kinetics by *Burkholderia xenovorans* LB400 in two-phase partitioning bioreactors. Chemosphere **63:**972-979.

35. **Rieske, J. S., D. H. Maclennan, and R. Coleman.** 1964. Isolation and properties of an iron-protein from the (reduced coenzyme Q)-cytochrome C reductase complex of the respiratory chain. Biochem. Biophys. Res. Commun. **15:**338-344.

36. **Rudell, D. R., J. P. Mattheis, and J. K. Fellman.** 2005. Evaluation of diphenylamine derivatives in apple peel using gradient reversed-phase liquid chromatography with ultraviolet-visible absorption and atmospheric pressure chemical ionization mass selective detection. J. Chromatogr. A. **1081:**202-209.

37. **Sato, S. I., J. W. Nam, K. Kasuga, H. Nojiri, H. Yamane, and T. Omori.** 1997. Identification and characterization of genes encoding carbazole 1,9a-dioxygenase in *Pseudomonas* sp. strain CA10. J. Bacteriol. **179:**4850-4858.

38. **Sato, S. I., N. Ouchiyama, T. Kimura, H. Nojiri, H. Yamane, and T. Omori.** 1997. Cloning of genes involved in carbazole degradation of *Pseudomonas* sp. strain CA10: nucleotide sequences of genes and characterization of *meta*-cleavage enzymes and hydrolase. J. Bacteriol. **179:**4841-4849.

39. **Schmidt, S., R. M. Wittich, D. Erdmann, H. Wilkes, W. Francke, and P. Fortnagel.** 1992. Biodegradation of diphenyl ether and its monohalogenated derivatives by *Sphingomonas* sp. strain SS3. Appl. Environ. Microbiol. **58:**2744-2750.

40. **Shindo, K., R. Nakamura, I. Chinda, Y. Ohnishi, S. Horinouchi, H. Takahashi, K. Iguchi, S. Harayama, K. Furukawa, and N. Misawa.** 2003. Hydroxylation of ionized aromatics including carboxylic acid or amine using recombinant *Streptomyces lividans* cells expressing modified biphenyl dioxygenase genes. Tetrahedron **59:**1895-1900.

41. **Spain, J. C., and S. F. Nishino.** 1987. Degradation of 1,4-dichlorobenzene by a *Pseudomonas* sp. Appl. Environ. Microbiol. **53:**1010-1019.

42. **Spain, J. C., G. J. Zylstra, C. K. Blake, and D. T. Gibson.** 1989. Monohydroxylation of phenol and 2,5-dichlorophenol by toluene dioxygenase in *Pseudomonas putida* F1. Appl. Environ. Microbiol. **55:**2648-2652.

43. **Spence, E. L., M. Kawamukai, J. Sanvoisin, H. Braven, and T. D. H. Bugg.** 1996. Catechol dioxygenases from *Escherichia coli* (MhpB) and *Alcaligenes eutrophus* (MpcI): Sequence analysis and biochemical properties of a third family of extradiol dioxygenases. J. Bacteriol. **178:**5249-5256.

44. **Suzuki, K., A. Ichimura, N. Ogawa, A. Hasebe, and K. Miyashita.** 2002. Differential expression of two catechol 1,2-dioxygenases in *Burkholderia* sp. strain TH2. J. Bacteriol. **184:**5714-5722.

45. **Thompson, J. D., D. G. Higgins, and T. J. Gibson.** 1994. CLUSTAL W: improving the sensitivity of progressive multiple sequence alignment through sequence weighting, position-specific gap penalties and weight matrix choice. Nucleic Acids Res. **22:**4673-4680.

46. **Tropel, D., and J. R. van der Meer.** 2004. Bacterial transcriptional regulators for degradation pathways of aromatic compounds. Microbiol. Mol. Biol. Rev. **68:**474-500.

47. **Urata, M., E. Uchida, H. Nojiri, T. Omori, R. Obo, N. Miyaura, and N. Ouchiyama.** 2004. Genes involved in aniline degradation by *Delftia acidovorans* strain 7N and its distribution in the natural environment. Biosci. Biotechnol. Biochem. **68:**2457-2465.

48. **van der Meer, J. R., C. Werlen, S. F. Nishino, and J. C. Spain.** 1998. Evolution of a pathway for chlorobenzene metabolism leads to natural attenuation in contaminated groundwater. Appl. Environ. Microbiol. **64:**4185-4193.

49. **Weisburg, W. G., S. M. Barns, D. A. Pelletier, and D. J. Lane.** 1991. 16S ribosomal DNA amplification for phylogenetic study. J. Bacteriol. **173:**697-703.

50. **Werlen, C., H. P. Kohler, and J. R. van der Meer.** 1996. The broad substrate chlorobenzene dioxygenase and *cis*-chlorobenzene dihydrodiol dehydrogenase of *Pseudomonas* sp. strain P51 are linked evolutionarily to the enzymes for benzene and toluene degradation. J. Biol. Chem. **271:**4009-4016.

51. **Wittich, R. M., H. Wilkes, V. Sinnwell, W. Francke, and P. Fortnagel.** 1992. Metabolism of dibenzo-*p*-dioxin by *Sphingomonas* sp. strain RW1. Appl. Environ. Microbiol. **58:**1005-1010.

# CHAPTER 4

# Biodegradation of Nitrobenzene, Aniline, and Diphenylamine at the Oxic/Anoxic Interface Between Sediment and Water

## 4.1 ABSTRACT

NB, aniline, and DPA are common contaminants at many aniline manufacturing sites. The release of these compounds from contaminated sediment to overlying water may pose a source of environmental exposure. The purpose of this study is to evaluate the aerobic biodegradation potential at the sediment/water interface to determine whether it is sufficient to eliminate the risk caused by the migration of the contaminants. Microcosm experiments with several samples from the interfaces showed that the three contaminants can be simultaneously degraded by bacteria associated with organic detritus at the sediment/water interface without any nutrient amendments. The presence of substantial populations able to grow on NB, aniline, or DPA was confirmed by most probable number (MPN) analysis and the bacteria responsible for the degradation were isolated. Degradation pathways employed by the isolates were tentatively identified by measuring the reaction products and metabolism of intermediates. In columns designed to simulate the sediment/water interface, the rates of NB degradation were 178 to 231 μg of NB/hr/$cm^3$ sediment when contaminated water passed through the thin layer of the interface samples. Mass balances of NB in the column were rigorously determined by the addition of $^{14}$C-ring-labeled NB. Radioactivity (58%) was recovered as $^{14}CO_2$ in the effluent. The results clearly indicate that NB can be mineralized as it transits the

sediment/water interface. This study provides the basis to establish the conditions for bioremediation and evaluate the potential for natural attenuation as a remedial strategy for contaminated sediments.

## 4.2 INTRODUCTION

Aniline is widely used as a feedstock for a variety of dyes and other organic products. It is made by the reduction of NB, which is often made by nitration of benzene at the manufacturing site. At many of the aniline manufacturing sites the groundwater and sediment are extensively contaminated with not only NB and aniline but also DPA, a byproduct of the process. The fate and transport of the above contaminants are of a great concern at contaminated sites where an anoxic contaminant plume emerges into a water body. The release of the toxic chemicals to overlying water poses a potential source of environmental exposure. The purpose of this study was to evaluate the impact of biodegradation on the transport of the three contaminants across the sediment/water interface.

The degradation mechanisms and bacteria responsible are well established for the biodegradation of NB, aniline, and DPA (1, 2, 7, 8, 11) (Fig. 4.1). There are two aerobic pathways for the degradation of NB. The most common involves the partial reduction of the nitro group to the hydroxylamine and then rearrangement to 2-aminophenol, which is mineralized (7). The alternative pathway involves an initial dioxygenase catalyzed removal of the nitro group as nitrite and the resultant catechol is mineralized (8). Similarly, aniline and DPA degradation under aerobic conditions are initiated by a dioxygenase attack at the carbon atom that is bonded to the nitrogen and then the

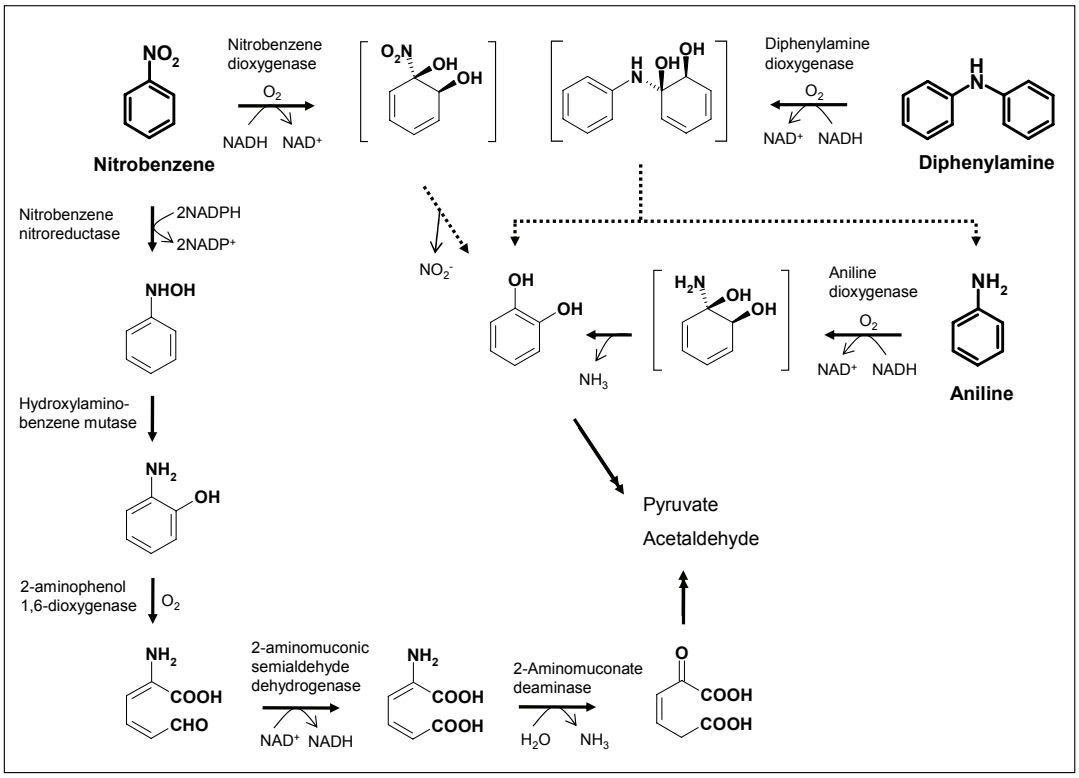


**Figure 4.1** Biodegradation pathways of NB, aniline, and DPA.

resulting products of the degradation are mineralized (6, 11).

Based on the understanding of the biodegradability and bacteria responsible it is relatively simple to evaluate the biodegradation potentials of chemicals in various matrices by identifying the following factors: i) the presence and distribution of appropriate bacteria, ii) the intermediates, endpoints, and final products, iii) the effect of mixtures of contaminants on the processes, and iv) other site-specific conditions such as the temperature, pH, oxygen, or nutrients. It is, however, not as simple to evaluate the impact of biodegradation on the behavior of the contaminants as they are transported across the interface between the anaerobic sediment and the overlying water.

One of the compelling questions at the Repauno site is the fate and transport of the above contaminants released from the sediment to overlying water (Fig. 4.2). There is migration of the groundwater from the subsurface toward the overlying water in the ditch. Although the groundwater and the sediment are extensively contaminated with NB, aniline, and DPA nitrobenzene is the main compound driving the risk at the site.

The overlying water contains negligible concentrations of the contaminants. Our hypothesis is that the sediments are anaerobic and that the lack of oxygen limits the biodegradation. As the contaminants migrate into the aerobic zone between the sediment and the overlying water there should be considerable potential for biodegradation by aerobic bacteria at the interface. Such a scenario is analogous to that in natural aquatic ecosystems where substantial populations of aerobic in the sediment/water interface prevent the escape of the methane produced in underlying anoxic sediment layers (4, 5, 10). The experiments described here were designed to evaluate the aerobic

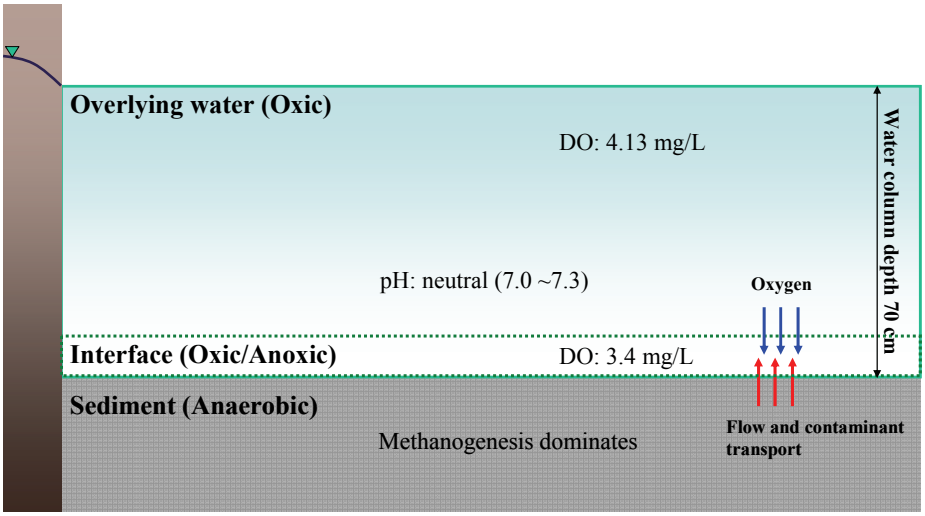


**Figure 4.2** Schematic view of a ditch at Repauno.

biodegradation potential of NB, aniline, and DPA at the sediment/water interface to determine whether it is sufficient to eliminate the transfer of contaminants to the overlying water.

## 4.3 MATERIALS AND METHODS

### 4.3.1 Microcosm construction

Sample collection was carried out by DuPont/URS Diamond field personnel on Sep 2005, May 2007, and Oct 2007. The samples were collected from the light organic layer at the surface of the sediment at various locations at the Repauno site. The pH of the samples was neutral and temperature was around 16 °C. Concentrations of ammonium and nitrite ions ranged 0.02 – 0.58 and 0.13 – 1.47 mg/L, respectively. Half of each sample was filter sterilized and the resulting filtered site water was used as the aqueous medium for microcosms. Non-filtered samples served as the inocula for the microcosm. The filtered material was dried in an oven (110 °C) to determine the dry weight of sediment actually added to microcosms. Microcosms were constructed in glass tubes (200 mm X 25 mm) sealed with Teflon-lined screw caps and consisted of sediment (5~60 mg dry weight) in 20 ml of the filter sterilized site water or nitrogen-free mineral salts medium (BLK) (3). Two active cultures and one killed control were prepared for each treatment. The elimination of biological activity for killed controls was achieved by autoclaving. NB and aniline (100 ~ 200 μM) were directly added to the liquid medium. DPA (1 M) in acetone was added to the glass tubes to yield a final concentration of approximately 100 μM and acetone was allowed to evaporate prior to addition of the slurries. Microcosms were incubated at room temperature on a Bellco roller drum

operated at 17 rpm.

### 4.3.2 Nitrobenzene degradation rate determination

To determine the rate of nitrobenzene degradation in μg of NB degraded/hr/mg of sediment, microcosms were prepared with different amounts of inocula (between 5 mg and 60 mg of sediment). Three active cultures and one killed control were prepared for each treatment as above. The rate constant (μg of NB degraded/hr) was determined under the assumption that NB degradation obeys zero-order kinetics after the lag period. A linear regression was conducted to obtain overall rate constants in units of μg of NB degraded/hr/mg of sediment.

### 4.3.3 Most probable number analysis

Samples were homogenized with a Molecular Grinding Resin (Geno Tech. Inc., St. Louis, MO) and then used in the enumeration of NB-degrading bacteria by most-probable-number (MPN) techniques. Serial dilutions of each sample were made in BLK media (3) in sterile 96-well microtiter plates (serial dilution of 8 replicates each) for MPN analysis. Plates were incubated in an atmosphere of nitrobenzene and changes in $A_{600}$ were measured in a microplate spectrophotometer for two weeks. Alternatively, accumulation of ammonium ions (9) was measured after the incubation to validate the turbidity measurement. For enumeration of aniline and DPA degraders, BLK media

containing 500 μM aniline or DPA was used. MPN was calculated from an 8-tube MPN table with 95% confidence limits.

### 4.3.4 Analytical Methods

HPLC analysis of NB, aniline, and DPA was performed with a Varian HPLC system equipped with a diode array detector. The compounds were separated by paired ion chromatography on a chromolith column (5 um, 4 mm x 8 cm). The mobile phase consisted of part A (5 mM PIC A low-UV reagent [Waters brand of tetrabutylammonium hydrogen sulfate] in 30% HPLC grade methanol-70% water) and part B (70% HPLC grade methanol-30% water). The flow rate was 3 ml/min. The mobile phase was changed from 100 % part A to 100 % part B over a 2-min period, and then 100 % part B for 2 min. Aniline was monitored at $A_{230,}$ NB was monitored at $A_{260}$, and DPA was monitored at $A_{280.}$ Alternatively, NB was analyzed with an isocratic mobile phase composed of 50% methanol-50% water. The flow rate was 1 ml/min

### 4.3.5 Column design

Samples collected from the light organic layer at the surface of the sediment were supported on Teflon frits (20 μm pore sized) in glass columns (1.2 cm ID X 2.5 cm length) and the column was sealed with Teflon stoppers (Fig. 4.3A). Stainless tubing (0.125 in. OD and 0.02 in. wall) was used for all connections to prevent the sorption of NB. Two active columns and one control column served for one set of experiments.

A.

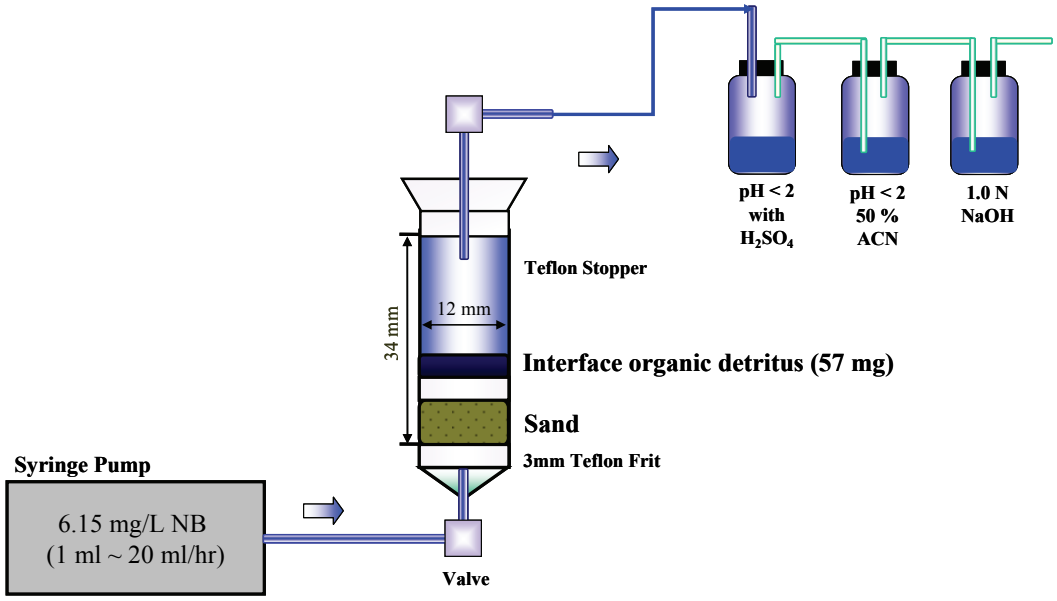


B.

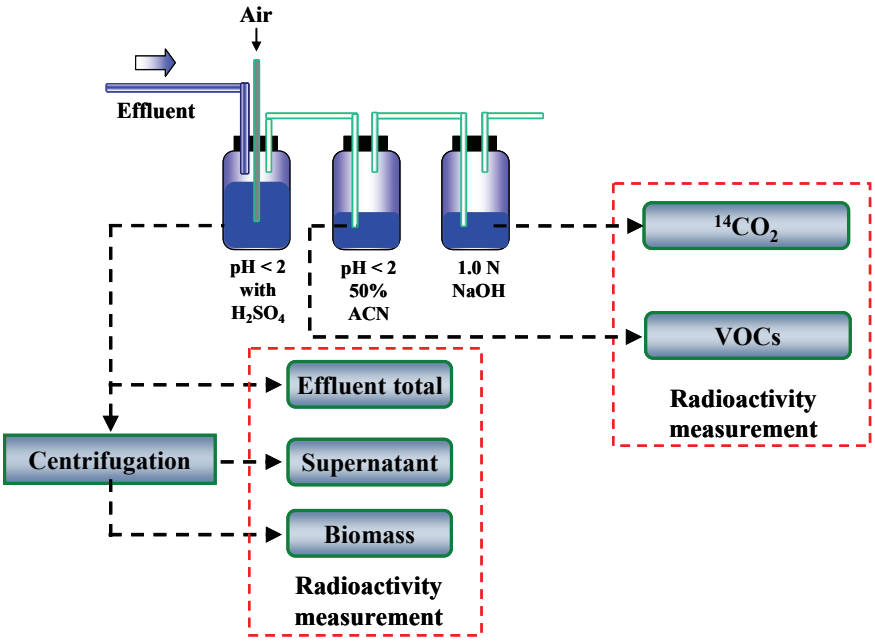


**Figure 4.3** (A) Column designed to stimulate the oxic/anoxic interface between sediment and water. (B) Apparatus for radioactivity fractionation.

Feed was prepared with groundwater from the site after aeration, removal of organics by activated carbon, addition of NB, and sterilization by filtration.

Autoclaved sediments were used in the control columns. Feed was prepared with groundwater from the site by aeration, removal of organics by activated carbon, addition of NB (50 μM), and sterilization by filtration. The system was operated at 1 ml/hr flow rate until it reached steady state, and then the flow was increased stepwise to 20 ml/hr. Column effluents were collected in a vial containing 0.5 N $H_2SO_4$ (1 ml) and analyzed by HPLC (Fig. 4.3A). The second vial contained acidified 50% acetonitrile (10 ml) to prevent loss of nitrobenzene due to volatilization. The degradation rates of NB were determined when the columns reached the new steady state.

### 4.3.6 Mineralization of NB in columns

Filter-sterilized site water supplemented with unlabeled (6.15 mg/l) and $^{14}$C-ring labeled nitrobenzene (4.5 μCi/l) was fed for 2 hours at flow rate of 2 ml/hr into the bottom of the columns via a syringe pump. Column effluent samples were collected in a series of scintillation vials sealed with Teflon septa. Vials 1-3 contain 0.5 N $H_2SO_4$ (1 ml), acidified 50% aetonitrile (10 ml), 1.0 N NaOH (10 ml), respectively. The analysis of column effluent was performed by the procedures described in Fig. 4.3B. Samples of column effluents were fractionated into aqueous, volatile organic compounds, biomass, and $^{14}CO_2$. Each fraction was mixed with scintillation cocktail and analyzed by liquid scintillation counting (LSC). At the end of experiments, materials in the column were separated into aqueous and solid phases by centrifugation or filtration. Each phase was mixed with scintillation cocktail and analyzed by LSC.

## 4.4 RESULTS AND DISCUSSION

### 4.4.1 Biodegradation of NB, aniline, and DPA in microcosms

All microcosms constructed with materials from Repauno showed degradation of NB, AN, and DPA, except for the killed controls (Fig. 4.4). The mixtures of the compounds could be simultaneously degraded without nutrient amendments in the microcosms. The presence of aniline and DPA did not influence the NB degradation in microcosms containing mixtures of the compounds. Aniline and NB degradation was fastest whereas DPA degradation was slowest. Degradation of the above compounds was immediate when the compounds were added a second time, which clearly indicates that the disappearance was due to biodegradation and that the microbial community became acclimated. When cells from active NB degrading microcosms were harvested, washed, and then resuspended in filtered site water with $^{14}$C-ring labeled NB, radioactivity was recovered as $^{14}CO_2$ (51.3 %) and biomass (40.0 %). Less than 4% of radioactivity was recovered as $^{14}CO_2$ and biomass in autoclaved controls. The results establish clearly that NB is mineralized by substantial populations of aerobic bacteria associated with organic detritus at the sediment/water interface.

### 4.4.2 Bacteria responsible for the degradation

The extent of microbial populations responsible for the degradations was evaluated by a most probable number (MPN) analysis. MPN for bacteria able to grow on NB, aniline, or DPA was $2.1 \pm 2.0\times10^3$, $5.6 \pm 2.9\times10^3$, and $0.8 \pm 0.3\times10^0$/mg sediment in samples (27 mg sediment/ml) collected on Jun 2007 respectively. The relative

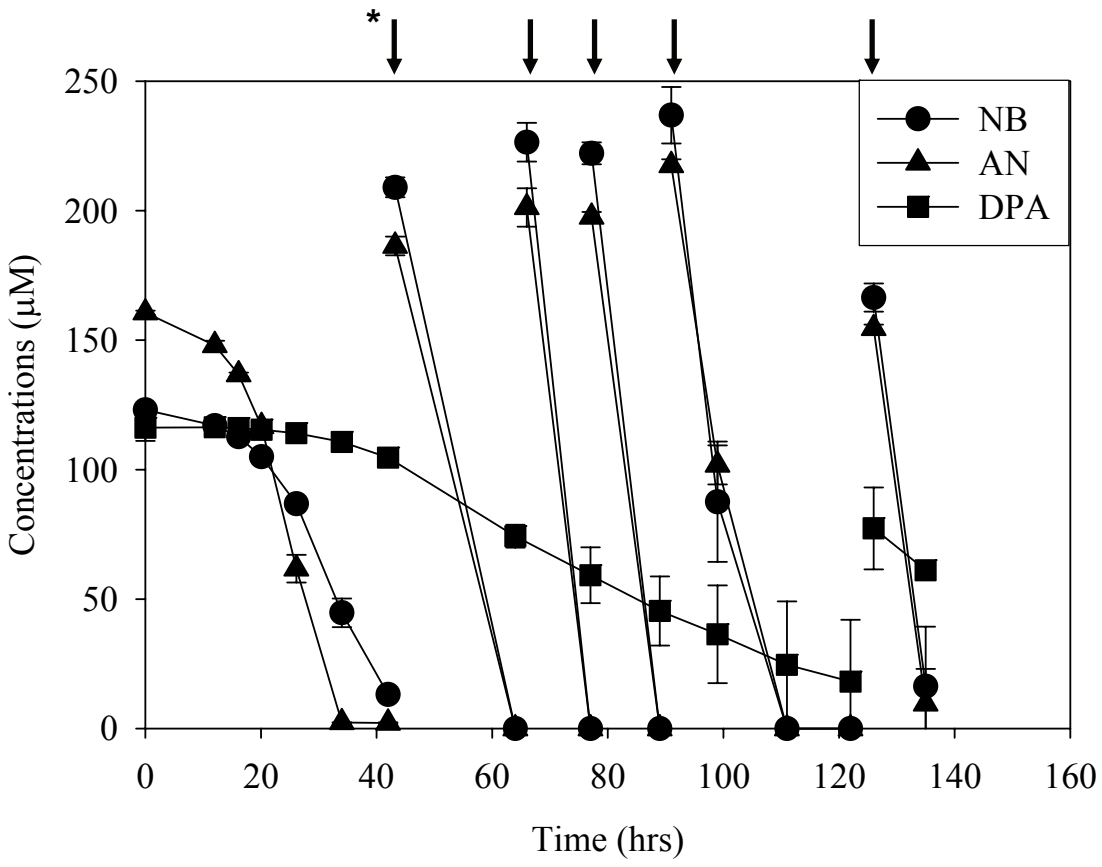


**Figure 4.4** Biodegradation of NB, aniline, and DPA in microcosms constructed with 27 mg of sediment in 20 ml of filtered site water.

population sizes correlate with rates of degradation of aniline, NB, and DPA (Fig. 4.4). The results suggest that the three different contaminants support the growth of relevant microbial populations at the contaminated site. The argument is further supported by the isolation of bacteria able to grow on NB, aniline, or DPA as sole carbon, nitrogen, and energy source (Table 4.1).

### 4.4.3 Final products of the degradation

All of the NB degraders released 0.35~0.49 mmoles of $NH_4^+$ during growth on NB (1 mM) in the absence of an added nitrogen source, but no $NO_2^-$ was produced. *Pseudomonas pseudoalcaligenes* JS45, a well characterized NB degrader, releases approximately 0.4 moles of $NH_4^+$ per mole of NB during growth via the partially reductive pathway (7). The results indicate that all of the isolates degrade NB via the partial reductive pathway (7) rather than the oxidative pathway (8). Similarly, aniline degrading bacteria released $NH_4^+$ during growth on aniline (1 mM) as a sole carbon, nitrogen, and energy source (Table 4.2). Aniline and catechol stimulated oxygen uptake with by cells grown on aniline. The difference (approximately 1 mole) in moles of oxygen required for the degradation of aniline and catechol indicates that a dioxygenase catalyzes the conversion of aniline to catechol (8). The results indicate that aniline is degraded via the common aniline degradation pathway (1, 6).

The pathway and final products of DPA degradation by strain JS667 were rigorously determined in Chapter 2. DPA is converted to aniline and catechol via dioxygenase attack at the 1,2 position of the aromatic ring and spontaneous rearomatization. Aniline and

**Table 4.1** Bacteria able to grow on NB, aniline, or DPA as sole carbon, nitrogen, and energy source and the closest relatives based on 16S rDNA (600 bp).

| Isolate | Growth Substrate | Closest strain | Identity (%) | Accession No. |
|---|---|---|---|---|
| JS1130 | NB | *Pseudomonas putida* PC30 | 99 | AY918068 |
| JS1131 | NB | *Pseudomonas putida* PC36 | 99 | DQ178233 |
| JS1132 | NB | *Pseudomonas* sp. PD7 | 99 | EF412971 |
| JS1133 | NB | *Pseudomonas putida* RE204 | 99 | EF143407 |
| JS1134 | NB | *Pseudomonas mendocina* PC10 | 99 | DQ178224 |
| JS1135 | Aniline | *Ralstonia* sp. T101 | 98 | AB212234 |
| JS1136 | Aniline | *Acidovorax* sp. U41 | 100 | EU375646 |
| JS1137 | Aniline | - | - | - |
| JS667 | DPA, Aniline | *Burkholderia* sp. 383 | 99 | CP000151 |
| JS668 | DPA, Aniline | *Ralstonia eutropha* HAMBI2380 | 99 | AF501365 |

**Table 4.2** Oxygen uptake and stoichiometric release of ammonia.

| | Oxygen Uptake Rates (nmoles/min/mg protein) | | Stoichiometry | | moles of $NH_4^+$ produced per mole of AN degraded |
|---|---|---|---|---|---|
| Strains | Aniline | Catechol | Aniline | Catechol | |
| JS1135 | 76 ± 13 | 119 ± 11 | 2.6 ± 0.1 | 1.5 ± 0.0 | 0.54 ± 0.08 |
| JS1136 | 40 ± 8 | 172 ± 5 | 3.1 ± 0.1 | 2.3 ± 0.1 | 0.35 ± 0.01 |
| JS1137 | 35 ± 12 | 107 ± 7 | 3.5 ± 0.1 | 2.2 ± 0.0 | 0.56 ± 0.13 |

catechol are further then biodegraded (6).

### 4.4.4 NB degradation rates in microcosms

NB is a major contaminant at the site. In order to provide useful estimates of the biodegradation potentials associated with sediment, rates of NB degradation were obtained as μg of NB degraded/hr/mg sediment. The initial rates (μg of NB degraded/hr) were determined in microcosms containing different amounts of sediment and then the rates were plotted versus the amounts of sediment in microcosms (Fig. 4.5). The NB degradation rates were proportional to the mass of sediment in the microcosms (Fig. 4.5), which indicates that bacteria associated with organic detritus at the sediment/water interface are responsible for the biodegradation. The resulting rate constant was 0.48 μg of NB /hr/mg of sediment which could be used to estimate overall biodegradation rates at the site based on measurement of the amounts of organic detritus at the sediment water interface.

### 4.4.5 Mineralization of NB in columns designed to simulate in situ conditions

In order to test the hypothesis that NB-degrading bacteria associated with organic detritus at the interface can eliminate NB across the surface layer of the sediment, we designed columns containing a representative sample of the surface detritus and a flow-through configuration with nitrobenzene contaminated water (Fig. 4.3A). Oxygen was provided in the feed water along with the NB (50 μM) in order to determine the biodegradation capacity of the sediment and to eliminate the possibility of oxygen

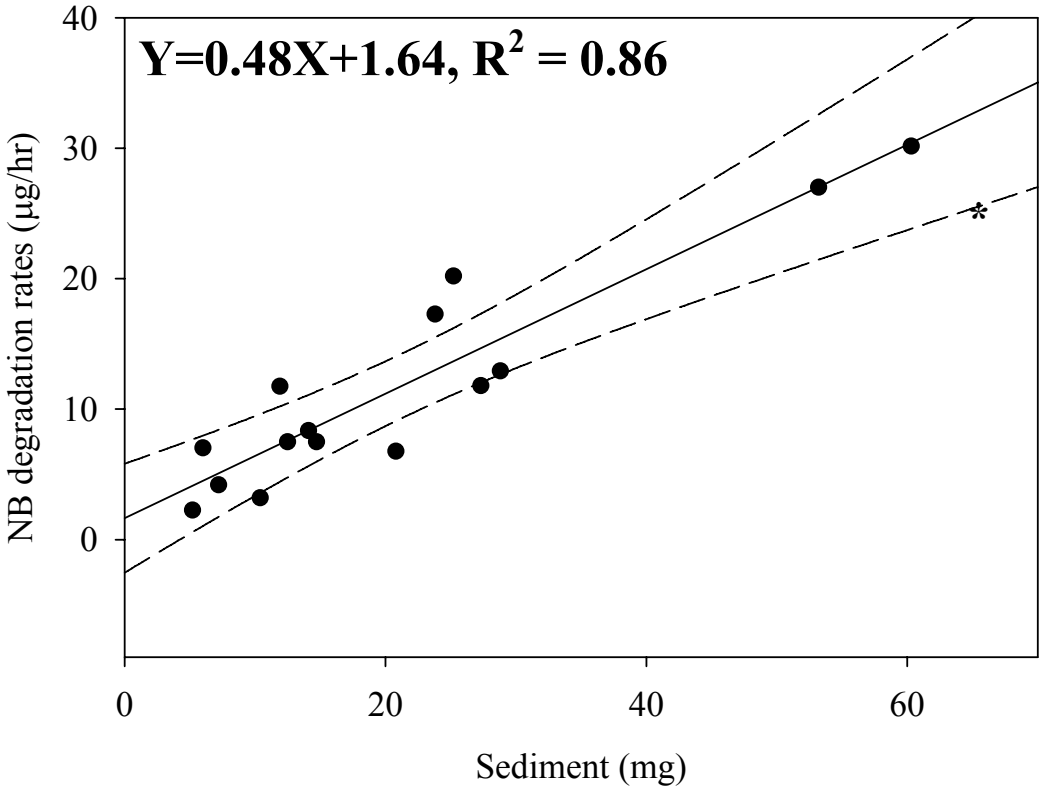


**Figure 4.5** Correlation between NB degradation rates (µg of NB/hr) and mass of detritus (mg). * 99% confidence interval

limitation for the experiment. In the field the oxygen would be provided by the overlying water or by phototrophs in the sediment.

Nitrobenzene (50 μM) was completely degraded at flow rates from 1 ml/hr to 2 ml/hr with no breakthrough (Fig. 4.6A). When flow rates were increased stepwise to 20 ml/hr, breakthrough of nitrobenzene was observed and then declined as the bacteria acclimated. The nitrobenzene degradation rates were 178 to 231 μg of NB/hr/$cm^3$ calculated at a flow rates of 20 ml/hr. The degradation rates can be expected to increase when more time is allowed for the microbial community to acclimate for each flow increment. The results clearly indicate a remarkably high capacity of the sediment for NB degradation. It is clear that nitrobenzene can be degraded as it migrates into the aerobic zone between the sediment and overlying water up to very high flow rates.

In order to determine a mass balance and the fate of a NB as it flows through the sediment/water interfaces. $^{14}$C-ring labeled NB was supplied to columns. A total of 58% of the radioactivity was recovered as carbon dioxide in the active columns at the end of experiment. The higher mineralization than those observed in batch (51%) suggests rapid turnover of NB degrading bacteria in the column. A further 19% of the radioactivity was associated with cells or bound to sediment (Table 4.3). It makes sense to consider the sediment-bound radioactivity as the portion of NB that was incorporated to biomass because negligible radioactivity was recovered from sediment in the control column. No other radioactive products were identified by HPLC. The results support the hypothesis that NB is mineralized by indigenous bacteria associated with organic detritus as it flows through the sediment/water interfaces.

**A.**

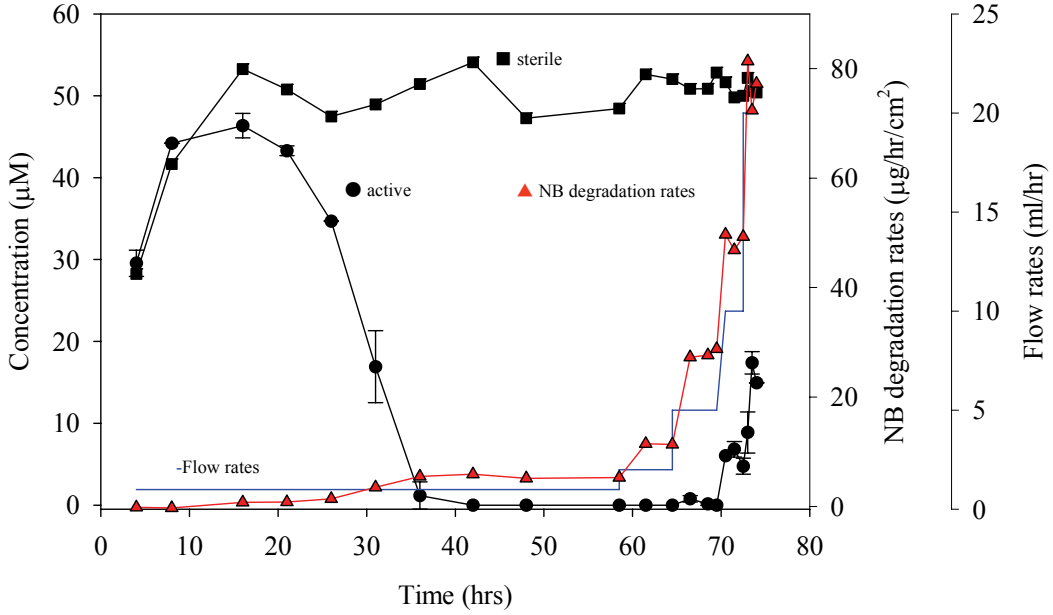


**B.**

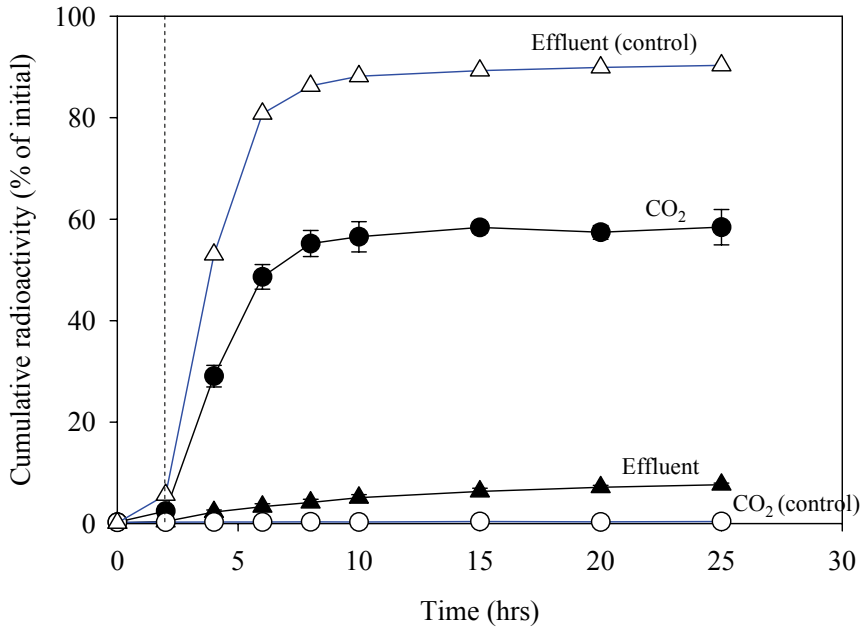


**Figure 4.6** (A) Rates of nitrobenzene degradation and (B) mass balance during the degradation in column.

Microcosm studies and enumeration and isolation of bacteria responsible for the degradation indicated that substantial populations of bacteria able to grow on NB, aniline, or DPA are associated with organic detritus at the sediment/water interface. The flux of the three chemicals from contaminated sediment across the interface would provide a selective pressure to develop and sustain the microbial community. The argument is supported by the predominance of aerobic methanotrophs and hydrogen sulfide oxidizing bacteria at oxic/anoxic interfaces where methane and hydrogen sulfide are supplied from underlying anoxic sediment layers in natural aquatic ecosystems (4, 5).

The continuous flow column studies demonstrated that aerobic bacteria associated with organic detritus overlying contaminated sediment rapidly biodegrade NB, aniline, and DPA, as they flow through the sediment/water interface. The findings support the ability of the natural attenuation processes to protect the water overlying contaminated sediments. Evaluation of *in situ* degradation rates by isotope fractionation of other strategies will be required to validate the extent of the processes in the field.

**Table 4.3** Mass balance of $^{14}$C-ring labeled nitrobenzene in column.

| | Column Effluent | | | Sediment | | | Total |
|---|---|---|---|---|---|---|---|
| | $CO_2$ | Aqueous | Cells | Total | Aqueous | Bound | Recovery |
| Active column | 58.4 ± 3.5 | 5.3 ± 0.4 | 1.8 ± 0.1 | 18.5 ± 0.6 | 0.3 ± 0.1 | 17.3 ± 0.6 | 85.8 |
| Sterile column | 0.4 | 89.4 | 1.7 | 0.6 | 0.4 | 0.6 | 91.4 |

## 4.5 REFERENCES


1. **Aoki, K., R. Shinke, and H. Nishira.** 1983. Metabolism of aniline by *Rhodococcus erythropolis* AN-13. Agric. Biol. Chem. **47:**1611-1616.
2. **Bachofer, R., F. Lingens, and W. Schafer.** 1975. Conversion of aniline into pyrocatechol by a *Nocardia* sp.; incorporation of oxygen-18. FEBS Lett. **50:**288-290.
3. **Bruhn, C., H. Lenke, and H.-J. Knackmuss.** 1987. Nitrosubstututed aromatic compounds as nitrogen source for bacteria. Appl. Environ. Microbiol. **53:**208-210.
4. **Buckley, D. H., L. K. Baumgartner, and P. T. Visscher.** 2008. Vertical distribution of methane metabolism in microbial mats of the Great Sippewissett Salt Marsh. Environ. Microbiol. **10:**967-977.
5. **Costello, A. M., A. J. Auman, J. L. Macalady, K. M. Scow, and M. E. Lidstrom.** 2002. Estimation of methanotroph abundance in a freshwater lake sediment. Environ. Microbiol. **4:**443-450.
6. **Fukumori, F., and C. P. Saint.** 1997. Nucleotide sequences and regulational analysis of genes involved in conversion of aniline to catechol in *Pseudomonas putida* UCC22(pTDN1). J. Bacteriol. **179:**399-408.
7. **Nishino, S. F., and J. C. Spain.** 1993. Degradation of nitrobenzene by a *Pseudomonas pseudoalcaligenes*. Appl. Environ. Microbiol. **59:**2520-2525.
8. **Nishino, S. F., and J. C. Spain.** 1995. Oxidative pathway for the biodegradation of nitrobenzene by *Comamonas* sp. stranin JS765. Appl. Environ. Microbiol. **61:**2308-2313.
9. **Parsons, T. T., Y. Maita, and C. M. Lalli.** 1984. A manual of chemical and biological methods for seawater analysis. Pergamon Press, Oxford, United Kingdom.
10. **Rahalkar, M., J. Deutzmann, B. Schink, and I. Bussmann.** 2009. Abundance and activity of methanotrophic bacteria in littoral and profundal sediments of lake constance (Germany). Appl. Environ. Microbiol. **75:**119-126.
11. **Shin, K. A., and J. C. Spain.** 2009. Pathway and evolutionary implications of diphenylamine biodegradation by *Burkholderia* sp. strain JS667. Appl. Environ. Microbiol. **75:**2694-2704.

# CHAPTER 5

# Conclusion and Recommendations

*cis*-Dichloroethene (*c*DCE) and diphenylamine (DPA) are toxic chemicals that drive the risk at many contaminated sites. Natural attenuation or bioremediation of the contaminated sites is potentially a cost efficient and environmentally benign approach but unknown degradation mechanisms and intermediates are bottlenecks for evaluating the potentials for natural attenuation processes and field applications involving bioremediation of the toxic chemicals. By establishing biodegradation pathways of *c*DCE and DPA in this study we demonstrated that both toxic chemicals are biodegraded without accumulation of toxic intermediates. Bioremediation would be, therefore, a promising strategy to clean up sites contaminated with *c*DCE or DPA. In addition, the understanding of appropriate conditions for the responsible bacteria will provide a basis for treatability studies to evaluate the biodegradation potentials at other contaminated sites.

Bioaugmentation with strain JS666 would be a promising strategy to clean up *c*DCE-contaminated plumes because *Polaromonas* sp. strain JS666 is the only bacterium known to grow on *c*DCE as the sole carbon and energy source under aerobic conditions. Field application of JS666 would require monitoring tools to validate the extent of *c*DCE degradation at contaminated sites. The large carbon isotope fractionation (-17.4 to -22.4‰) during *c*DCE degradation was suggested as a tool to predict the extent of *c*DCE degradation in field (3), but the lack of understanding about the *c*DCE degradation

mechanism was a deterrent to application of the technology for *c*DCE degradation. The discovery of the initial reaction in *c*DCE degradation that is catalyzed by cytochrome P450 monooxygenase will enable future experiments to determine how isotope fractionation can be used to monitor bioremediation. The validation should be carried out in future work by measuring isotope fractionation during *c*DCE transformation by the cloned cytochrome P450 monooxygenase.

The cytochrome P450 monooxygenase in JS666 appears to be specialized for dichloroacetaldehyde rather than epoxide production from *c*DCE, which channels the carbon into a productive pathway to prevent accumulation of the toxic and reactive products. This is the first example of a productive pathway involving P450 catalyzed transformation of chlorinated ethenes to aldehyde compounds. Similar reactions were reported previously during the oxidation of trichloroethene by cytochrome P450 enzymes from rat liver microsomes (4), but mass balances of the reactions were not rigorously determined. Closely related cytochrome P450 alkane hydroxylases appear to be specialized for the hydroxylation of medium-chain-length alkanes (C6-C10) and the epoxidation of styrene, cyclohexene, and 1-octene, but their activities for *c*DCE are unknown. A binding model to simulate the reaction compared with structures of well established cytochrome P450 enzymes will suggest how the cytochrome P450 monooxygenase in JS666 has evolved the ability to transform *c*DCE to dichloroacetaldehyde. Site-directed mutagenesis will rigorously reveal what causes differences in substrate specificity of cytochrome P450 monooxygenase in JS666 and other alkane hydroxylases.

Molecular phylogeny of the cytochrome P450 gene and organization of neighboring genes suggest that the genes encoding the cytochrome P450 monooxygenase were recruited from alkane assimilating bacteria. The recruitment and expression of the genes encoding the cytochrome P450 monooxygenase could allow the relatively common chloroacetaldehyde degrading bacteria to grow with *c*DCE as a sole source of carbon and energy. Instability and rapid loss by JS666 of the ability to degrade *c*DCE under non selective conditions suggests that the system was recently assembled and sustained at the field site in response to contamination by *c*DCE. The hypothesis can be tested by introducing the cytochrome P450 monooxygenase genes into chloroacetaldehyde degrading bacteria to determine whether such gene recombination can evolve the productive *c*DCE degradation pathway.

DPA is converted to aniline and catechol via dioxygenation at the 1,2 position of the aromatic ring and spontaneous rearomatization. Aniline and catechol are then completely degraded via the common aniline degradation pathway. The enzymes that catalyze the initial reaction in DPA degradation belong to the family of Rieske non-heme iron oxygenases that hydroxylate aromatic rings (8). The DPA dioxygenase system comprising a terminal dioxygenase component (*dpaAa*), ferredoxin reductase (*dpaAd*), and ferredoxin (*dpaAc*) is closely related to carbazole 1,9a-dioxygenase (1) that catalyzes attack at the angular position of carbazole , but DPA dioxygenase is highly specialized for DPA and the carbazole dioxygenase could not transform DPA. Alignment of the deduced amino acid sequence of the DPA dioxygenase with the carbazole dioxygenase revealed that three amino acids (Ala-259, Ile-184, and Ile-262) of fourteen amino acids forming

the substrate-binding pocket are substituted with Ile, Val, and Ala in the DPA dioxygenase. Site-directed mutagenesis will rigorously reveal causes of the difference in substrate specificity of carbazole and DPA dioxygenases.

2-Hydroxydiphenylamine appears to be a minor side product resulting from decomposition of a dihydrodiol intermediate during DPA degradation. Stimulation of oxygen uptake in DPA grown cells by hydroxydiphenylamines suggests that the compound is further degraded. Preliminary results showed that the *E. coli* clone expressing DPA dioxygenase transformed 3-hydroxydiphenylamine (27%) and 4-hydroxydiphenlamine (30%) of the rate of DPA transformation, but the products of the degradation were not identified. In order to rigorously determine the fate of 2-hydroxydiphenylamine, it should be tested whether DPA dioxygenase transforms the compound to biodegradable intermediates that feed back into the pathway. Elucidation of the degradation products will provide additional insight about how dioxygenases recapture the small amounts of phenols produced during dioxygenase catalyzed pathways.

The recruitment of the genes encoding DPA dioxygenase would be sufficient to allow the relatively common aniline degrading bacteria to grow with DPA as a sole source of carbon, nitrogen, and energy. It seems reasonable to speculate that the system was assembled at the field site in response to contamination by DPA. Genes involved in carbazole and aniline biodegradation would be the potential origins of the DPA degradation pathway. Such a scenario was strongly supported for assembly of a chlorobenzene degradation pathway in response to chlorobenzene contamination (5).

The evolutionary relationships among bacteria able to grow on DPA, aniline, or carbazole should be determined to enable prediction of the distribution of the DPA degradation pathway and effectiveness for bioremediation. In a preliminary study, other areas of the DPA contaminated sites were screened to evaluate the distribution of DPA degraders and whether they can be expected to support bioremediation at the site. New DPA degraders were readily isolated, which indicated that DPA degradation should be widespread at the site. The bacteria belong to the genera *Burkholderia*, *Ralstonia*, and *Pseudomonas* and they have identical DPA dioxygenase genes involved in the initial steps of DPA degradation. The results suggested that the ability to degrade DPA was spread at the site by horizontal gene transfer. In addition, bacteria able to grow on aniline or carbazole were isolated from the same sites where DPA degraders were isolated. There was some evidence that the strains evolved at the DPA contaminated sites by recombination between aniline and carbazole degraders and the hypothesis should be tested to determine whether such mechanisms might operate at other DPA contaminated sites. The nucleotide sequence similarities of the homologous initial dioxygenase and aniline dioxygenase among aniline, carbazole, and DPA degraders will provide insight about the origins of DPA biodegradation pathway and will enable predictions of how catabolic pathways are assembled in response to synthetic pollutants at Repauno and other sites.

The fate and transport of contaminants are of a great concern at several historically contaminated sites where an anoxic contaminant plume emerges into a water body. The release of the toxic chemicals to overlying water poses a potential source of

environmental exposure. In this study, bench scale studies demonstrated that substantial populations of bacteria associated with organic detritus at the interface rapidly biodegrade toxic chemicals as they migrate from contaminated sediment to overlying water. The findings demonstrated the feasibility of the natural attenuation processes as a remedial strategy to protect the water overlying contaminated sediments, but the results can not directly represent the degradation capacity in the field because of unknown factors that may affect the biodegradation. Evaluation of in situ degradation rates will require additional work including isotope fractionation or other strategies.

Recent advances in the use of isotope fractionation have enabled dramatic improvements in the ability to distinguish among mechanisms of fate and transport of contaminants in the subsurface. Hofstetter et al extended the approach to include aerobic biodegradation of nitrobenzene (2). The results of C and N isotope fractionation during the oxidation of nitrobenzene indicate that the fractionation should be similar with amines such as aniline and DPA where the initial enzymatic attack is by a dioxygenase enzyme at the carbon atom that is bonded to the nitrogen. Therefore, the potential for isotope fractionation of aniline and DPA should be determined to provide evidence of biodegradation. Pathways that begin with oxidative removal of the nitro group give distinctly different fractionation patterns from pathways that begin with reduction of the nitro group, which makes it possible distinguish the extent of nitrobenzene biodegradation via the two different pathways (6, 7). Subsequent validation should be conducted in bench scale to field scale systems.

In summary, i) the elucidation of the biodegradation mechanisms of DPA and *c*DCE provide the basis to predict the fate of the two toxic chemicals in the environment and set the stage for field applications to enable bioremediation. ii) The discovery of enzymes that catalyze the initial reactions in DPA and *c*DCE biodegradation increases our understanding of catabolic versatibility of the two existing enzyme families, Rieske iron non heme oxygenases and cytochrome P450 enzymes. iii) Molecular phylogeny of the enzymes and organization of neighboring genes support current understanding that new biodegradation pathways for synthetic chemicals can evolve through mutations that alter the substrate specificities of the existing enzymes and/or recruitment of genes that channel degradation intermediates to central metabolism. iv) The natural attenuation processes at the sediment/water interface can be applied as a remedial strategy to protect the overlying contaminated sediments.

## REFERENCES


1. **Ashikawa, Y., Z. Fujimoto, H. Noguchi, H. Habe, T. Omori, H. Yamane, and H. Nojiri.** 2006. Electron transfer complex formation between oxygenase and ferredoxin components in Rieske nonheme iron oxygenase system. Structure **14:**1779-1789.
2. **Hofstetter, T. B., J. C. Spain, S. F. Nishino, J. Bolotin, and R. P. Schwarzenbach.** 2008. Identifying competing aerobic nitrobenzene biodegradation pathways by compound-specific isotope analysis. Environ. Sci. Technol. **42:**4764-4770.
3. **Jennings, L. K., M. M. Chartrand, G. Lacrampe-Couloume, B. S. Lollar, J. C. Spain, and J. M. Gossett.** 2009. Proteomic and transcriptomic analyses reveal genes upregulated by *cis*-dichloroethene in *Polaromonas* sp. strain JS666. Appl. Environ. Microbiol. **75:**3733-3744.
4. **Meunier, B., S. P. de Visser, and S. Shaik.** 2004. Mechanism of oxidation reactions catalyzed by cytochrome P450 enzymes. Chem. Rev. **104:**3947-3980.
5. **Muller, T. A., C. Werlen, J. Spain, and J. R. Van Der Meer.** 2003. Evolution of a chlorobenzene degradative pathway among bacteria in a contaminated groundwater mediated by a genomic island in *Ralstonia*. Environ. Microbiol. **5:**163-173.
6. **Nishino, S. F., and J. C. Spain.** 1993. Degradation of nitrobenzene by a *Pseudomonas pseudoalcaligenes*. Appl. Environ. Microbiol. **59:**2520-2525.
7. **Nishino, S. F., and J. C. Spain.** 1995. Oxidative pathway for the biodegradation of nitrobenzene by *Comamonas* sp. stranin JS765. Appl. Environ. Microbiol. **61:**2308-2313.
8. **Wackett, L. P.** 2002. Mechanism and applications of Rieske non-heme iron dioxygenases. Enzym. Microb. Tech. **31:**577-587.

# VITA
# KWANGHEE SHIN

Shin was born in Daegu, South Korea. He graduated from Simin High School in 1996 and attended Yeungnam University earning a Bachelor of Environmental Engineering in 2002. He served in Republic of Korea Army for two years from 1997. He received a Master of Environmental Science and Engineering in 2004 from Gwangju Institute of Science and Technology (GIST), South Korea. After graduating from GIST, he worked as research technician in molecular biology at Bio/Molecular Informatics Center in Seoul, Korea. He began studying for a Ph.D. in Environmental Engineering at the Georgia Institute of Technology in the Fall of 2005.